

FINAL STUDY REPORT

HUNTSMAN STUDY NUMBER:	HMSC-169
SPONSOR:	ITOPF
PROJECT NAME:	Photomodification Of Low-sulfur-fuel-oils Investigations of Toxic Effects (POLITE).
TEST MATERIAL:	U/VLSFO
LOCATION:	Huntsman Marine Science Centre St. Andrews, NB Canada
Principal Investigator:	Benjamin de Jourdan, PhD. Huntsman Marine Science Centre St. Andrews, NB Canada
Co-Principal Investigator:	Christoph Aeppli, PhD Bigelow Laboratory for Ocean Sciences East Boothbay, ME USA
EXPERIMENTAL INITIATION DATE:	May 1 st , 2022
REPORTING PERIOD DATE:	May 1 st 2022 – May 1 st , 2024
PROJECT COMPLETION DATE:	May 1 st , 2024

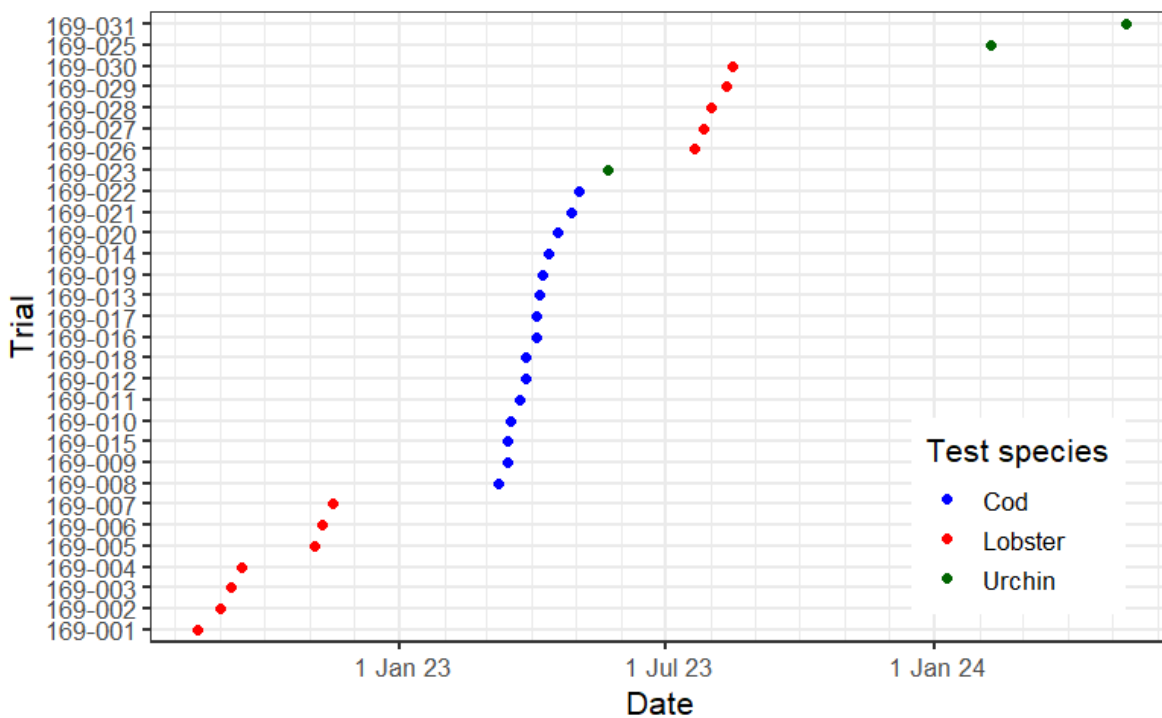
2 Executive Summary

3 The following report outlines the activities from the entire project that began May 1st 2022
 4 and ended May 1st, 2024. During this project we completed work that addressed aspects
 5 of all three of our goals;

6

- 7 1. How toxic are U/VLS fuel oils compared to conventional fuel oils?
- 8 2. How does photomodification change toxicity?
- 9 3. Can we effectively predict the toxicity photomodified and non-photomodified
 U/VLS fuel oils?

10 In this study we conducted 31 distinct toxicity bioassays (Figure 1) with American lobster
 11 (*Homarus americanus*), Atlantic cod (*Gadus morhua*), and green sea urchin
 12 (*Strongylocentrotus droebachiensis*) using a conventional heavy crude oil (CONV), an
 13 offshore Newfoundland crude oil (ESRF), an ultra-low sulfur fuel oil (ULSFO), and 14 very
 14 low sulfur fuel oils (VLSFO) provided by the Australian Maritime Safety Authority (AMSA).
 15 The bioassays were conducted with exposure media generated from paired water
 16 accommodated fractions (WAFs) of the oil and seawater, with one WAF prepared in the
 17 dark (e.g., standard preparation) and one prepared under a UV light (e.g., irradiated) to
 18 induce photomodification.



Following irradiation, the exposure metrics (e.g., fluorometry units (RFU), total organic carbon (TOC), biomimetic extraction solid phase microextraction (BE-SPME), and polycyclic aromatic compounds (PACs)) for many of the products tested significantly increased, suggesting that there were photoproducts being formed. The amount of photoproducts formed varied between oil samples, with some of the tested VLSFOs not showing any detectable changes following irradiation. In nearly all cases the observed toxicity in the UV treated WAF was equal or greater than the WAF prepared in the dark. Larval lobster immobilization was the most sensitive endpoint across the tested species, and it showed a full range of responses with the tested products varying from 10 - 100% immobilization (Figure 2).

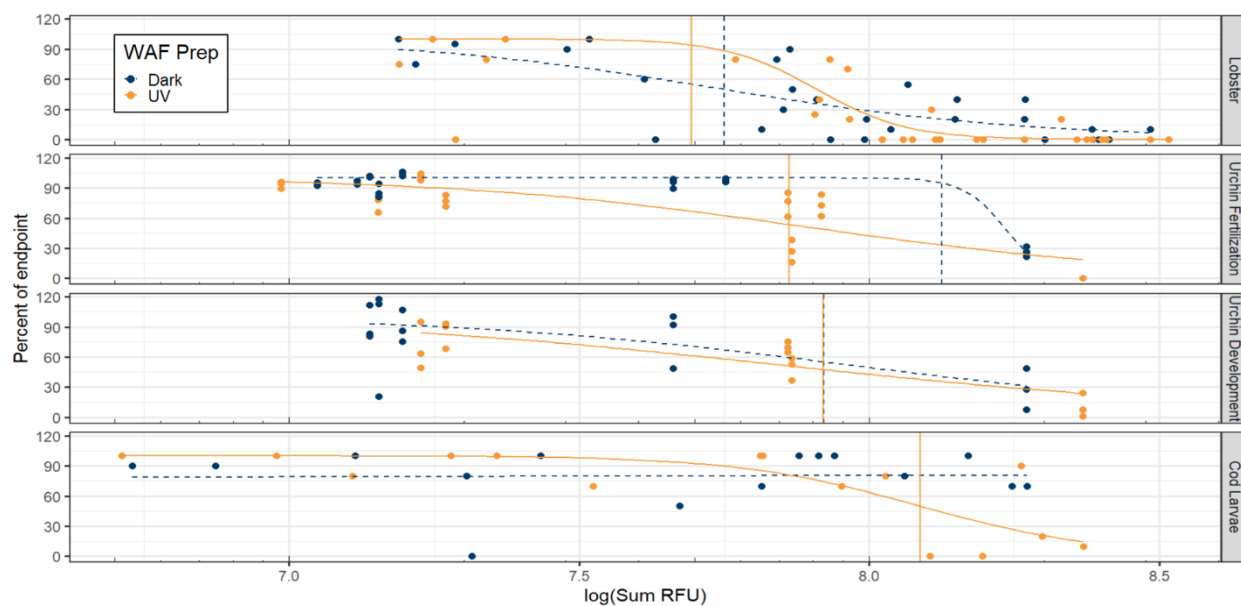


Figure 2: Normalized responses showing lobster immobilization (top), urchin fertilization and development (middle) and cod mortality (bottom) following exposure to irradiated (solid orange circles) and non-irradiated (solid blue circles) WAFs. The species are ordered by sensitivity top to bottom, with the vertical lines showing the EC50 on the basis of fluorometry units

The immobilization response largely followed a concentration gradient with TOC, BE-SPME, and PAC based toxic units. However, using only waterborne PAC concentrations to calculate toxic units, the predicted toxicity was consistently lower than what was observed for many of the VLSFOs products, both with and without UV irradiation. These results suggest that there are other aspects that aren't measured by traditional GC-MS (e.g., oxidized products) which are contributing to the toxicity of the VLSFOs.

The results highlight a wide range of responses across fuel types, with significant differences in sensitivity across species. The impact of UV light on the observed toxicity underscores the importance of addressing and incorporating modifying factors when

45 determining the toxicity of complex mixtures. The SARA fraction (Saturates, Aromatics,
46 Resins, and Asphaltenes), specifically the aromatics and asphaltenes, have significant
47 correlations with the formation of photoproducts and their associated toxicity.

48 The data generated within this study will be used to develop and validate models, to
49 predict and assess the toxicity of these new generation fuel oils.

50

Contents

Executive Summary	2
1. Study Overview	12
2. Methods	13
2.1. Test Materials	13
2.2. WAF Preparation	15
2.3. UV light exposure	16
2.4. Test organism	16
2.4.1. American lobster	16
2.4.2. Atlantic cod	17
2.4.3. Green sea urchin	18
2.5. Bioassay	19
2.5.1. American lobster methodology	19
2.5.2. Atlantic cod methodology	20
2.5.3. Green sea urchin methodology	21
2.6. Chemical characterization	23
2.6.1. Total Organic Carbon	23
2.6.2. Fluorometry	23
2.6.3. Biomimetic Extraction using Solid Phase Microextraction	23
2.6.4. Gas Chromatography–Mass Spectrometry	24
2.6.5. VLSFO Characterization	25
3. Results	26
3.1. Test Material Characterization	26
3.1.1. Physical and chemical data	26
3.1.1.1. Gas Chromatography–Mass Spectrometry	29
3.1.1.2. GC × GC	32
3.1.1.3. UV-Vis	34
3.2. Impact of WAF Preparation Method	35
3.2.1. Timing of irradiation	35
3.2.2. Variable loading	37

81	3.3. Toxicity Testing	40
82	3.3.1. American lobster results	40
83	3.3.2. Atlantic cod results.....	51
84	3.3.3. Green sea urchin results.....	58
85	3.4. Modelling.....	60
86	3.4.1. Relationships in water chemistry	62
87	3.4.2. Relationships between properties of the VLSFOs and bioassay results ..	63
88	4. Conclusions	65
89	5. Dissemination.....	66
90	6. References.....	67
91	7. Appendix	69
92	7.1. Alkanes and PAC Data from VLSFOs.....	69

93

94 **Figures**

95	Figure 1: Timeline of the bioassays conducted over the course of this study.....	2
96	Figure 2: Normalized responses showing lobster immobilization (top), urchin fertilization 97 and development (middle) and cod mortality (bottom) following exposure to irradiated 98 (solid orange circles) and non-irradiated (solid blue circles) WAFs. The species are 99 ordered by sensitivity top to bottom, with the vertical lines showing the EC50 on the 100 basis of fluorometry units	3
101	Figure 3: Sulphur content, API gravity, pour point (showing the test temperatures 102 employed in this study, 6, 10, and 15°C) and %mass less than 370°C from simulated 103 distillation (SIMDIST) of the 49 VLSFOs provided by AMSA, the ULSFO, and two 104 conventional crudes (ESRF and CONV) grouped by viscosity, with the blue triangles 105 indicating the products (n = 17) selected for toxicity screening.	14
106	Figure 4: Representative WAFs displaying a range of physical appearance and 107 behaviours upon contact with seawater.	15
108	Figure 5: Overview of the process of working with berried lobsters. A) Collection of 109 lobsters from local fishers after receiving required permission to do so, B) holding and 110 feeding of berried female lobsters in individual holding cells, C) staging and measuring	

111	the clutch to assess fecundity and development stage in anticipation of larval release,	
112	D-H) developmental progression of the embryos.....	17
113	Figure 6: Overview of Atlantic cod embryo and larvae generation for toxicity testing. A)	
114	technician holding a mature cod prior to gamete collection during artificial spawning	
115	procedures, B) reference image of cod embryos 24-48hrs post fertilization C) image of	
116	cod embryos prior to hatch, D-H) reference image of ~200 degree day cod larvae.....	18
117	Figure 7: Holding of adult urchins under “perpetual spring” conditions prior to spawning	
118	them.....	19
119	Figure 8: Lobster testing overview A) allocating the larval lobster into exposure vessels.	
120	B) Stage I larvae. C) Assessing a lobster larvae in the exposure vessel.....	20
121	Figure 9: Distribution of the ages and sizes of the reference organisms at for each	
122	toxicity trial (different shapes) conducted with embryos (left) and larvae (right)	21
123	Figure 10: A) Representative eggs (unfertilized) and embryos (fertilized) following a	
124	fertilization bioassay. B) 40 hrs post fertilization, C) ~200 hrs post fertilization showing	
125	normal development.....	22
126	Figure 11: (Top) High temperature simulated distillation curves for the 49 AMSA	
127	products and the Huntsman reference oils. The dashed horizontal lines represent the	
128	boiling point cutoffs associated with the C11 (204°C), C25 (343°C), and C40 (524°C)	
129	alkanes. (Bottom) Overlay of the HTSD curves for the products screened for toxicity	
130	with larval lobsters. O-43 (light purple) shows a distinctly different pattern with 75% of	
131	the cumulative mass having been lost by 343°C. Note the HTSD data for ULSFO,	
132	CONV, and ESRF were generated separately from the other 49 AMSA products.....	28
133	Figure 12: Grouped alkane concentrations for the products, top: concentration, bottom:	
134	percent composition.....	30
135	Figure 13: Sum PACs for each of the examined products as the source, extract, and UV	
136	treated.....	31
137	Figure 14: Concentration (top row) and percent composition (bottom row) of the	
138	measured PACs for two products, O-14 (least toxic to lobsters) and O-2 (most toxic to	
139	lobsters).....	32
140	Figure 15: Representative GC × GC plots from select products demonstrating a range of	
141	toxicity responses.....	33

142	Figure 16: Annotated GC × GC profiles for the ULSFO and CONV products.	34
143	Figure 17: UV spectra profiles for 12 oils. The vertical lines 295 nm for pure	
144	phenanthrene, 328 nm for aromatic chromophores with three or four aromatic rings, and	
145	401 nm for the Soret electronic absorption band of vanadyl porphyrins.....	35
146	Figure 18: Schematic of the various ways the 18 hour UV dose was applied to the	
147	treatments, either directly on the oil (Treatment 1), on the dissolved phase test solution	
148	(Treatment 3), or while mixing (Treatment 5). The non-UV treatments (2, 4, and 6) were	
149	treated in the same manner as their UV counterparts only in a dark location within the	
150	same room.	36
151	Figure 19: Summary of the measurements of BE (top row), fluorometry (second row),	
152	PACs (third row) and TOC (bottom row) following the different Treatment methods and	
153	UV irradiation.	37
154	Figure 20: BE values (fiber concentration) for the different loadings of ULSFO (left) and	
155	CONV (right) prepared under UV light (orange) and in the dark (blue). The numbers	
156	indicate the fold difference between the irradiated and dark samples.	38
157	Figure 21: Concentration response relationship for lobsters exposed to variable loadings	
158	of ULSFO (left) and CONV (right) that were irradiated (orange) or prepared in the dark	
159	(blue). The immobilization response is shown with open circles and dashed line, while	
160	mortality is shown with solid circles and lines, both were fit with a 3-parameter Type 1	
161	Weibull model.....	39
162	Figure 22: Amount of each product used in making the WAFs. The dashed blue line is	
163	the target loading, while the dashed red lines are the acceptable ranges.	40
164	Figure 23: Visual summary of the lobster immobilization response for the 2022	
165	exposures to irradiated (solid orange circles) and non-irradiated (open blue triangles)	
166	WAFs.	42
167	Figure 24: Concentrations of total organic carbon (TOC) and the lobster immobilization	
168	response.	44
169	Figure 25: Relative fluorescence units (RFU) and the lobster immobilization response.	
170	45
171	Figure 26: Summary of the larval lobster immobilization response data following 24-hour	
172	exposure to irradiated (orange) and non-irradiated (blue) WAFs in the 2022 (open	

173	triangles) and 2023 (filled circles) testing season. The dashed vertical line is the	
174	calculated BE-critical value of 6.3 μmol per mL PDMS.	46
175	Figure 27: Sum of the polycyclic aromatic compounds (PAC) and the lobster	
176	immobilization response.....	47
177	Figure 28: Predicted and observed toxicity. Dashed line is 1:1 with the dotted lines	
178	bounding 20%.	48
179	Figure 29: Summary of the lobster immobilization in response to 24-hr exposure to	
180	irradiated (orange) and non-irradiated (blue) WAFs in the 2022 (open triangles) and	
181	2023 (filled circles) testing season. Where the product was tested in both years the	
182	boxplot illustrates the range and mean response.....	49
183	Figure 30: Summary of the photo-modification and photo-sensitization combined trial.	
184	The panel on the left represent WAF media that was prepared in the dark (no photo-	
185	modification), while the panel on the right is WAF media prepared under UV light	
186	(photo-modification). The colours of the points within each panel indicate whether	
187	following 24-hrs of exposure to media the replicate (individual point) was placed under	
188	UV light for 3-hours (photo-sensitization; orange circles), or left in the dark (blue circles).	
189	50
190	Figure 31: Summary of embryo responses following either 72 (circles) or 96 (triangles)	
191	exposure to UV-treated (orange) or dark (blue) WAF.....	51
192	Figure 32: Summary of the larval mortality (left; each point represents a replicate, with	
193	the box bounding the interquartile range), total organic carbon measurements (middle-	
194	left), the relative fluorometry signal (middle-right), and the BE-SPME (right) for the UV-	
195	treated (orange) and dark (blue) WAFs. The products are listed on the y-axis in	
196	decreasing order of toxicity based on the UV-treated WAFs (e.g., products on the	
197	bottom are more toxic)	54
198	Figure 33: Fitting the larval cod mortality data to the exposure metrics of total organic	
199	carbon (top), relative fluorometry signal (middle), and BE (bottom) for the UV-treated	
200	(orange) and dark (blue) WAFs.....	55
201	Figure 34: Summary of the photo-modification and photo-sensitization combined trial.	
202	The panel on the left represent WAF media that was prepared in the dark (no photo-	
203	modification), while the panel on the right is WAF media prepared under UV light	
204	(photo-modification). The colours of the boxes within each panel indicate whether	
205	following 24-hrs of exposure to media the replicate (individual point) was placed under	

206	UV light for 3-hours (photo-sensitization; orange boxes), or left in the dark (blue boxes).	57
207	
208	Figure 35: Urchin fertilization (top) and development (bottom) results for the UV-treated (orange) and dark (blue) WAFs.....	58
209		
210	Figure 36: (top) The sum of the fluorometric signals from the urchin exposures for the (blue circles) and under UV (orange triangles). (bottom) WAFs prepared in the dark (blue circles) and under UV	59
211	Summary of the fluorometry excitation and emission spectra (colour represents signal	
212	intensity with yellow being the most intense and purple the least) and toxicological	
213	responses for O-32.....	
214		
215	Figure 37: Concentration response relationship for the UV-treated (orange) and dark (blue) WAFs.	60
216		
217	Figure 38: Predicted toxicity (as immobilization) to American lobster larvae based on the measured concentrations in the source oil following the preparation of a WAF in the dark (left) or under UV light (right). The dashed line is showing 1:1 and the dotted lines	61
218	bound a +/- 20%.....	
219		
220		
221	Figure 39: Comparison between the measured exposure metrics TOC (A), RFU (B), and (blue circles) and under UV light (orange circles).The dashed BE-SPME (C) between lobster (x-axis) and cod (y-axis) for the same products (n = 15) prepared in the dark (blue circles) and under UV light (orange circles).The dashed	62
222	diagonal line is 1:1 and the solid line is the linear regression relationship with the	
223	equation in the insert.....	
224		
225		
226	Figure 40: Relationship between the exposure metrics TOC and RFU (A), TOC and BE (B), and RFU and BE (C) prepared in the dark (blue circles) and under UV light (orange circles).....	63
227		
228		
229	Figure 41: Correlation matrix with scatterplots (lower half), histograms (diagonal), and (upper half) for a suite of measures.....	64
230		
231		
232	Tables	
233	Table 1: Additional physical and chemical characterization of the source oils including	
234	simulated distillation (Sim. Dist.) and SARA (Saturates, Aromatics, Resins,	
235	Asphaltenes) analysis. The products tested in this program are shaded blue.....	26
236	Table 2: Summary of lobster immobilization (Imm.) results for 2022 and the various	
237	exposure metrics. Fold change refers to the Light to Dark.....	41

238	Table 3: Summary of the O-43 testing with larval lobster in 2023	43
239	Table 4: Results of larval cod toxicity screening prepared in the dark and under 18	
240	hours of irradiation.....	53
241		

242 Photomodification Of Low-sulfur-fuel-oils Investigations of Toxic Effects (POLITE)

243 **1. Study Overview**

244 The changes in International Maritime Organization (IMO) regulations regarding the lower
245 limits of sulfur content in marine fuel oils (IMO 2020) have initiated the transition to a new
246 generation of low sulfur fuel oils (LSFO) that meet the requirements for lower atmospheric
247 sulfur emissions. These new generation fuels are diverse, and their physical, chemical
248 and toxicological properties are less well understood compared to their traditional
249 counterparts. Only limited data are available about the range of properties and chemical
250 composition LSFOs can exhibit. These properties are subject to change following a spill
251 as environmental processes and weathering begin to take place. The significance of
252 these processes, especially the effect of photooxidation by ultraviolet or visible light is a
253 significant data gap.

254 Through chemical characterization, toxicity assays, and modeling, we addressed the
255 following THREE GOALS and advanced our understanding of the environmental effects
256 of LSFOs after oil spills:

- 257 • **GOAL 1: COMPARE THE TOXICITY AND CHEMICAL COMPOSITION OF
258 VLSFOs RELATIVE TO CONVENTIONAL FUEL OILS:** Low-energy water-
259 accommodated fractions (WAFs) were prepared with a set of U/VLSFO products
260 (at least 4 distinct products). These WAFs are used in toxicity assays with Atlantic
261 cod (*Gadus morhua*) larvae, American lobster (*Homarus americanus*) larvae, and
262 green-sea urchin (*Strongylocentrotus droebachiensis*) embryos, along with
263 appropriate positive and negative controls.
- 264 • **GOAL 2: INVESTIGATE HOW PHOTOOXIDATION CHANGES THE TOXICITY
265 AND CHEMICAL COMPOSITION OF VLSFOs:** The selected VLSFOs were
266 subjected to photooxidation by irradiating the oil in a full-spectrum solar simulator
267 for 18h during WAF preparation. The resultant WAFs were used in bioassays and
268 were chemically evaluated.
- 269 • **GOAL 3: EVALUATE AND COMPARE METHODS TO PREDICT TOXICITY OF
270 PHOTOOXIDIZED AND NON-PHOTOOXIDIZED LSFOs:** The relationship
271 between chemical composition toxic effects was evaluated based on a set of
272 available models.

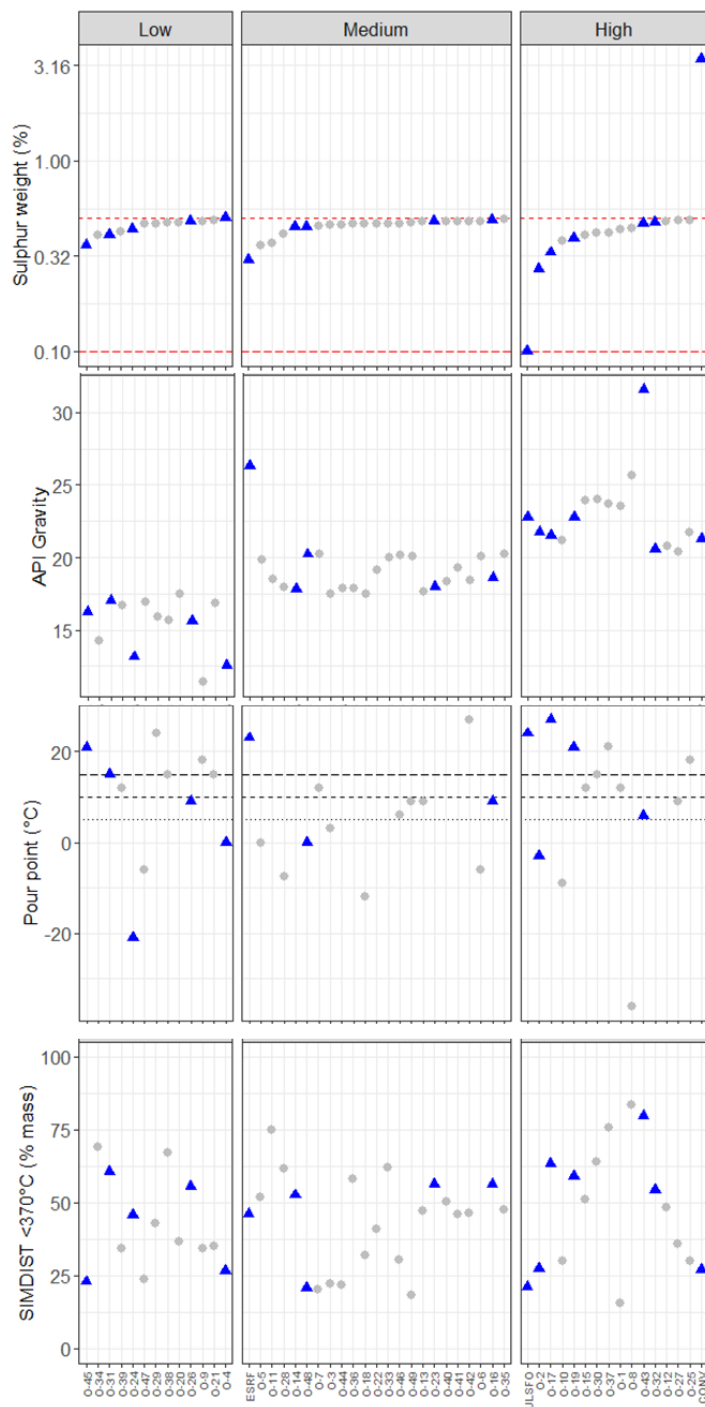
273 The toxicological effects of photooxidized and non-photooxidized oils were determined
274 on early-life stages of marine organisms, while state-of-the-art analytical capabilities were
275 be used to investigate the formation of photoproducts. Collectively these data may be
276 used to validate models which predict toxicity based on the chemical composition of the
277 product and species-specific sensitivity.

278 **2. Methods**279 **2.1. Test Materials**

280 Materials included an ultra-low sulfur fuel oil (ULSFO Shell 2019, supplied through the
281 2019 ITOPF R&D Award Winner¹ in collaboration with the Department of Fisheries and
282 Oceans Canada's Multi-Partner Oil Spill Research Initiative [MPRI] program), a
283 conventional heavy crude (CONV, sulfur content ~3.4%, also provided through MPRI),
284 and an artificially weathered (artificially weathered by nitrogen stripping until 10% loss by
285 mass) crude oil sourced from offshore Newfoundland and Labrador (ESRF, sulfur content
286 ~3%). These oils were used to optimize exposure methods and serve as a basis for
287 comparison.

288 We received an additional 49 VLSFO products from the Australian Maritime Safety
289 Authority (AMSA). The VLSFO products from AMSA were grouped according to their
290 viscosity as low (<48.5 Cst 50 °C), medium (48.5 – 125 Cst 50 °C) and high (>125 Cst 50
291 °C). Within each grouping, the percent by weight of sulfur was compared and a total of
292 14 oils were selected for additional toxicological screening based on the distribution of
293 percent sulfur, API gravity, pour point (if water temperatures are below the pour point of
294 the product it is unlikely to flow and will become solid), and the percent of mass that is
295 below 370°C in a boil point distribution (Figure 3).

¹ Sørheim, K.R., Daling, P.S., Cooper, D., Buist, I., Faksness, L., Altin, D., Pettersen, T.A., Bakken, O.M. 2020. Characterization of Low Sulfur Fuel Oils (LSFO) – A new generation of marine fuel oils. https://www.itopf.org/fileadmin/uploads/itopf/data/Documents/RDaward/Final_report_LSFO_Multipartner_3.1_.pdf



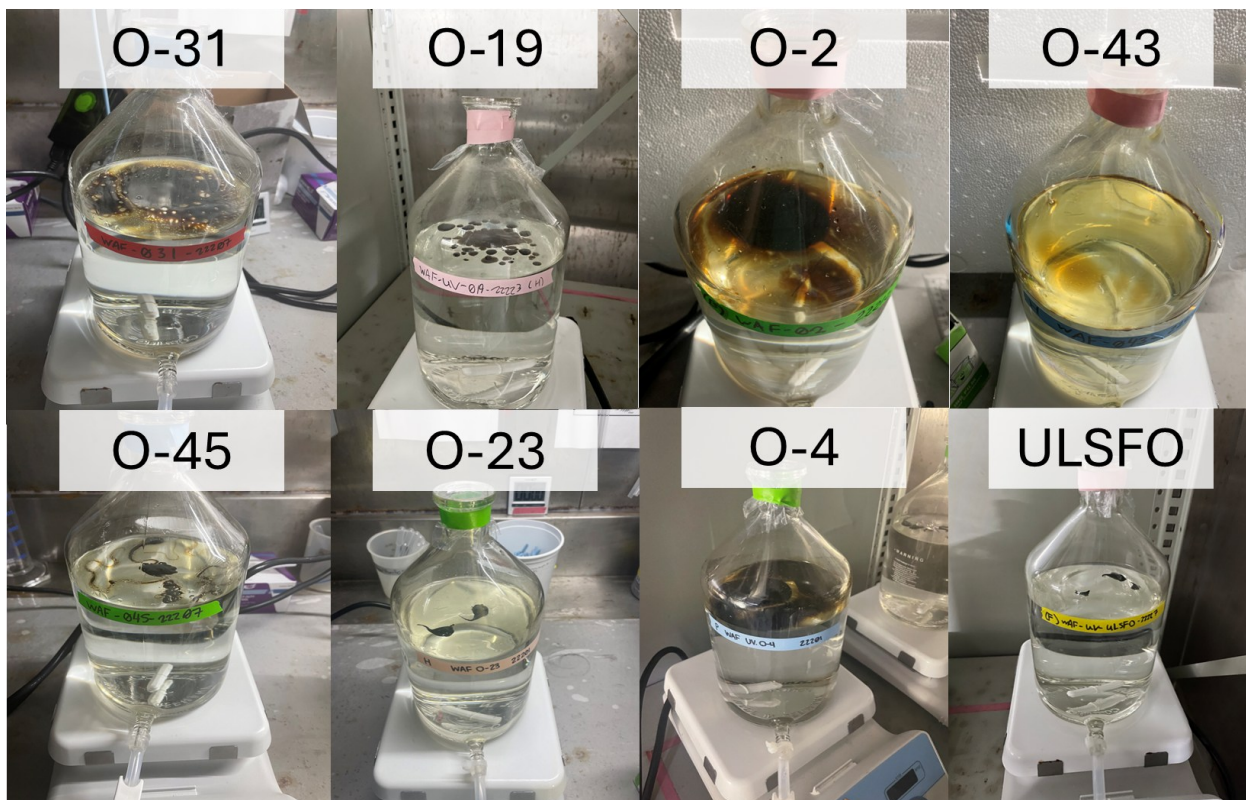
296

297 *Figure 3: Sulphur content, API gravity, pour point (showing the test temperatures employed in this study,
 298 6, 10, and 15°C) and %mass less than 370°C from simulated distillation (SIMDIST) of the 49 VLSFOs
 299 provided by AMSA, the ULSFO, and two conventional crudes (ESRF and CONV) grouped by viscosity, with
 300 the blue triangles indicating the products (n = 17) selected for toxicity screening.*

301 **2.2. WAF Preparation**

302 Low energy water accommodated fractions (WAFs) were prepared following the methods
303 described in Singer et al., (2000). In brief, a known amount of oil was added to a 2L glass
304 aspirator bottle containing 1.6 L of 0.22 μ m filtered seawater. The vessel was then set to
305 stir on a stir plate with a magnetic stir bar either under UV light or in the dark on the
306 benchtop, in an environmentally controlled room at test temperature (e.g., 6, 10 or 15 °C).
307 The WAF was stirred for 20 hours, left to settle for 4 hours and then sampled for chemical
308 analyses and use in toxicity testing. All exposures were conducted with 100%
309 concentration WAF solution.

310 Each WAF was imaged (Figure 4), and an incredible diversity of the products was
311 observed in terms of the physical appearance and behaviour, with some oils spreading
312 and forming a sheen, while others aggregate in waxy clumps.



313
314 *Figure 4: Representative WAFs displaying a range of physical appearance and behaviours upon contact
315 with seawater.*

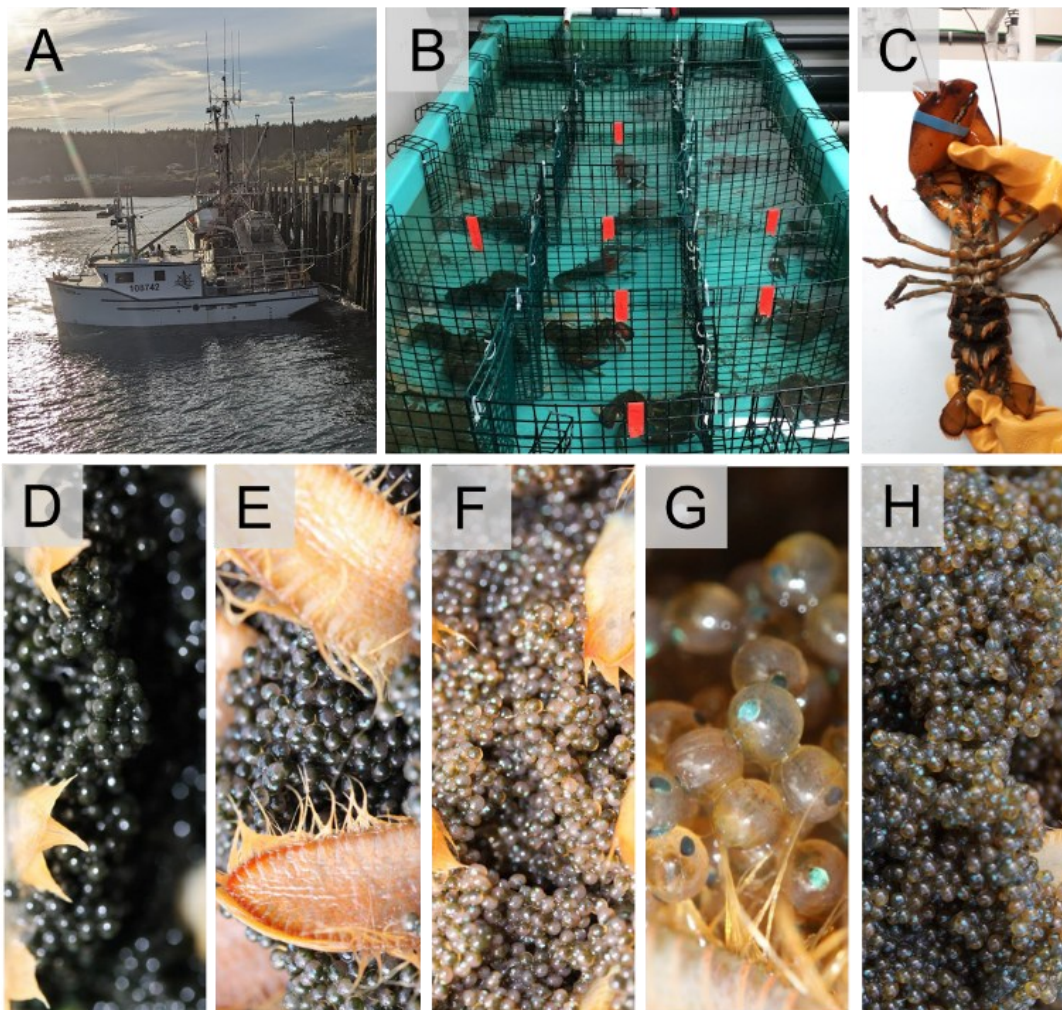
317 2.3. *UV light exposure*

318 Full spectrum light exposures (composed of both UV and visible light) were generated
319 using an Atlas Solar Constant MGH 1200 simulator (Atlas Material Testing Technology;
320 Mount Prospect, IL). The spectrum ranges from 280nm to 3000nm and is designed to
321 emulate natural sunlight. Irradiance was measured at the beginning of the UV exposure
322 near the surface of the exposure media using a model UV203-3 Irradian portable
323 radiometer (Irradian Limited, East Lothian, UK). UV doses were also be quantified using
324 a surrogate unit containing a chemical actinometer. The UV light intensity used in the
325 study was selected based on previously published literature of photo-enhanced toxicity
326 at the values recorded on a sunny summer day in St. Andrews, NB using the Irradian
327 radiometer. The radiometer measured the UV dose at the height of the oil being exposed.
328 The average values measured \pm the standard deviation were as follows: UV A = 5.43 \pm
329 1.11 W/m², UV B = 0.57 \pm 0.13 W/m², and total visible light = 55.56 \pm 5.53 W/m². Based
330 on the intensity measured (UV-A + UV-B) the total UV dose for the 18 hours of exposure
331 was 108.0 \pm 21.8 W/m² x hour.

332 2.4. *Test organism*

333 2.4.1. American lobster

334 Adult commercial size (0.5 - 2.0 kg) ovigerous ("berried") female American lobsters
335 (*Homarus americanus*) were captured by local fishers in the Bay of Fundy Lobster Fishing
336 Area 36 under authority of a Fisheries and Oceans Canada license. Upon collection,
337 females were transferred to the Huntsman Marine Science Centre (St. Andrews, New
338 Brunswick, Canada) and held in communal tanks in ambient natural seawater (8-14 °C)
339 on a 16:8 light: dark cycle. The berried females were assessed and staged for embryo
340 development weekly to predict release of larvae. Berried females with mature egg
341 clutches were transferred to an individual tank with seawater heated to 18 °C to
342 encourage synchronous larval release. Released larvae were collected daily, with freshly
343 released Stage I larvae (< 72 hours old) used for all bioassays.



344

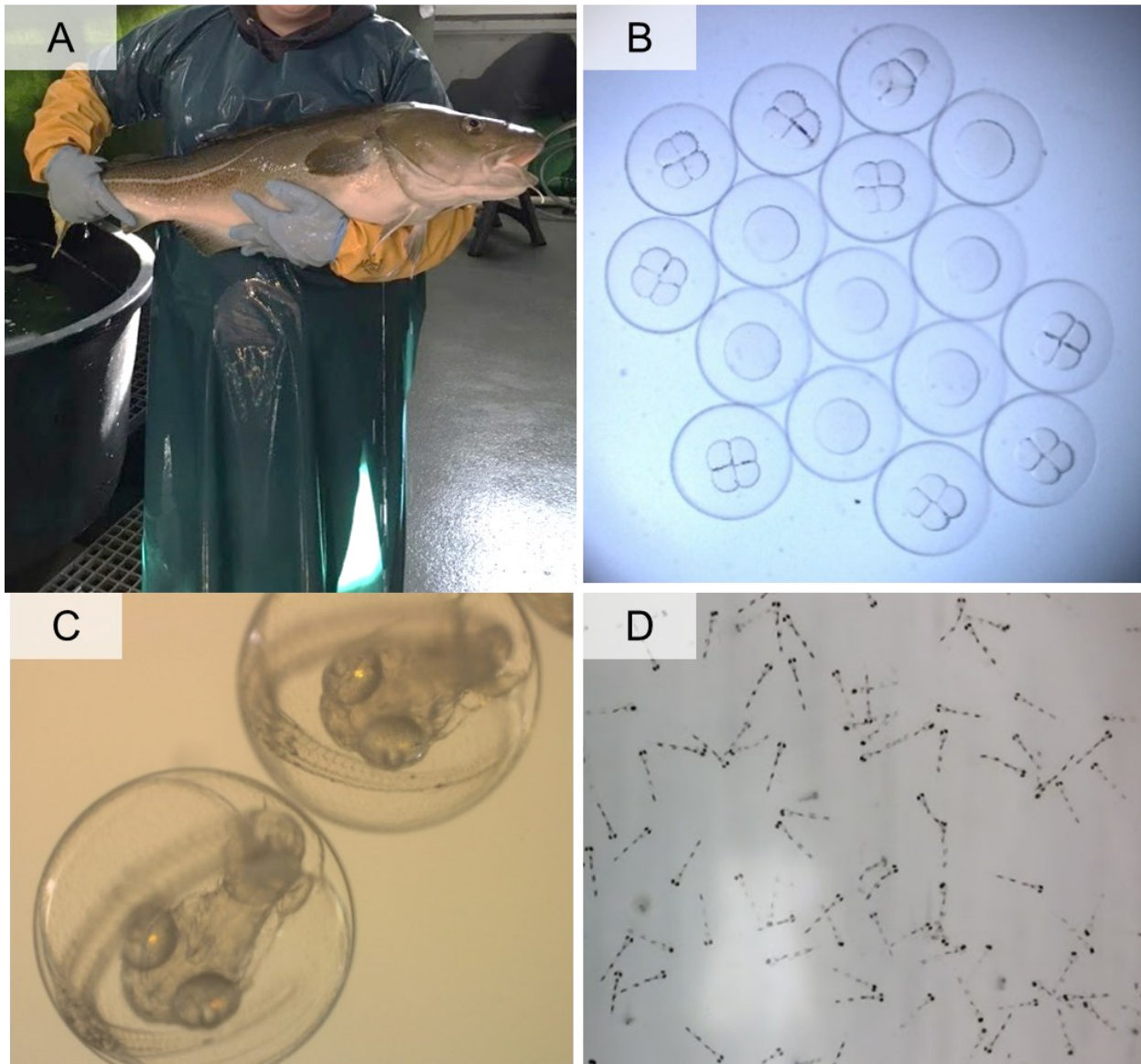
345 *Figure 5: Overview of the process of working with berried lobsters. A) Collection of lobsters from local*
 346 *fishers after receiving required permission to do so, B) holding and feeding of berried female lobsters in*
 347 *individual holding cells, C) staging and measuring the clutch to assess fecundity and development stage in*
 348 *anticipation of larval release, D-H) developmental progression of the embryos.*

349
 350
 351
 352
 353
 354
 355
 356
 357
 358
 359

2.4.2. Atlantic cod

Wild, sexually mature cod were captured August 2020 and were maintained year-round in communal tanks with flow-through natural seawater (4-14°C) and lighting to mimic ambient conditions. To obtain the embryos and larvae needed for toxicity both natural and artificial spawning methods are used. Prior to spawning, female and male fish are assessed to determine the gamete maturity. Once high-quality gametes were observed during the pre-spawning assessments, fish were handled weekly to ensure a regular supply of embryos and larvae throughout the cod spawning season (February – April). In addition to the targeted crosses made in lab, cod also spawned naturally in their holding tank and were captured using egg collectors which were monitored daily. Cod embryos are incubated without feed until hatch, after which they are fed enriched rotifers 3x daily

360 until they are used for testing. Freshly fertilized embryos (>48hrs post fertilization) and
 361 ~200 degree day larvae were used for all studies.



362
 363 *Figure 6: Overview of Atlantic cod embryo and larvae generation for toxicity testing. A) a technician*
 364 *holding a mature cod prior to gamete collection during artificial spawning procedures, B) reference image*
 365 *of cod embryos 24-48hrs post fertilization C) image of cod embryos prior to hatch, D-H) reference image*
 366 *of ~200 degree day cod larvae.*

367 2.4.3. Green sea urchin

368 Green sea urchin (*Strongylocentrotus droebachiensis*) collected from the Bay of Fundy
 369 were maintained at the Huntsman Marine Science Centre in a flowthrough system at $6 \pm$
 370 2°C to enhance gonad development and fed *ad libitum* with macroalgae (kelp or
 371 rockweed) (Figure 7).



372

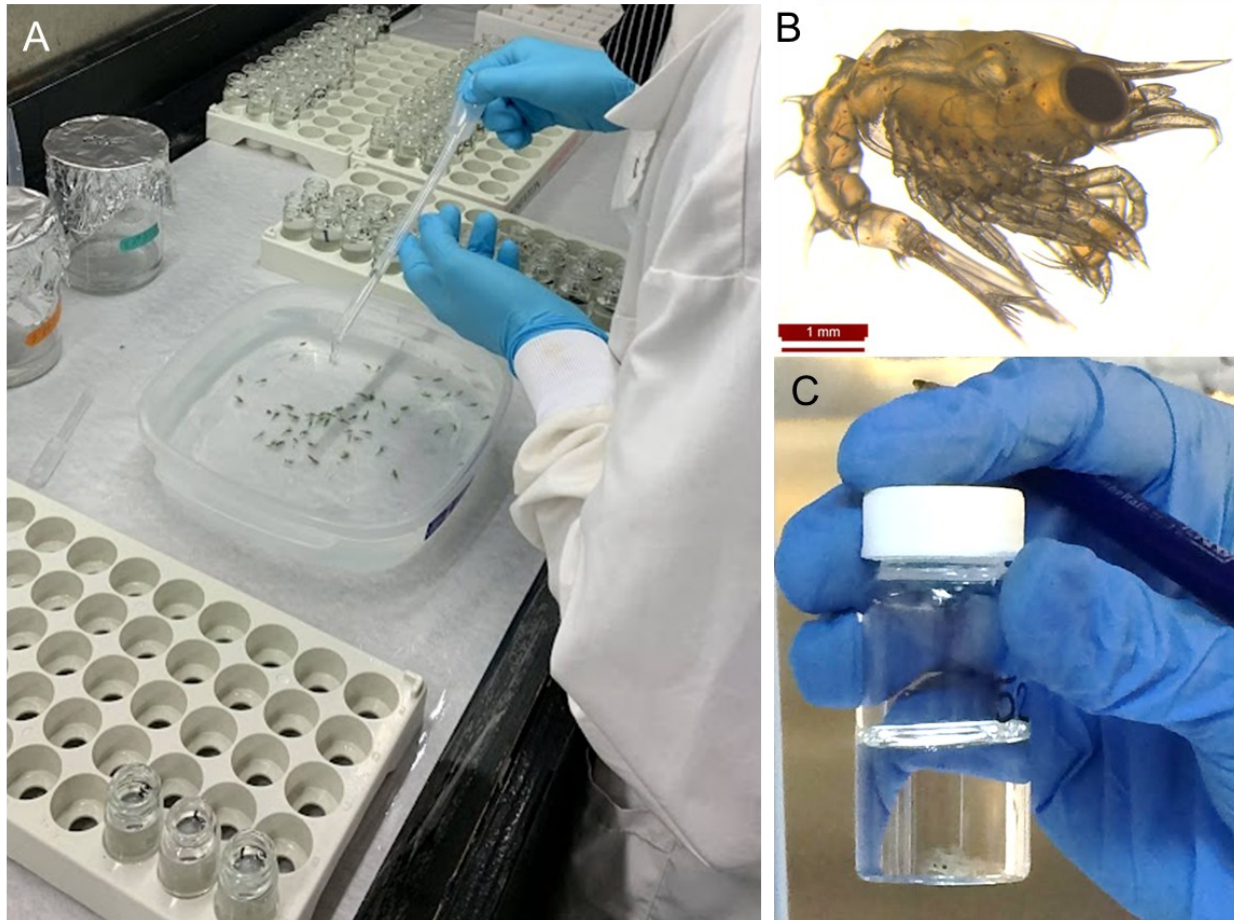
373 *Figure 7: Holding of adult urchins under “perpetual spring” conditions prior to spawning them.*

374 **2.5. Bioassay**

375 **2.5.1. American lobster methodology**

376 Bioassays were conducted in temperature-controlled chambers at 15 °C (+/- 2°C). For
377 each exposure, 20 reference individual organisms were imaged to confirm the
378 developmental stage and ensure larval size did not contribute to the observed differences
379 in toxicity. Mortality and immobilization were assessed after 24-hours of exposure
380 following the methods described in Philibert et al. (2021) and de Jourdan et al. (2022). In
381 all bioassays, water quality (pH, dissolved oxygen content, salinity and temperature) was
382 measured at test start and in pooled samples after 24 hours of exposure. Exposure media
383 was generated using low energy WAFs prepared at a loading of 1 g of oil per L of filtered
384 natural seawater. WAFs were prepared either under UV light (Full spectrum light
385 generated using an Atlas Solar Constant MGH 1200 simulator, Atlas Material Testing

386 Technology; Mount Prospect, IL) or in the dark on the benchtop. Test solutions were
 387 prepared using a gradient dilution design.



388

389 *Figure 8: Lobster testing overview A) allocating the larval lobster into exposure vessels. B) Stage I larvae.*
 390 *C) Assessing a lobster larvae in the exposure vessel.*

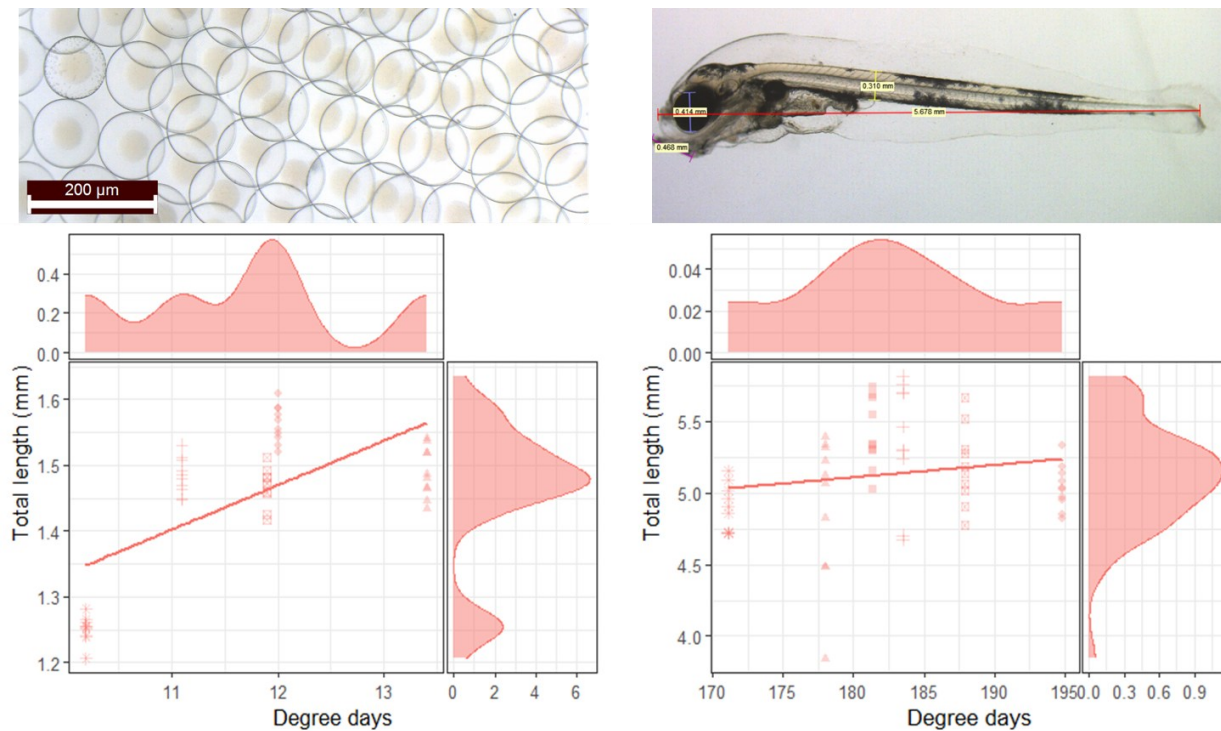
391 For all trials, exposure solution water quality (pH, dissolved oxygen content, salinity and
 392 temperature) was measured at test start and in pooled samples after 24 hours of
 393 exposure. The trial was considered valid if the control survival was greater than 80%,
 394 dissolved oxygen remained over 60% saturation, and solution temperature change
 395 remained within 1.5 °C for the duration of the trial. Trials were performed and data were
 396 collected consistent with OECD Principles of Good Laboratory Practice. All assessments
 397 were blinded to observational staff and data entry, followed by data quality control, were
 398 completed by separate staff independent of the assessments.

399 2.5.2. Atlantic cod methodology

400 Bioassays were conducted in temperature-controlled chambers at 6 °C (+/- 2°C). For each
 401 exposure, 20 reference individual organisms were imaged to confirm the developmental

402 stage and ensure embryo and larval size/quality did not contribute to the observed
 403 differences in toxicity. The age as degree days (summation of the temperature for each
 404 day post hatch) and the size distribution from each trial is shown in Figure 9.

405 For all trials, exposure solution pH, dissolved oxygen content, salinity and temperature
 406 were measured at test start and in pooled samples after 24 hours of exposure. The trial
 407 was considered valid if the control survival was met ($\geq 60\%$ for embryo and $\geq 80\%$ for
 408 larval exposures), dissolved oxygen remained over 60% saturation, and solution
 409 temperature change remained within 1.5°C for the duration of the trial. Trials were
 410 performed and data were collected consistent with Good Laboratory Practice standards.
 411 All assessments were blinded to observational staff and data entry, followed by data
 412 quality control, were completed by separate staff independent of the assessments.



413

414 *Figure 9: Distribution of the ages and sizes of the reference organisms at for each toxicity trial (different*
 415 *shapes) conducted with embryos (left) and larvae (right)*

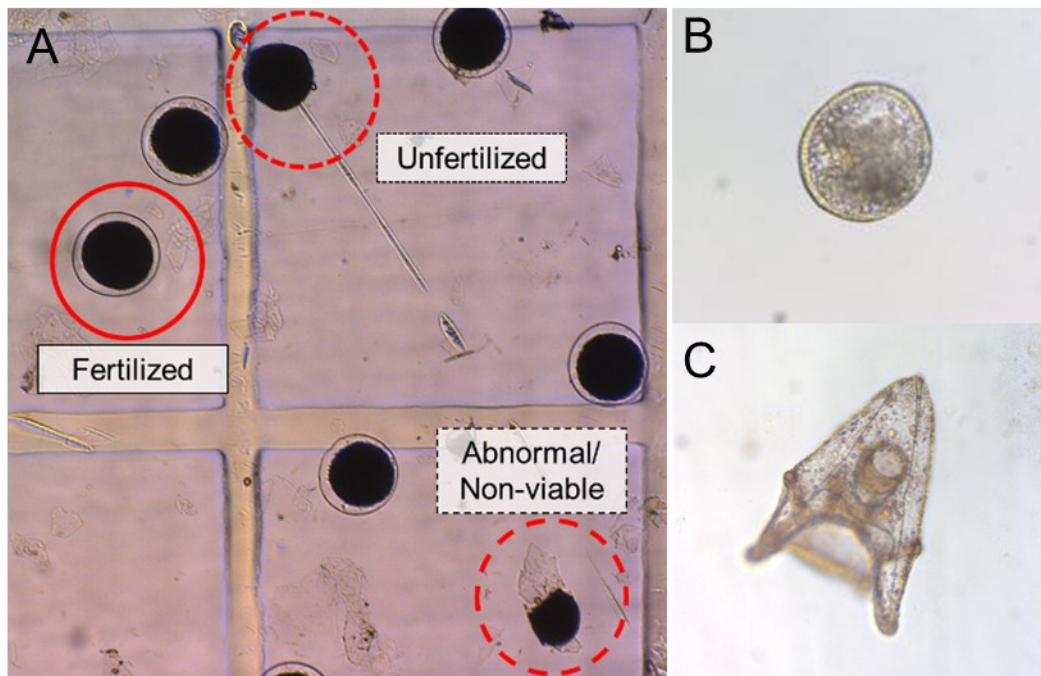
416

417 2.5.3. Green sea urchin methodology

418 To perform fertilization tests, the method described by Environment Canada (2011) was
 419 followed. Briefly, sea urchins were induced to release gametes with a 1 mL injection of
 420 1.5 M KCl. Sperm and eggs were collected and kept separated until needed. Toxicity of
 421 the WAFs was tested by exposing gametes to the dilutions (e.g., 100, 10, 1% strength)

422 plus a negative control (1.0 μ m filtered seawater) and a positive control of copper sulfate
 423 (0.038 mg/L). Each condition was replicated three times. Exposure was carried out in
 424 glass scintillation vials with a final volume of 10 mL, in an environmental chamber
 425 (temperature set at 10 ± 2 °C). Sperm was activated in each test solution (salinity 30 ± 2
 426 PSU), after 10 minutes 2000 ± 200 eggs per vial were added, and after an additional 10
 427 minutes the fertilization assay was stopped by adding 1 mL of glutaraldehyde. Fertilization
 428 success was measured by counting the number of fertilized embryos (presence of a
 429 fertilization membrane, Figure 10) in 1 mL subsample on a Sedgewick rafter slide under
 430 a compound microscope (Olympus model BH2).

431 The urchin development bioassay was conducted with the same test solutions as the
 432 fertilization. Upon confirmation of fertilization, embryos less than 2-hours post fertilization
 433 were transferred into the test solution at a loading of 20 embryos/mL (equivalent to 400
 434 embryos per exposure vessel; non fertilized eggs are transferred as well and their
 435 presence is accounted for in the final assessment). An additional set of control units were
 436 assessed daily to confirm developmental stage, and the trial was terminated when >80%
 437 pluteus was observed in the developmental check units. Upon termination of the trial, the
 438 contents of the exposure vials were assessed and scored according to developmental
 439 stage as either normal pluteus, slightly abnormal pluteus, abnormal pluteus, or affected
 440 (e.g., did not develop to pluteus).



441
 442 *Figure 10: A) Representative eggs (unfertilized) and embryos (fertilized) following a fertilization bioassay.*
 443 *B) 40 hrs post fertilization, C) ~200 hrs post fertilization showing normal development*

444 All trials were performed and data were collected consistent with Good Laboratory
445 Practice standards. All assessments were blinded to observational staff and data entry,
446 followed by data quality control, were completed by separate staff independent of the
447 assessments.

448 **2.6. Chemical characterization**

449 **2.6.1. Total Organic Carbon**

450 Total organic carbon (TOC), was measured in each WAF by an external laboratory (RPC,
451 Fredericton, NB). TOC was measured using the combustion method following the APHA
452 5310 B method. The measurement of TOC can track the presence of carbon in the water
453 even as the concentrations of measured analytes have seemingly decreased to minimal
454 levels, supporting research into new types of toxic compounds including photoproducts
455 (Lara-Jacobo et al., 2021; Heshka et al., 2022).

456 **2.6.2. Fluorometry**

457 Fluorometry data (3D excitation and emission matrix) was collected for each of the test
458 solutions both at the start and at the end of the exposure period. Fluorometry, paired with
459 PAH and alkyl-PAH measurements, provide semi-quantitative analysis of the PAC
460 content in each of the different test solutions. For this study, measurements were
461 collected with a Horiba Aqualog under the following conditions: excitation wavelengths
462 ranging from 200-800nm, an integration of 0.5s, accumulations of 1, increments of 3, CCD
463 gain was set to high, and samples were run concurrently with a 0.22 μ m filtered seawater
464 blank.

465 **2.6.3. Biomimetic Extraction using Solid Phase Microextraction**

466 A solid phase microextraction coupled to a gas chromatography-flame ionization
467 detection (SPME-GC-FID) instrument was used for biomimetic extraction (BE)
468 measurements following established protocols as described in Katz et al. 2022. Briefly,
469 portions of 20 mL sample were transferred into 20-mL headspace vials, and extracted
470 using a solid phase microextraction (SPME) fiber (30 μ m PDMS fiber; Supelco; 0.132 μ L
471 PDMS; 23Ga, yellow hub part # 57289-U), installed in an autosampler with automated
472 and temperature-controlled stirring was used (CTC CombiPAL). The extraction time was
473 100 min at 30 °C, using orbital shaking (250 rpm). A GC-FID system (Agilent 7890B)
474 equipped with an Rtx-1 column (Restek; 15m x 0.53mm i.d., 1.5um film) was used. An
475 inlet liner with a narrow diameter was used (1.8 mm, Restek Topaz; 280 °C inlet
476 temperature). The GC oven temperature was 40 °C for 3 min and then ramped to 300 °C
477 at a 45 °C/min rate. The carrier gas (He) flow was 17 mL/min. The FID trace was recorded
478 using a software (ChromaTOF, Leco). External calibration was performed using certified
479 reference material containing toluene, o-xylene, 2-methylnaphthalene, 2,3-
480 dimethylnaphthalene, and 9-methylantracene (Sigma-Aldrich Certified Reference

481 Material 42127). Serial dilutions of the calibration solution were automatically injected (1
482 μ L injection volume, using a CombiPAL autosampler). The FID signals were exported as
483 machine-readable files (CSV) using the ChromaTOF software and integrated using an R
484 script. The FID signals were baseline-corrected (to subtract the column bleeding) by fitting
485 the column bleed signal from a no-inject temperature ramp run to the BE FID signal. BE
486 calibration was performed using an external calibration using liquid injection of a certified
487 reference material containing DMA (Sigma-Aldrich 42127-2ML, Oil Sand-Affected Water
488 Calibration Standard Kit; 2,3-dimethylnaphthalene concentration 2,000 μ g/mL). Using the
489 slope from these calibration curves along with the PDMS volume of the used SPME fiber
490 (0.132 μ L), the fiber concentration of each BE sample was calculated as “ μ mol DMA
491 equivalent per mL PDMS”. All BE samples were measured in analytical duplicates.

492 **2.6.4. Gas Chromatography–Mass Spectrometry**

493 Water samples from the WAFs were sent to an external laboratory (RPC, Fredericton,
494 NB) for analytical characterization of polycyclic aromatic compound (PACs) and alkyl
495 PAHs by solvent extraction and gas chromatography–mass spectrometry (GC–MS; using
496 the method previously described in the United States Environmental Protection Agency
497 3510C/8270C document). Using the results of the water characterization, a toxic unit (TU)
498 approach was employed, where the concentration of the analytes was used to predict the
499 toxicity of the mixture. The toxicity of dissolved oil components was evaluated using an
500 additive TU model:

501
$$TU_{oil,dis} = \sum_i^N \frac{C_i}{L(E)C_{50,i}}$$
 (Eq. 1)

502 where:

503 $TU_{oil,dis}$ = dissolved phase toxic units

504 i = individual PAC

505 N = number of PACs measured in the oil

506 C_i = dissolved concentration of individual PAC, i

507 $L(E)C_{50,i}$ = dissolved LC₅₀ (lethal concentration) or EC₅₀ (effect concentration)
508 causing 50% response for each individual PAC i

510 To estimate the EC₅₀ for each measured PAC, the target lipid model (TLM) was applied.
511 The TLM posits that effect endpoints can be explained when the molar concentration at
512 a hypothetical target lipid site within the test organism exceeds a critical threshold value
513 (Parkerton et al., 2023). Based on the TLM, toxicity is described by:

514
$$\log L(E)C_{50} = -0.94 \log K_{ow} + \log \Delta c_i + \log CTLBB$$
 (Eq. 2)

515 where:

516 $L(E)C_{50}$ = lethal or sublethal molar concentration in water causing a 50% effect,
517 (mmol/L_{water})

518 K_{ow} = octanol-water partition coefficient of hydrocarbon (L_{water}/L_{octanol})

519 CTLBB = critical target lipid body burden causing a 50% effect (mmol/L_{octanol} =
520 $\mu\text{mol/g}_{\text{octanol}}$). A CTLBB for lobster of 87.7 $\mu\text{mol/g}$ octanol was applied based on
521 the 24-hour exposure data (Philibert et al. 2021).

522 Δc_i = class-specific correction. The Δc_i is required for monoaromatics ($\Delta c = -$
523 0.025), polycyclic aromatics ($\Delta c = -0.364$) and heterocycles such as thiophenes ($\Delta c = -$
524 0.412) to account for differences in partitioning between octanol and target lipid
525 (McGrath et al. 2018; McGrath et al. 2021).

526
527 The Toxic Units for each compound were calculated by dividing the dissolved
528 concentration of each hydrocarbon by the corresponding predicted effect concentration,
529 and then summing to derive $TU_{TPAH32,\text{dis}}$ (the subscript denotes the individual compounds
530 considered in the TU calculation, here the 32 analytes measured by RPC). The
531 $TU_{TPAH32,\text{dis}}$ is then multiplied by 50 in order to estimate the percent effect (e.g., a TU of 1
532 would have 50% mortality).

533 2.6.5. VLSFO Characterization

534 The products from AMSA were provided with various physical and chemical
535 characterization (3.1.1). Additional analysis included determining the UV-vis spectrum of
536 each product, and a more comprehensive analysis of the chemical components of the
537 products. GC-MS was also employed at Bigelow to examine the PAC concentration (46
538 analytes) in the source oil, and following the preparation of the WAF, both in the dark and
539 under UV. And lastly, the VLSFO samples were analyzed using comprehensive two-
540 dimensional gas chromatography coupled to a flame ionization detector (GC \times GC-FID)
541 according to Aeppli et al. (2014). Briefly, 1 μL of each sample in dichloromethane (DCM)
542 was injected in a GC \times GC-FID system with a dual stage cryogenic modulator (Leco, Saint
543 Joseph, MI), equipped with a Restek Rtx-1 first- dimension column (60 m, 0.25 mm ID,
544 0.25 μm film thickness) and a SGE BPX-50 second-dimension column (1.5 m, 0.10 mm
545 ID, 0.10 μm film thickness). The inlet temperature was held at 300 °C. The injection mode
546 was splitless, and the carrier gas was H₂ at a constant flow rate of 1.00 mL min⁻¹. The first
547 oven was programmed isothermal at 40 °C for 10 min, 40 to 340 °C at 1.25 °C min⁻¹ (held
548 for 5 min). The second oven was programmed as follows: isothermal at 45 °C for 10 min,
549 45 to 355 °C at 1.29 °C min⁻¹ (held for 5 min). The modulation period was 15 s. The
550 constituents of the source oils were identified based on their position on GC \times GC
551 chromatograms, and FID signals were integrated on the ChromaTOF software (Leco).

552

3. Results

 553

3.1. Test Material Characterization

 554

3.1.1. Physical and chemical data

 555 Physical and chemical data was made available from AMSA regarding the physical and
 556 chemical properties of these products, specifically the high temperature simulated
 557 distillation (HTSD) curves and the SARA values (SARA = Saturates, Aromatics, Resins,
 558 Asphaltenes). This data is presented in Table 1.

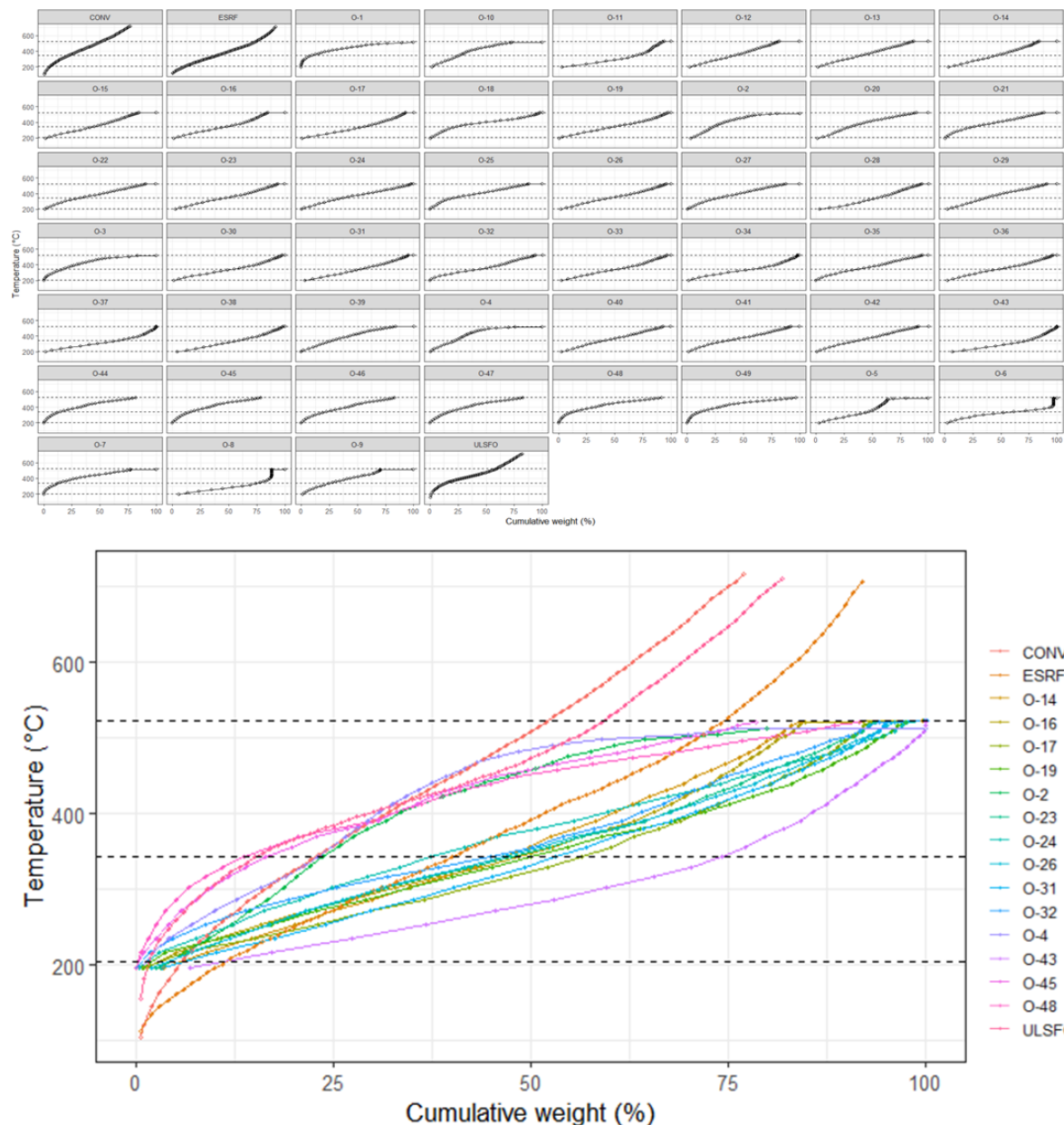
 559 *Table 1: Additional physical and chemical characterization of the source oils including simulated
 560 distillation (Sim. Dist.) and SARA (Saturates, Aromatics, Resins, Asphaltenes) analysis. The products
 561 tested in this program are shaded blue.*

Sample ID	Country Bunkered	Sulphur (% wt)	Sim. Dist. (% mass)		SARA (Saturates, Aromatics, Resins, Asphaltenes; % mass)			
			<370°C	>370°C	S	A	R	A
O-1	South Korea	0.4339	15.7	84.3				
O-2	Japan	0.27	27.5	72.5				
O-3	China	0.46	22.2	77.8				
O-4	Germany	0.5	26.5	73.5	38.4	24.5	27.6	9.4
O-5	China	0.36	51.8	48.2				
O-6	New Zealand	0.482	*					
O-7	Singapore	0.452	20.2	79.8				
O-8	Canada	0.44	83.4	16.6				
O-9	China	0.48	34.4	35.6				
O-10	Japan	0.38	30	70				
O-11	China	0.37	75	25				
O-12	Singapore	0.477	48.4	51.6				
O-13	Singapore	0.48	47.1	52.9				
O-14	Turkey	0.45	52.6	47.4	46.1	24.1	22	7.8
O-15	Taiwan	0.406	51.2	48.8	62.5	22.5	10.2	4.8
O-16	Singapore	0.49	56.4	43.6	51.9	20.2	20.2	7.6
O-17	Australia	0.33	63.2	36.8	61.8	28.2	7.6	2.5
O-18	USA	0.47	32.1	67.9	49.1	31.6	17.5	1.9
O-19	Australia	0.39	59.1	40.9	60	32.8	5.7	1.5
O-20	Singapore	0.476	36.6	63.4	51	14.3	27.1	7.6
O-21	Netherlands	0.49	35	65	51.4	17.2	22.3	9
O-22	Singapore	0.47	41	59	59.5	19.7	17	3.8
O-23	Singapore	0.48	56.5	43.5	49.9	19.3	18.2	12.5
O-24	USA	0.44	45.8	54.2	49	27.6	15.9	7.5
O-25	Turkey	0.49	29.8	70.2	61	20	15.5	3.5
O-26	China	0.48	55.6	44.4	49.2	25.9	18.5	6.4
O-27	Singapore	0.487	35.8	64.2				
O-28	Japan	0.41	61.6	38.4				
O-29	China	0.468	42.9	57.1	48.4	25.9	19.7	6

O-30	Taiwan	0.42	64	36				
O-31	USA	0.41	60.5	39.5				
O-32	South Korea	0.473	54.2	45.8	58.9	23.5	13.6	4
O-33	Sweden	0.47	62.2	37.8				
O-34	Vietnam	0.407	69	31				
O-35	Singapore	0.491	47.4	52.6	53.4	20	20.2	6.4
O-36	China	0.465	58.1	41.9				
O-37	Taiwan	0.421	75.8	24.2	61	24.9	9.6	4.6
O-38	China	0.475	67.2	32.8				
O-39	China	0.423	34.4	65.6				
O-40	Singapore	0.48	50.2	49.8				
O-41	Singapore	0.48	46.2	53.8	54.6	24.9	14.5	6
O-42	Singapore	0.482	46.4	53.6	49.8	22.5	20.7	7
O-43	Russia	0.47	79.7	20.3	77.4	15.6	6.8	0.2
O-44	China	0.462	21.6	78.4				
O-45	China	0.36	22.9	77.1				
O-46	Korea	0.47	30.3	59.7				
O-47	China	0.465	23.9	76.1				
O-48	Singapore	0.45	20.6	79.4				
O-49	Singapore	0.475	18.3	81.7				

*According to the AMSA report, sample O-6 was omitted due to the appearance of light gas oil components presumed to be from sample contamination when sampling on the vessel.

This data became available after the first year of toxicity testing was underway so it was not able to inform the initial selection of products for testing, however it was used to identify certain products that had characteristics that had not been covered in our first year of testing and allowed us to include two additional oils. We selected O-19 (high aromatic content) and O-32 (mid-range aromatic and saturates content) to ensure our dataset covered a wide range of physical and chemical characteristics. The HTSD curves (Figure 11) and the report from AMSA also indicated that O-43 is likely a misidentified oil, with AMSA suspecting that it is RMD80 and not appropriate for an RMD380 specification based on its kinematic viscosity of 6.22 cSt (in the bottom panel of Figure 11 the curve for O-43 shows 75% of the cumulative mass has been lost by 343°C). We did include O-43 in our testing initially as it was notably less viscous than our other oil samples. The information from the HTSD curves is used to highlight any trends in the tested products with respect to their likelihood of undergoing photomodification and their general toxicity, following the guidance described in Dettman et al. 2023.



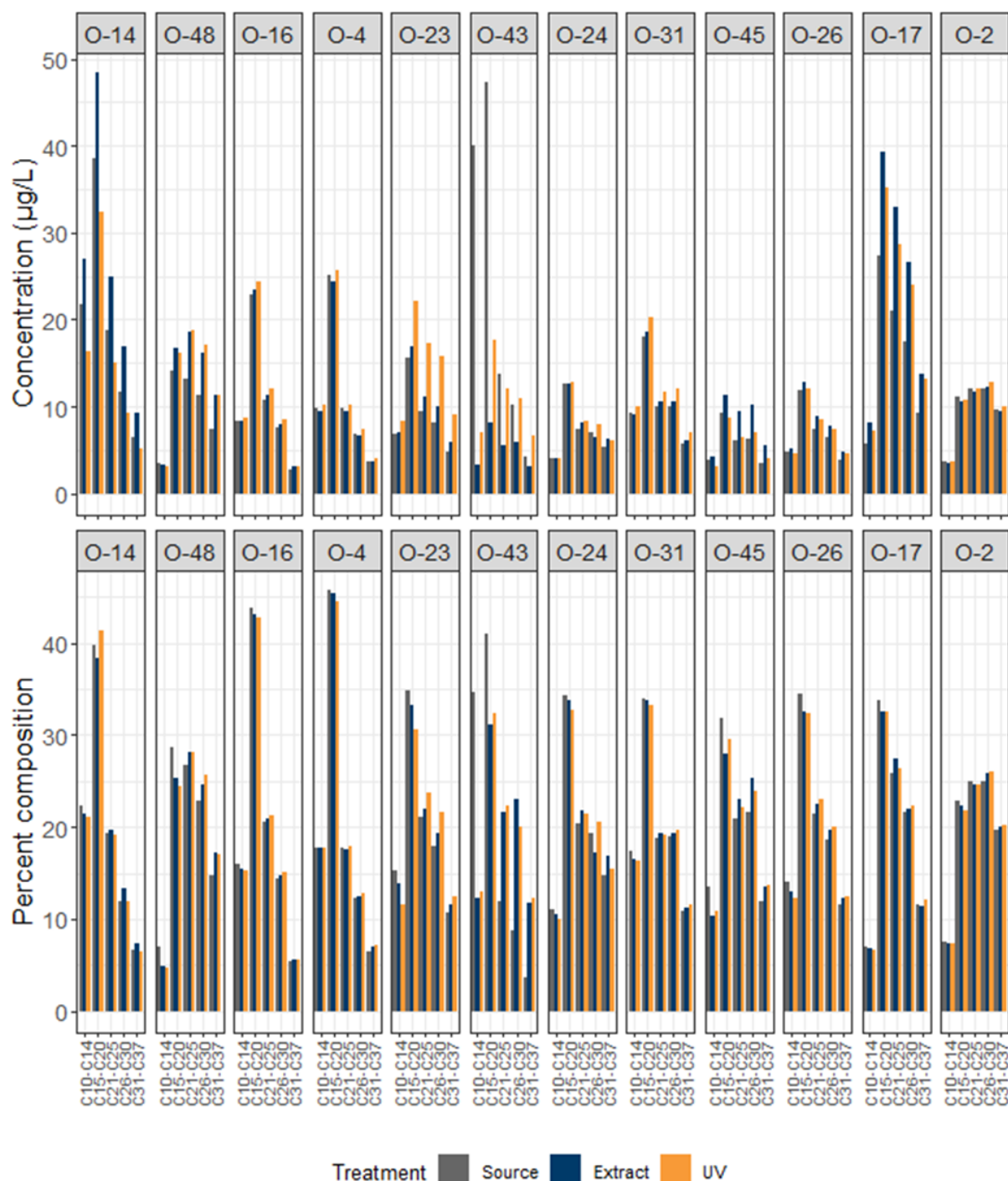
578

579 *Figure 11: (Top) High temperature simulated distillation curves for the 49 AMSA products and the*
 580 *Huntsman reference oils. The dashed horizontal lines represent the boiling point cutoffs associated with*
 581 *the C11 (204°C), C25 (343°C), and C40 (524°C) alkanes. (Bottom) Overlay of the HTSD curves for the*
 582 *products screened for toxicity with larval lobsters. O-43 (light purple) shows a distinctly different pattern*
 583 *with 75% of the cumulative mass having been lost by 343°C. Note the HTSD data for ULSFO, CONV,*
 584 *and ESRF were generated separately from the other 49 AMSA products.*

585

586 3.1.1. Gas Chromatography–Mass Spectrometry
587 Select products were evaluated for alkanes (n-C10 to n-C39 normal aliphatics), and
588 branched alkanes (pristine, phytane), and polycyclic aromatic compounds (PACs) using
589 GC-MS. These analyses were completed on the raw product (“Source”), the product after
590 making a WAF in the dark (“Extract”) and the product collected after making the UV WAF
591 (“UV”).

592 For illustrative purposes, alkanes were grouped as C10-C14, C15-C20, C21-C25, C26-
593 C30, and C31-C37 (Figure 12).



594

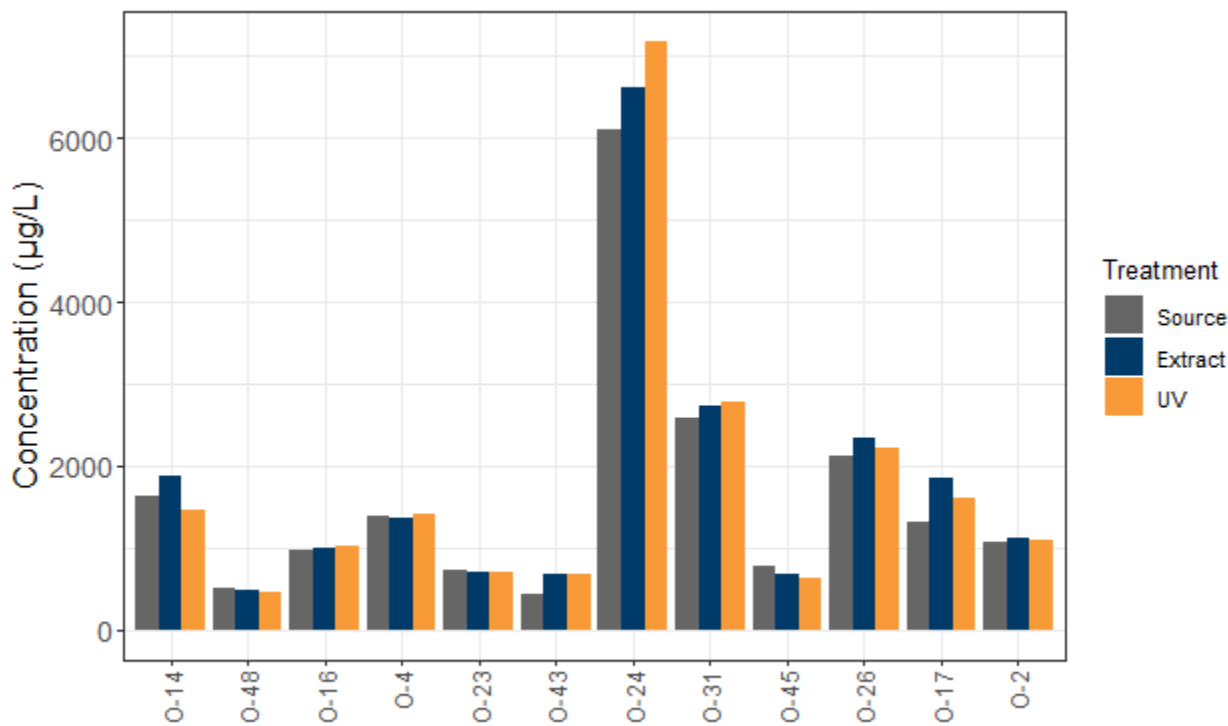
595 *Figure 12: Grouped alkane concentrations for the products, top: concentration, bottom: percent*
 596 *composition.*

597 In most cases the concentration of the alkanes was similar across treatments, with C15-
 598 C20 being the most abundant grouping, with some notable exceptions. O-4 and O-17

599 have slightly greater concentration in the oil that was collected from the dark WAF
 600 ("Extract") than the Source or UV treated oil. O-23 shows an increase in concentrations
 601 of the higher carbon alkanes (e.g., >C15) following UV treatment. O-43 shows a unique
 602 pattern where the Source oil has the highest concentration of the low weight alkanes
 603 (<C20), which are considerably reduced in both the light and dark WAF collected oil.

604 It is generally true that most oils exhibit decreasing concentrations of n-alkanes with
 605 increasing carbon number. This trend occurs because higher molecular weight alkanes
 606 are less volatile and less soluble in the lighter fractions of crude oil. Additionally, the
 607 formation of these long-chain alkanes requires specific geological conditions and longer
 608 periods, making them less abundant compared to shorter-chain alkanes. This general
 609 trend does not hold for many of the VLSFOs analyzed in this project, where the low
 610 molecular weight alkanes (<C15) are largely depleted in the samples and there is an
 611 appreciable amount of long-chain alkanes (e.g., >C30). This pattern is likely due to the
 612 blending and catalytic process used to produce these products and achieve the low sulfur
 613 requirement while meeting the RMD380 specification.

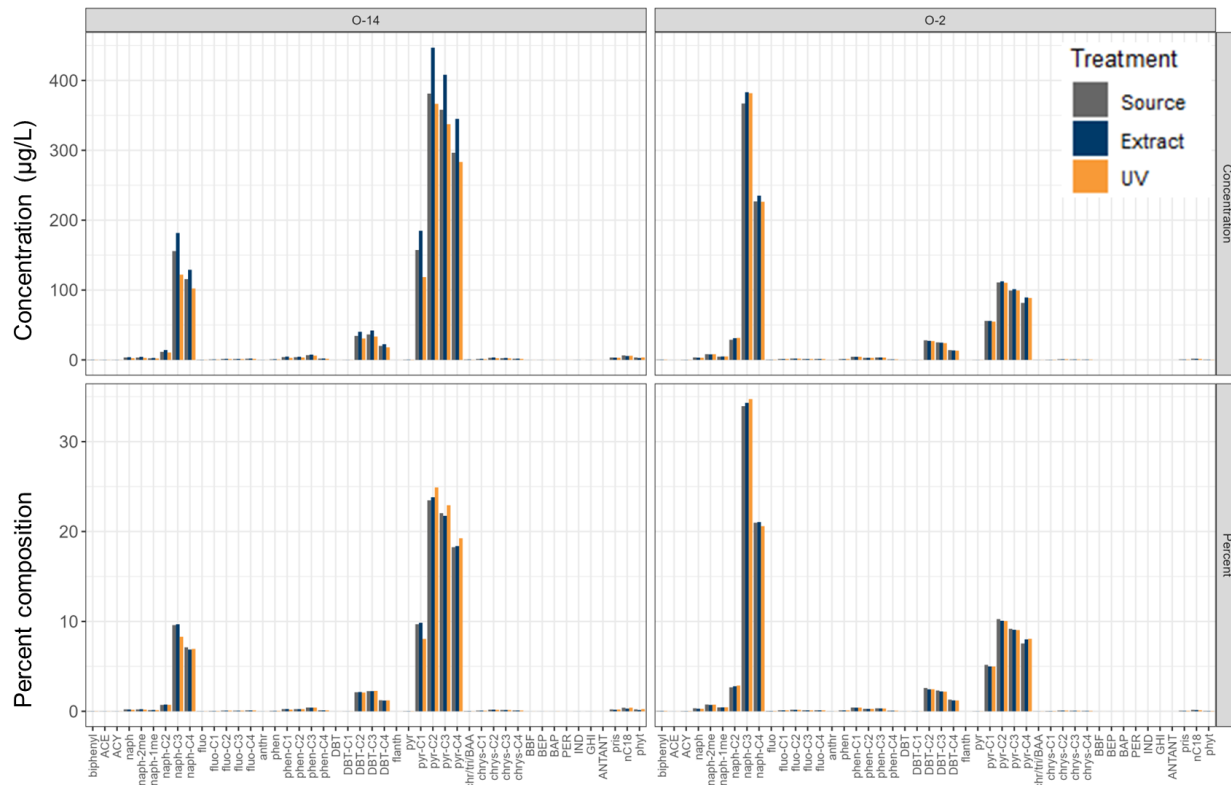
614 The products were analyzed for PACs ($n = 46$), and for visualization purposes the sum
 615 PACs are presented in Figure 13.



616

617 *Figure 13: Sum PACs for each of the examined products as the source, extract, and UV treated.*

618 The products in Figure 13 are ordered from left to right as least to most toxic to lobster
619 larvae (see section 3.3.1). The fact the O-14 (least toxic) has a greater sum PAC
620 concentration than O-2 (most toxic) highlights that sum PAC is not a reliable metric as it
621 does not consider the differences in compositional profiles and the varying toxicity of the
622 components (Figure 14).



623

624 **Figure 14: Concentration (top row) and percent composition (bottom row) of the measured PACs for two**
 625 **products, O-14 (least toxic to lobsters) and O-2 (most toxic to lobsters).**

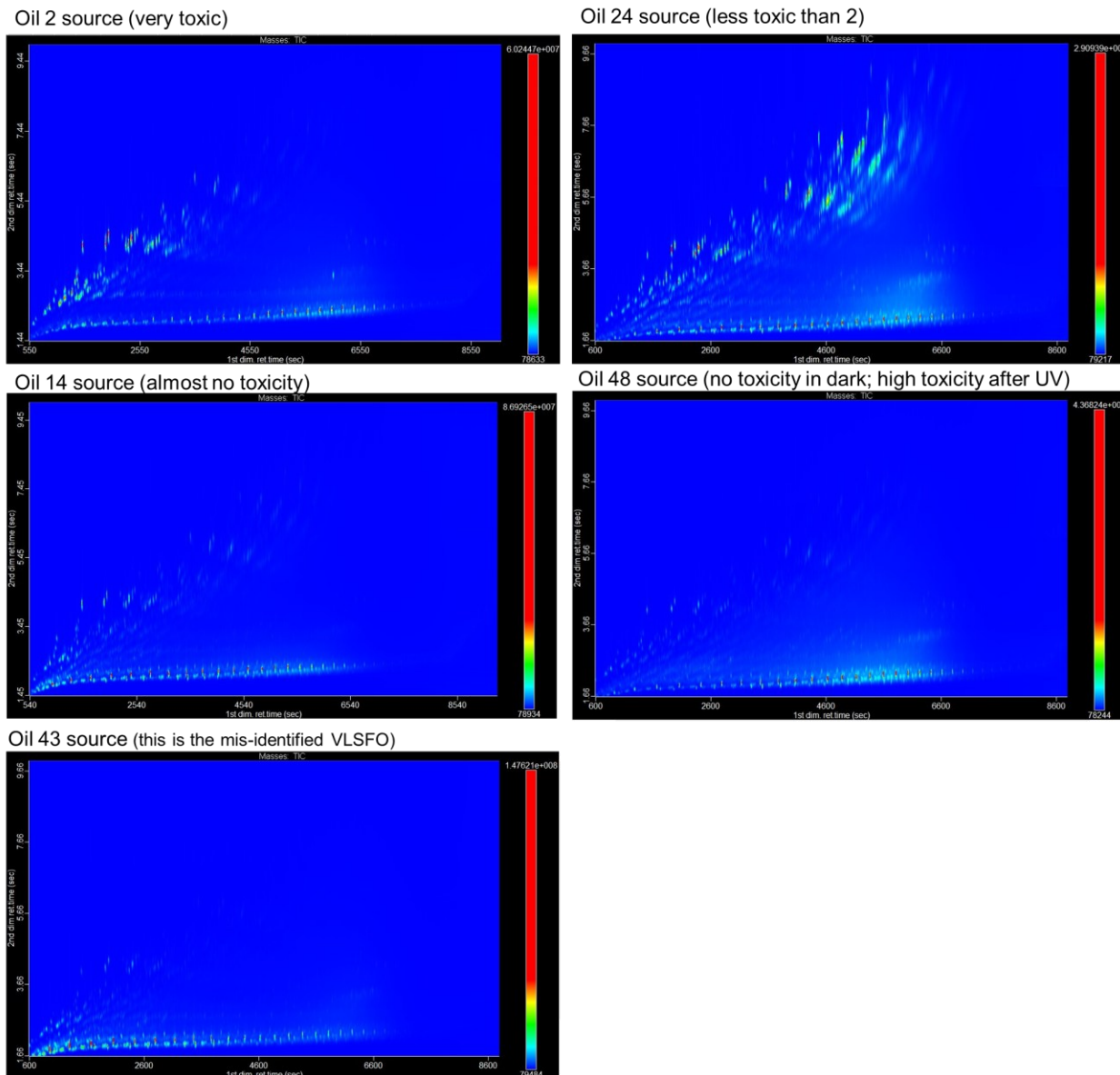
626 The main difference between the two profiles shown in Figure 14, is the relative
627 abundance of naphthalenes (C3 and C4-naphthalenes) in O-2 compared to O-14.
628 Naphthalene is more acutely toxic than pyrene (the most abundant grouping in O-14),
629 thus the greater contribution of naphthalenes in O-2 is responsible for the greater toxicity
630 observed, despite the lower overall sum PAC concentration than O-14.

631 The full suite of analytical characterization of the VLSFOs is provided in Appendix.

3.1.1. $GC \times GC$

633 The samples were analysed by GC × GC – MS, and their profiles revealed differences
634 in abundance and composition of the individual components within the product.

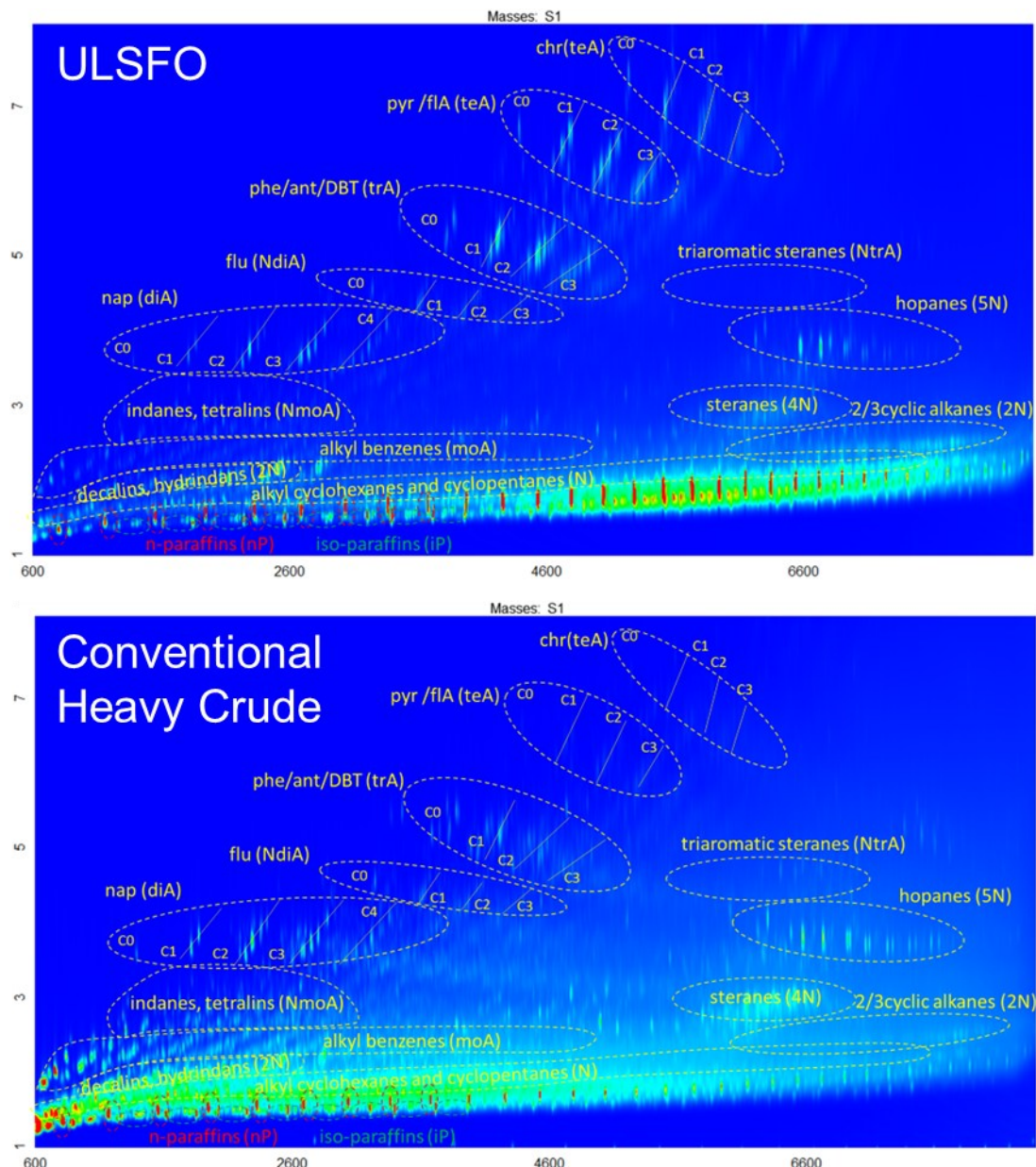
635 Representative profiles are provided in Figure 15 for products that had varying toxicity
 636 towards American lobster larvae.



637

638 *Figure 15: Representative GC × GC plots from select products demonstrating a range of toxicity*
 639 *responses.*

640 Annotation of the GC × GC profiles (Figure 16) will provide inputs for environmental fate
 641 and toxicity models which require hydrocarbon blocks or pseudo-components as their
 642 input.



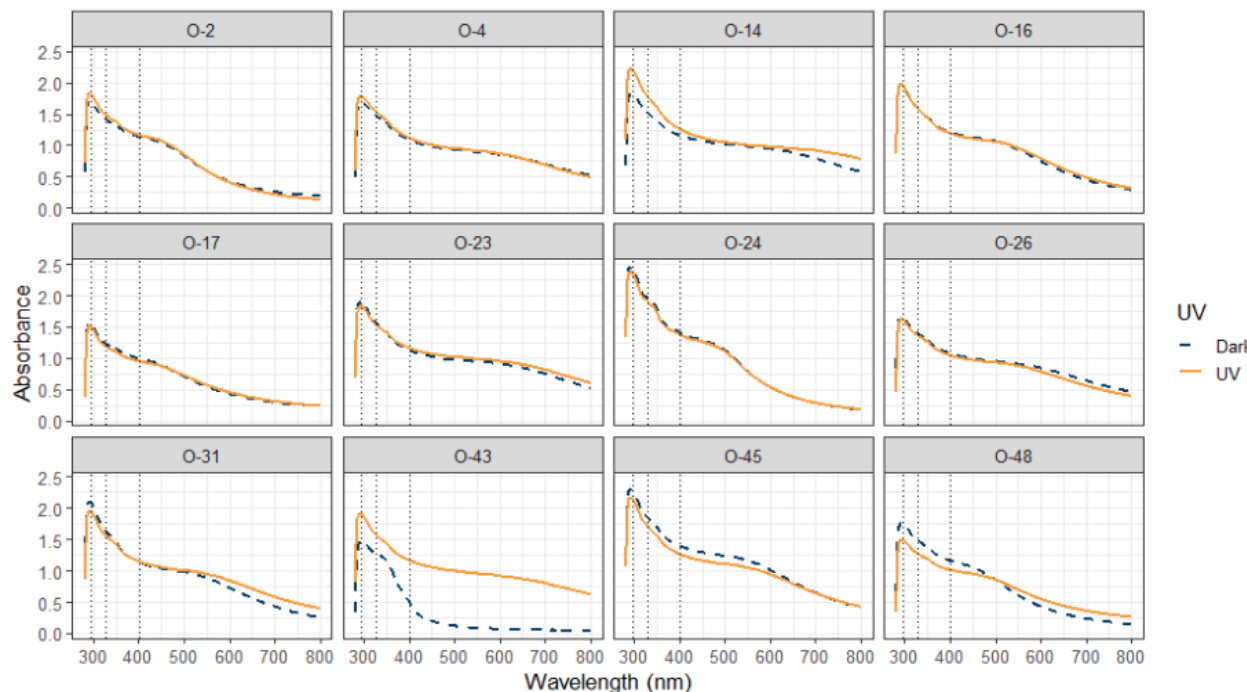
644 *Figure 16: Annotated GC × GC profiles for the ULSFO and CONV products.*

645

646 **3.1.2. UV-Vis**

647 Select VLSFOs had their UV-Vis spectra examined, for both a dark and UV irradiated
 648 sample. Each solution was analyzed on a spectrophotometer in the range of 200–800
 649 nm. Evolution of the different absorbance signals (A) in the spectra were plotted with
 650 respect to wavelength (λ) to examine changes in the shape and amplitude following UV
 651 irradiation (Figure 17).

652



653

654 *Figure 17: UV spectra profiles for 12 oils. The vertical lines 295 nm for pure phenanthrene, 328 nm for*
 655 *aromatic chromophores with three or four aromatic rings, and 401 nm for the Soret electronic absorption*
 656 *band of vanadyl porphyrins*

657 Most of the products examined showed similar profiles following irradiation, with O-14, O-
 658 31 and O-48 showing slight increases in amplitude following irradiation, while O-43 had
 659 both a different shape and amplitude following irradiation. These changes in absorbance
 660 may be an indicator of the likelihood of whether a product is likely to undergo
 661 photomodification.

662 **3.2. Impact of WAF Preparation Method**

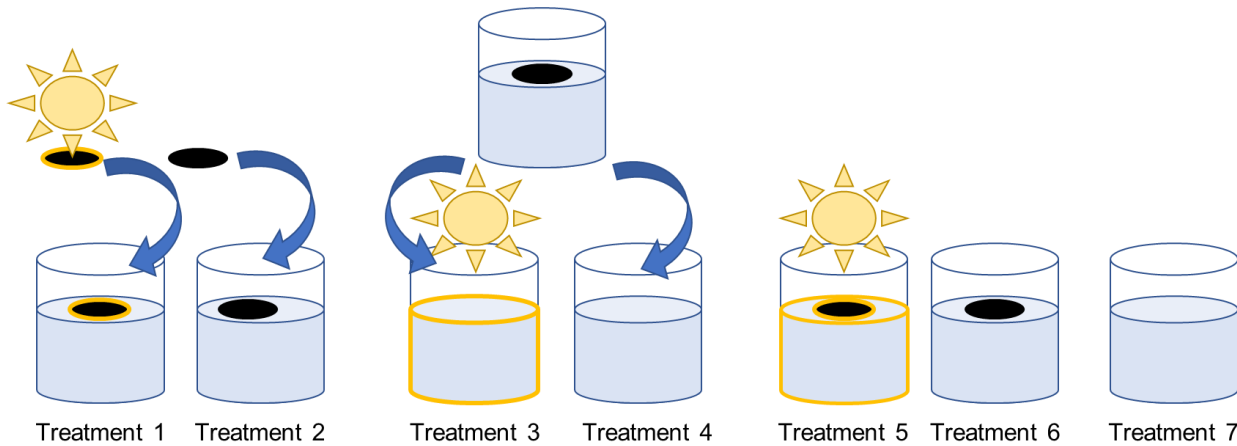
663 **3.2.1. Timing of irradiation**

664 The oil was exposed to light in multiple different steps to compare the effect of photo-
 665 modification methods on water chemistry and biological effects. We conducted two trials
 666 (one trial using ULSFO, the second trial using CONV) with the following 7 treatments
 667 (Figure 18):

668

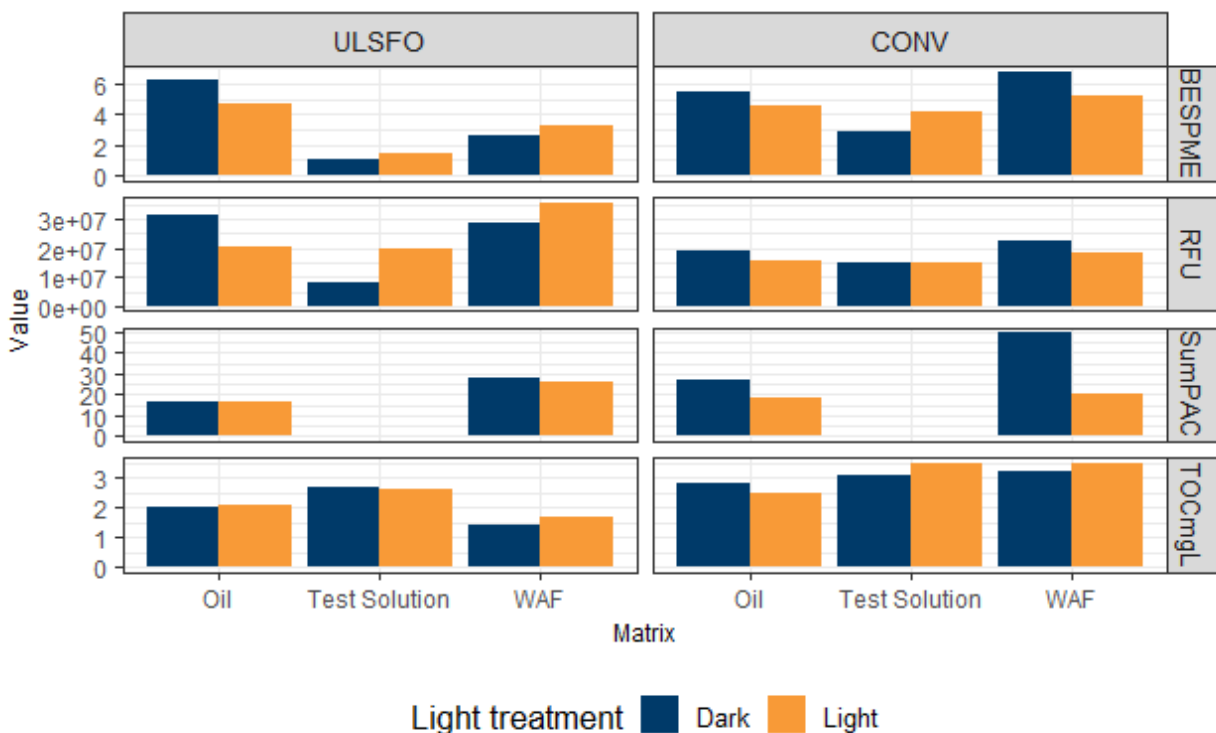
- 669 • Treatment 1 – Oil was spread to a 1 mm thick layer in a petri dish and exposed to
 UV light for 18 hours prior to WAF preparation,
- 670 • Treatment 2 – Oil was left in a petri dish with no UV light exposure,

671 • WAF was prepared on a lab bench, collected after 24 hours, and then divided into
 672 2 beakers, one beaker was placed under the UV light for irradiation (Treatment 3)
 673 and the other left without UV light exposure (Treatment 4),
 674 • Treatment 5 – WAF was exposed to UV light for 18 hours while mixing,
 675 • Treatment 6 – WAF was prepared normally on a bench without UV exposure, and
 676 • Treatment 7 – was a seawater only control.



677
 678 *Figure 18: Schematic of the various ways the 18 hour UV dose was applied to the treatments, either directly
 679 on the oil (Treatment 1), on the dissolved phase test solution (Treatment 3), or while mixing (Treatment 5).
 680 The non-UV treatments (2, 4, and 6) were treated in the same manner as their UV counterparts only in a
 681 dark location within the same room.*

682 The media generated from these trials was characterized with fluorometry and had
 683 analytical measurements of total organic carbon (TOC), PAH and alkyl-PAH (PAC; with
 684 the exception of Treatments 3 and 4 where there was not sufficient volume to complete
 685 the analysis), and biomimetic extraction solid-phase microextraction (BE-SPME). The test
 686 media was used to expose Stage I larval lobsters for 24 hours to assess their
 687 immobilization and mortality response. There was no observed toxicity in these trials and
 688 as such the focus is on the changes in concentration in the WAFs following the different
 689 UV treatments. There were changes in the measured concentrations depending on the
 690 Treatment method, the product, and the measurement method (Figure 19).



691
 692 *Figure 19: Summary of the measurements of BE (top row), fluorometry (second row), PACs (third row) and*
 693 *TOC (bottom row) following the different Treatment methods and UV irradiation.*

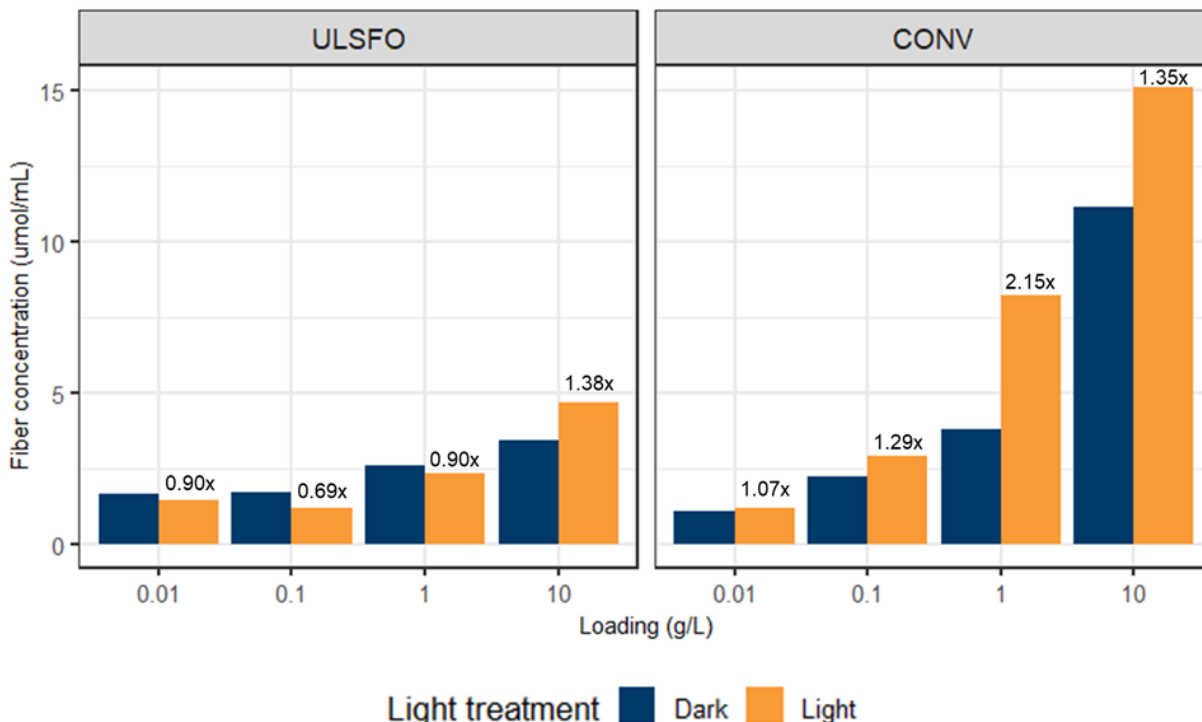
694 For consistency, volume, and relevance purposes, the method of irradiating the WAF
 695 was selected for the remainder of the testing program.

696 3.2.2. Variable loading

697 To examine the role of slick thickness and photomodification, trials were conducted with
 698 variable oil loadings of ULSFO and CONV. Duplicate WAFs were prepared with loading
 699 rates of 0.01, 0.1, 1, and 10 g/L oil, and one of each loading rate were either exposed to
 700 UV light for 18hrs while mixing or left on the lab bench without any UV light exposure.

701 There was a concentration dependent increase in BE values with increased loading, and
 702 irradiation lead to a slight (ULSFO) and larger (CONV) increase in BE values (Figure 20).

703



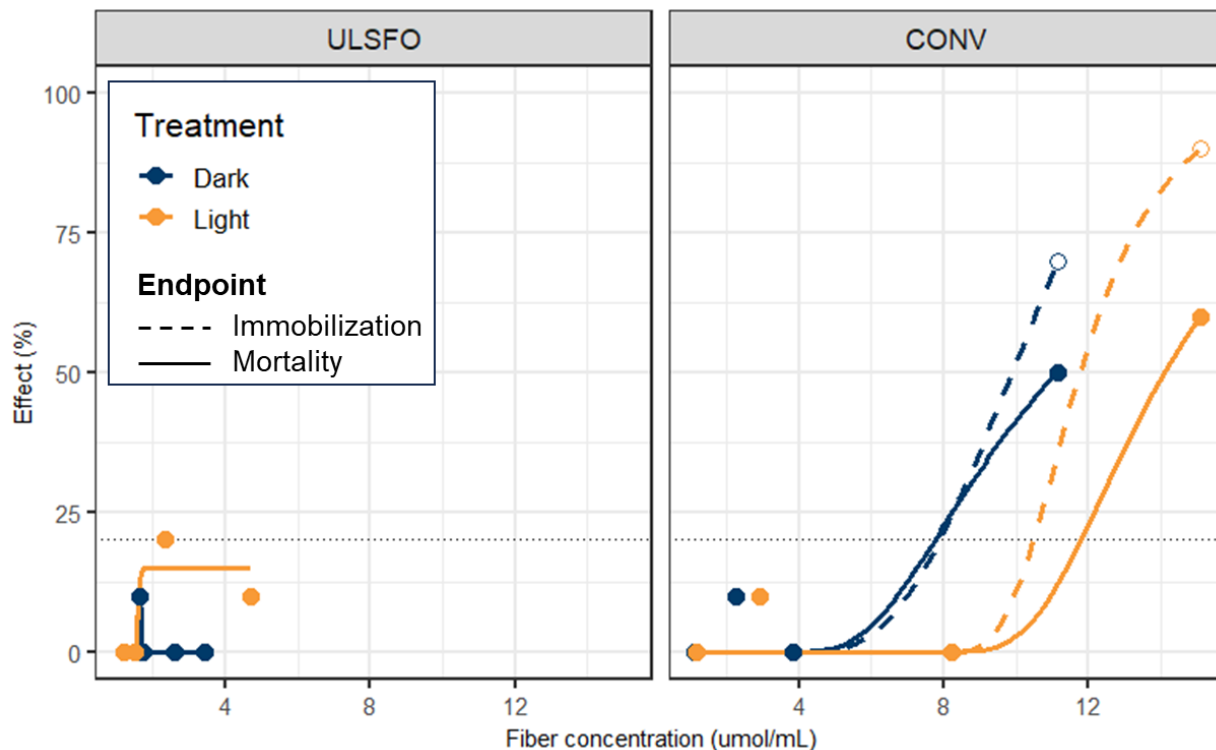
704

705 *Figure 20: BE values (fiber concentration) for the different loadings of ULSFO (left) and CONV (right)*
 706 *prepared under UV light (orange) and in the dark (blue). The numbers indicate the fold difference between*
 707 *the irradiated and dark samples.*

708 The ULSFO generally had lower BE values than the CONV, suggesting that at equal
 709 loadings there is less bioavailable material in the ULSFO preparation than in the CONV.
 710 The higher the loading, the higher the BE, and the greater the increase in BE from the
 711 irradiated sample, highlighting the importance of slick thickness for the formation of
 712 photoproducts.

713 The increase in BE values mirrored the observed toxicity in a lobster bioassay, where at
 714 the 10 g/L loading of CONV there was notable (e.g., >20%) immobilization and mortality,
 715 with the irradiated sample having greater effect (Figure 21).

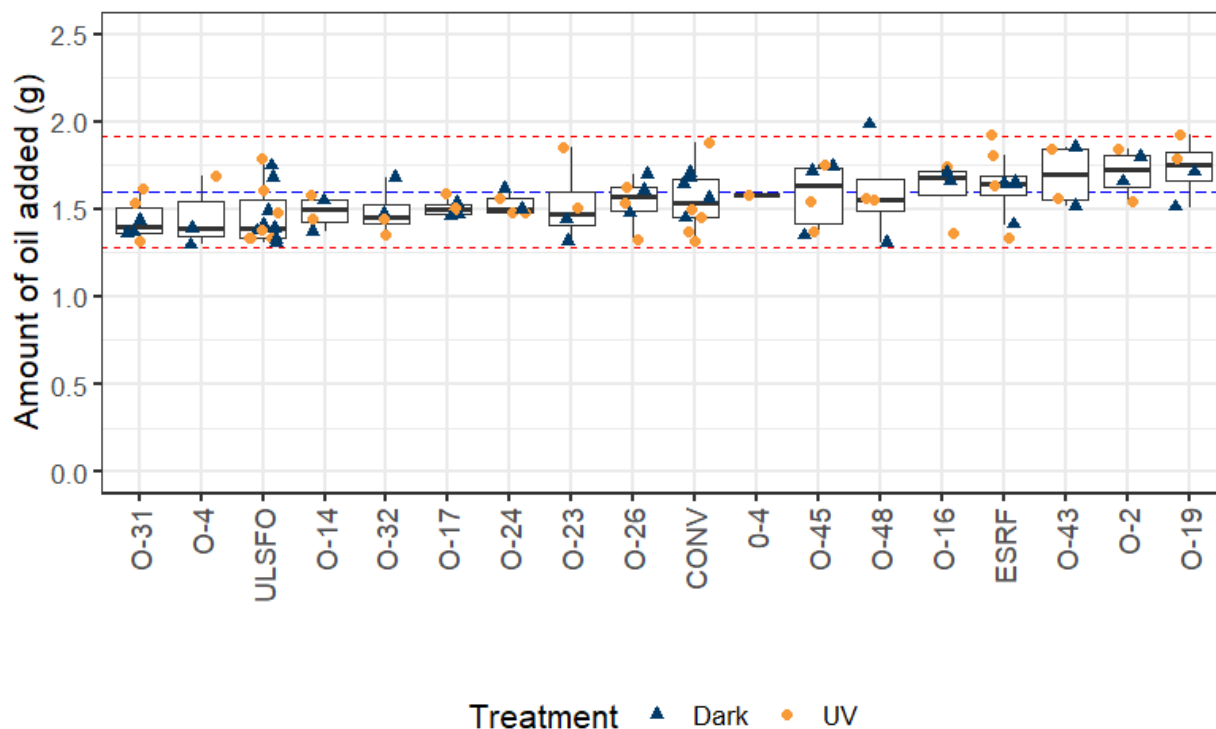
716



717

718 *Figure 21: Concentration response relationship for lobsters exposed to variable loadings of ULSFO (left)*
 719 *and CONV (right) that were irradiated (orange) or prepared in the dark (blue). The immobilization response*
 720 *is shown with open circles and dashed line, while mortality is shown with solid circles and lines, both were*
 721 *fit with a 3-parameter Type 1 Weibull model.*

722 Given the small volume of VLSFOs available, the decision was made to proceed with a
 723 single loading to maximize the amount of trials that could be conducted with an individual
 724 product. All subsequent WAFs for the toxicity testing were made with a 1 g/L loading.
 725 WAFs were made with 1.6 L of seawater, and as such the target loading was 1.6 g (+/-
 726 20%) (Figure 22). From the 150 WAFs made a total amount of 278 g of VLSFO product
 727 was utilized in this project.



728

729 *Figure 22: Amount of each product used in making the WAFs. The dashed blue line is the target loading,*
 730 *while the dashed red lines are the acceptable ranges.*

731 **3.3. Toxicity Testing**

732 **3.3.1. American lobster results**

733 WAFs were prepared at a single loading (1 g/L) under UV light and in the dark and were
 734 tested using only 100% strength solution of the WAF. The objective of this screening was
 735 to determine the relative toxicity of the different products, and to identify any products
 736 which showed a significant effect of photomodification (e.g., a change in toxicity relative
 737 to the dark preparation) (Table 2).

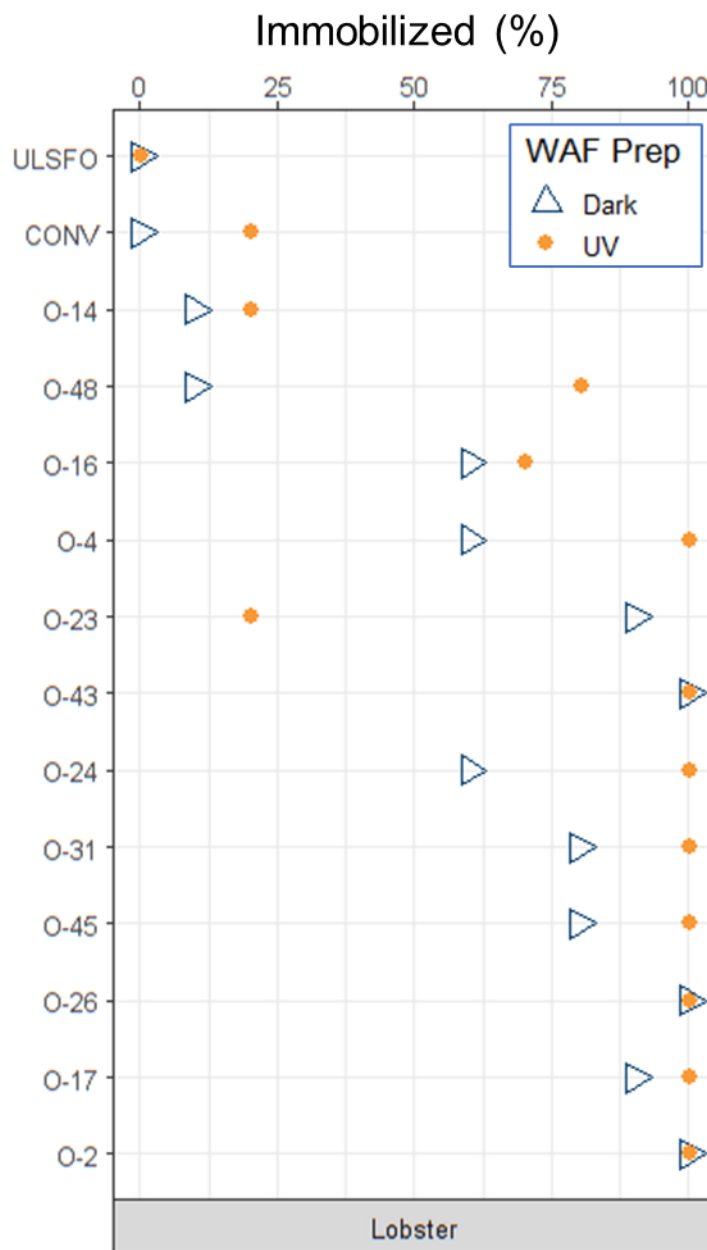
738

Table 2: Summary of lobster immobilization (Imm.) results for 2022 and the various exposure metrics. Fold change refers to the Light to Dark.

Product	UV	Imm. (%)	Fold Change	TOC (mg/L)	Fold Change	Sum RFU	Fold Change	BE SPME	Fold Change	Sum PAC (µg/L)	Fold Change	Predicted Toxic Units	Predicted Imm.	Observed - Predicted Imm.
O-43	Dark	100		2.8		4E+07		12.1		168		0.10	5	95
	Light	100	1.00	8.2	2.93	1E+08	3.09	14.7	1.22	240	1.43	0.35	18	82
O-17	Dark	90		2.6		3E+08		24.5		1053		0.80	40	50
	Light	100	1.11	3.3	1.27	3E+08	0.83	18.9	0.77	1264	1.20	0.86	43	57
O-2	Dark	100		2.5		2E+08		30.7		900		0.78	39	61
	Light	100	1.00	4.7	1.88	3E+08	1.23	30.4	0.99	1045	1.16	0.93	46	54
O-24	Dark	60		2.6		2E+08		16.0		454		2.97	100	-40
	Light	100	1.67	5.4	2.08	2E+08	1.23	28.4	1.77	702	1.55	6.16	100	0
O-16	Dark	60		2.4		1E+08		10.9		222		0.25	12	48
	Light	70	1.17	3	1.25	1E+08	0.90	10.1	0.93	219	0.98	0.23	11	59
O-48	Dark	10		2		3E+07		3.3		65		0.05	3	7
	Light	80	8.00	3.8	1.90	9E+07	3.07	5.9	1.77	133	2.04	0.35	17	63
O-26	Dark	100		5.2		3E+08		19.9		1125		2.25	100	0
	Light	100	1.00	8	1.54	3E+08	1.27	25.8	1.29	1571	1.40	4.33	100	0
O-31	Dark	80		3		1E+08		18.8		454		1.72	86	-6
	Light	100	1.25	4.7	1.57	2E+08	1.12	16.9	0.90	428	0.94	1.26	63	37
O-45	Dark	80		2.2		1E+08		9.9		243		0.22	11	69
	Light	100	1.25	4.7	2.14	2E+08	1.87	0.00		420	1.73	0.79	40	60
O-23	Dark	90		1.9		7E+07		4.0		273		0.18	9	81
	Light	20	0.22	1.9	1.00	6E+07	0.90	6.7	1.68	278	1.02	0.18	9	11
O-14	Dark	10		2		7E+07				326		0.18	9	1
	Light	20	2.00	2.5	1.25	9E+07	1.17	9.5		315	0.97	0.19	9	11
O-4	Dark	60		2.6		8E+07		8.6		153		0.11	6	54
	Light	100	1.67	2.9	1.12	1E+08	1.46	9.6	1.12	229	1.50	0.19	10	90
ULSFO	Dark	0		2		2E+07		2.6		17		0.05	2	-2
	Light	0	-	4.6	2.30	2E+07	1.53	2.3	0.90	33	1.89	0.04	2	-2
CONV	Dark	0		2.1		3E+07		3.8		22		0.03	1	-1
	Light	20	-	2.3	1.10	2E+07	0.66	8.2	2.15	16	0.74	0.13	6	14

739

740 In nearly all cases there was an increase in toxicity following UV irradiation (Figure 23),
 741 which was mirrored by increases in the various exposure metrics (TOC, RFU, BE-SPME
 742 and PAC). Using the PAC data the Toxic Units (TU) were calculated, and the predicted
 743 toxicity (as immobilization) was compared to the observed response. The TU approach
 744 was able to predict the toxicity within +/- 20% for 12 of the 28 products, however it
 745 generally was underpredicting the toxicity of the VLSFOs both with and without UV.



746

747 *Figure 23: Visual summary of the lobster immobilization response for the 2022 exposures to irradiated (solid
 748 orange circles) and non-irradiated (open blue triangles) WAFs.*

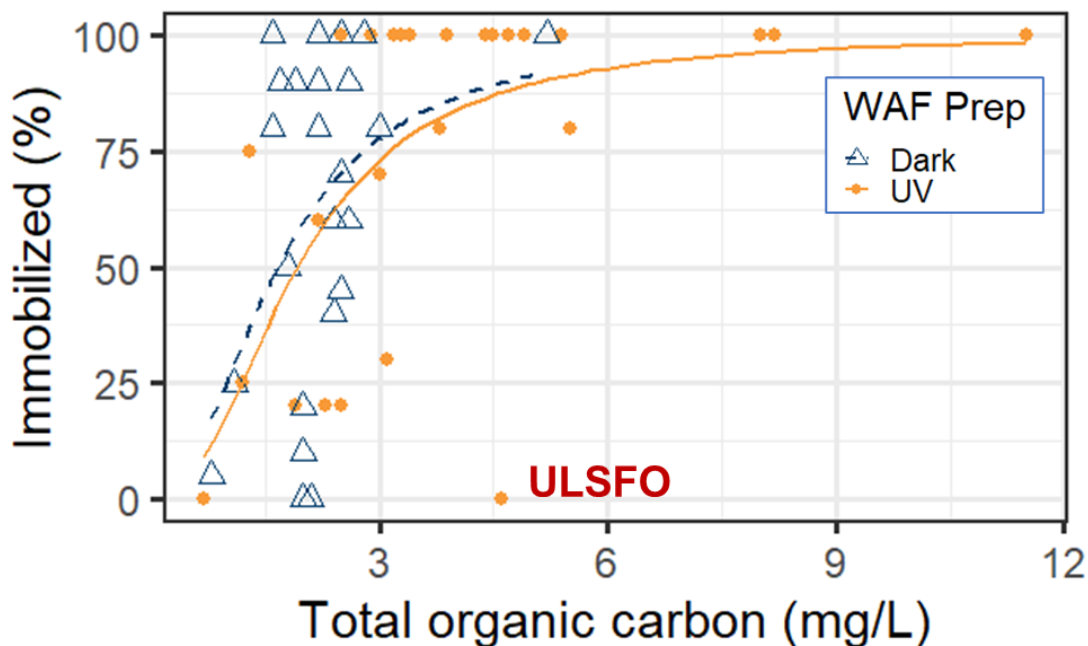
749 In 2023, two additional products, O-19 and O-32, were selected for testing based on their
 750 physical properties, specifically SARA. The other products that were selected for re-
 751 testing included fuels that saw 100% immobilization in the UV treated WAFs including O-
 752 2, O-4, O-17, O-24, O-26, O-43 and O-45, and the product O-23 which saw greater toxicity
 753 in the dark WAF (90% immobilization) than in the one prepared under UV (20%
 754 immobilization). As the products which had 100% immobilization were unable to discern
 755 how much toxicity was being “added” due to photo-modification, a dilution series was
 756 prepared from each WAF such that the 100, 10 and 1% strength were tested. In nearly
 757 each case, the dilution range proved too wide, as at the 10% strength there was minimal
 758 toxicity for most products. The notable exception was O-43 which saw sustained toxicity
 759 in the UV treated WAF even at 1% strength (90% immobilization, Table 3).

760 *Table 3: Summary of the O-43 testing with larval lobster in 2023*

Percent	UV	Immobilized (%)	RFU
1	Dark	0	3,206,626
	UV	90	4,336,892
10	Dark	0	8,040,701
	UV	90	24,622,922
100	Dark	40	40,920,218
	UV	100	220,328,001

761
 762 The fluorometric signal for the UV treated O-43 WAF was ~5.4 times greater than its dark
 763 counterpart. The 10 and 1% strength UV solution had a lower fluorometric signal than the
 764 100% strength Dark WAF yet produced a significantly greater immobilization response.
 765 This suggests that the photo-products formed in the during the irradiation of O-43 are not
 766 detectable by fluorometer (e.g., addition of an oxygen atom will often decrease
 767 fluorescence of aromatic compounds). The 100% strength sample of UV treated O-43
 768 WAF also showed the greatest increase in TOC (4.8 x) and BE-SPME (2.29 x) across all
 769 products tested, suggesting that this product is highly photo-reactive, and based on the
 770 results of the lobster (and cod, see section 3.3.2.2) bioassay the products formed are very
 771 toxic.

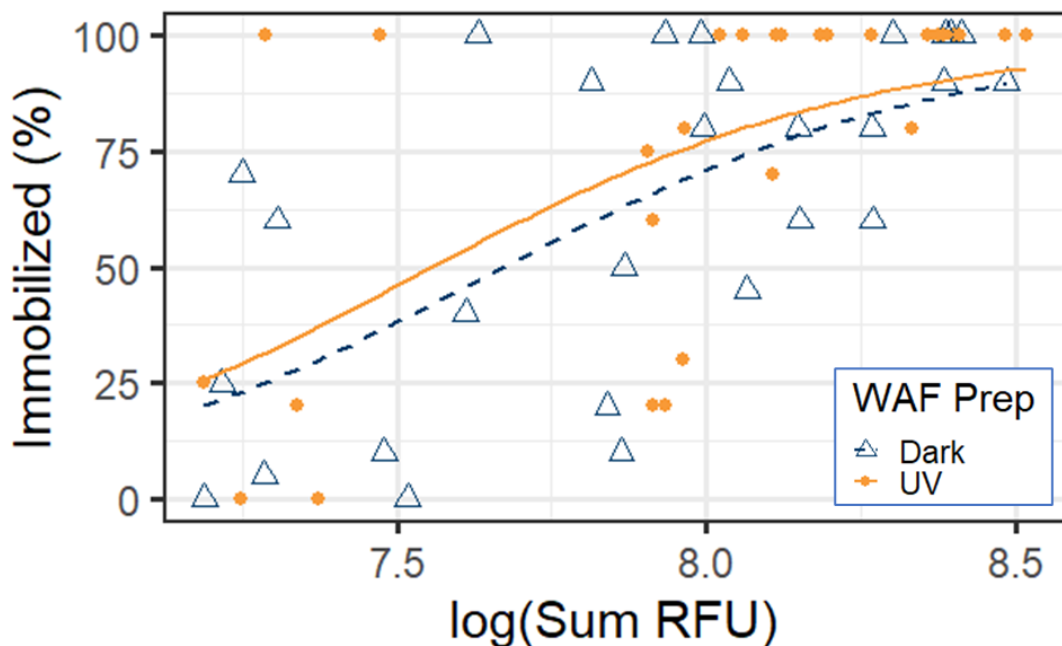
772 The lobster data from 2022 and 2023 were combined to model the relationship between
 773 the exposure metrics, TOC (Figure 24), RFU (Figure 25), BE-SPME (Figure 26), PACs
 774 (Figure 27), and TUs (Figure 28), and immobilization.



775

 776 *Figure 24: Concentrations of total organic carbon (TOC) and the lobster immobilization response.*

777 TOC concentrations generally had a consistent relationship with immobilization, where
 778 increasing concentrations of TOC (especially above 3 mg/L) resulted in nearly complete
 779 immobilization. However, the lack of resolution in this measurement and its non-specificity
 780 may limit its widespread adoption for predicting toxicity outside of a laboratory setting.
 781 The irradiated ULSFO result is unexpected, showing a 2.3-fold increase in TOC relative
 782 to the dark preparation, but no change in toxicity (a similar result was observed in the
 783 Atlantic cod trials, Table 4). This highlights a challenge in the non-specificity of TOC as it
 784 cannot be assumed that all photoproducts that are formed are equally toxic, and in the
 785 case of ULSFO where there was a notable increase in TOC, these products did not
 786 contribute to toxicity.

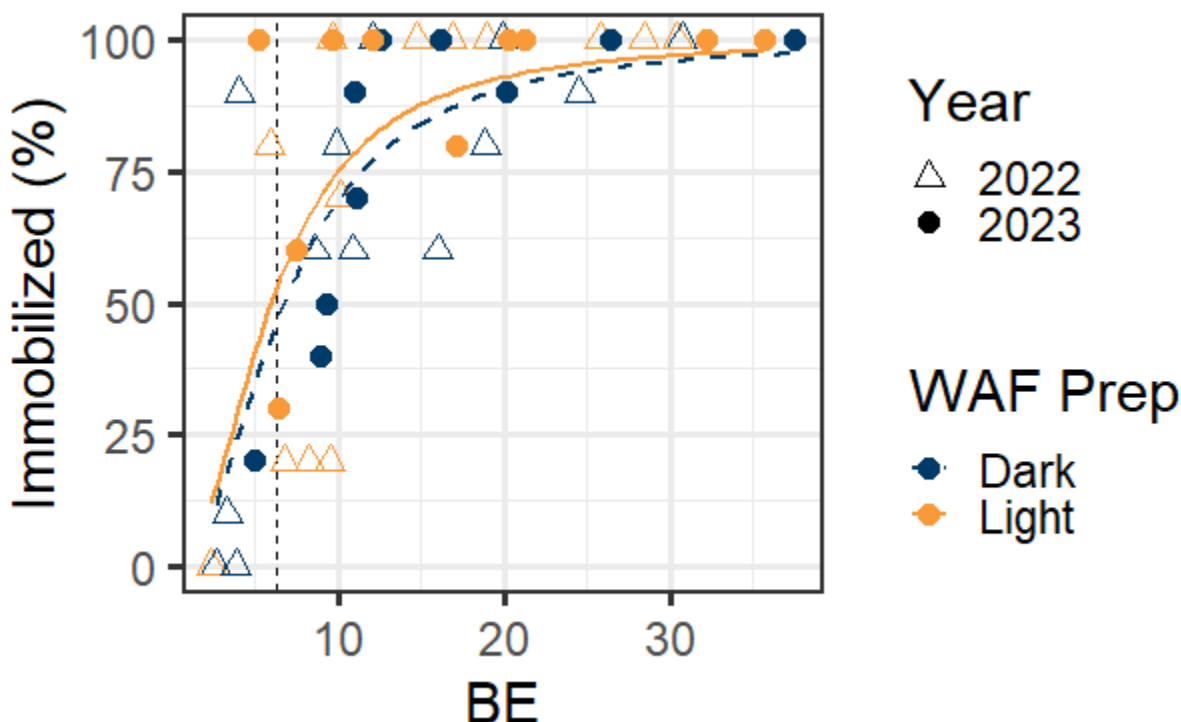


787

Figure 25: Relative fluorescence units (RFU) and the lobster immobilization response.

Fluorometry proved to be quite variable in being able to describe the observed toxicity and may not be a reliable predictor of observed toxicity in lobsters. This may be due to the presence of compounds in the VLSFOs (both the dark and irradiated) that are not detectable by fluorometry but contribute to the observed toxicity.

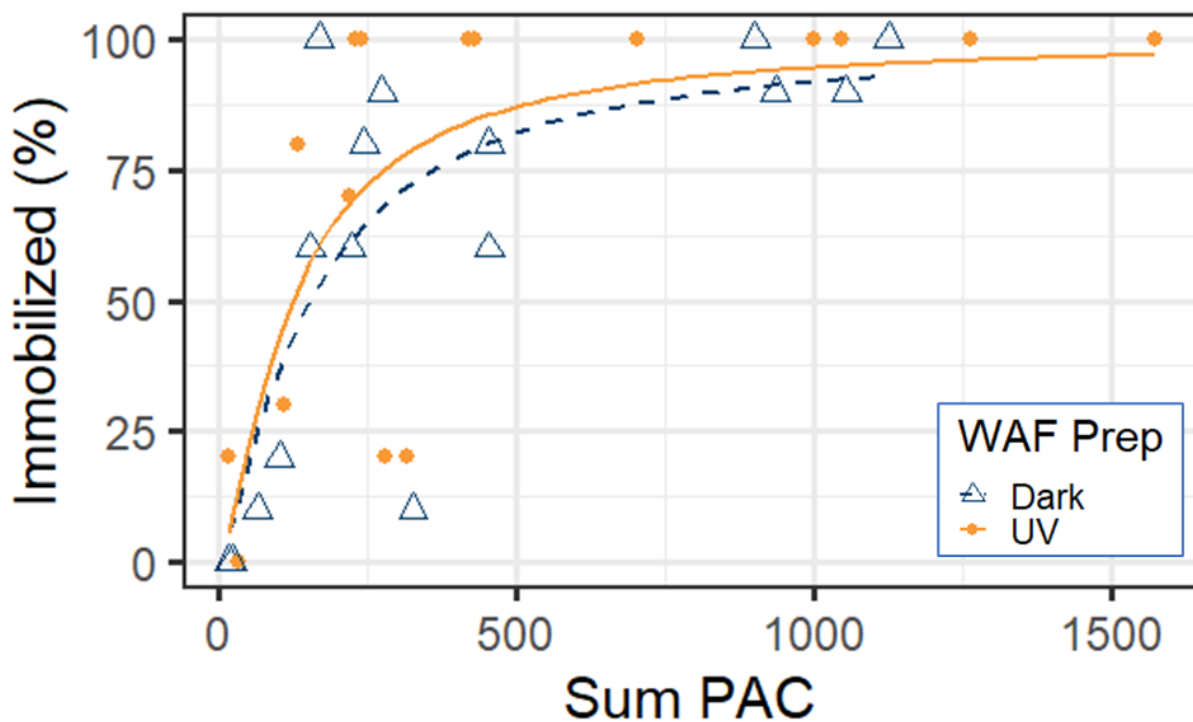
793



794

795 *Figure 26: Summary of the larval lobster immobilization response data following 24-hour exposure to*
 796 *irradiated (orange) and non-irradiated (blue) WAFs in the 2022 (open triangles) and 2023 (filled circles)*
 797 *testing season. The dashed vertical line is the calculated BE-critical value of 6.3 $\mu\text{mol per mL PDMS}$.*

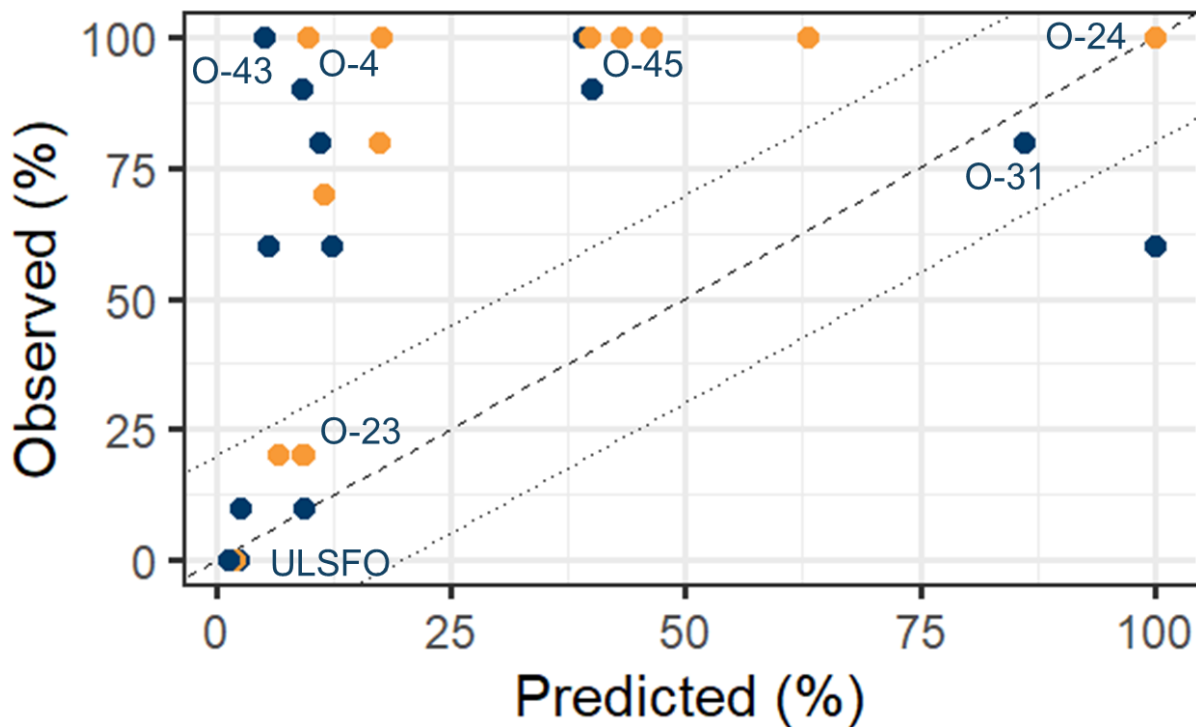
798 When comparing the lobster results from 2022 (circles) to 2023 (triangles), there was very
 799 good agreement between BE values and toxicity, which supports the derivation of a BE-
 800 critical value (value that corresponds to 50% mortality, analogous to an LC50 value with
 801 the exposure metric expressed as a fiber concentration, rather than a water
 802 concentration), that can be used to reasonably approximate the toxicity of an unknown
 803 WAF, and potentially an environmental sample, to American lobster larvae. The lobster
 804 BE-critical value was calculated as a fiber concentration of 6.3 $\mu\text{mol per mL PDMS}$ (0.7
 805 standard error) and can be used to compare sensitivity across species.



806

807 *Figure 27: Sum of the polycyclic aromatic compounds (PAC) and the lobster immobilization response.*

808 The immobilization response increases with increasing sum PAC concentrations,
 809 however there are a few instances where the immobilization response is less than would
 810 be expected for a sample with that sum PAC ($\mu\text{g/L}$) value. This is largely due to the
 811 varying toxicity of the different PACs within that summary metric of sum PAC (or total
 812 PAC), where the contribution of each PAC towards toxicity is considered equal. The toxic
 813 unit approach accounts for the composition and concentration of the PACs in the mixture
 814 and allows for the prediction of toxicity (Figure 28).



815

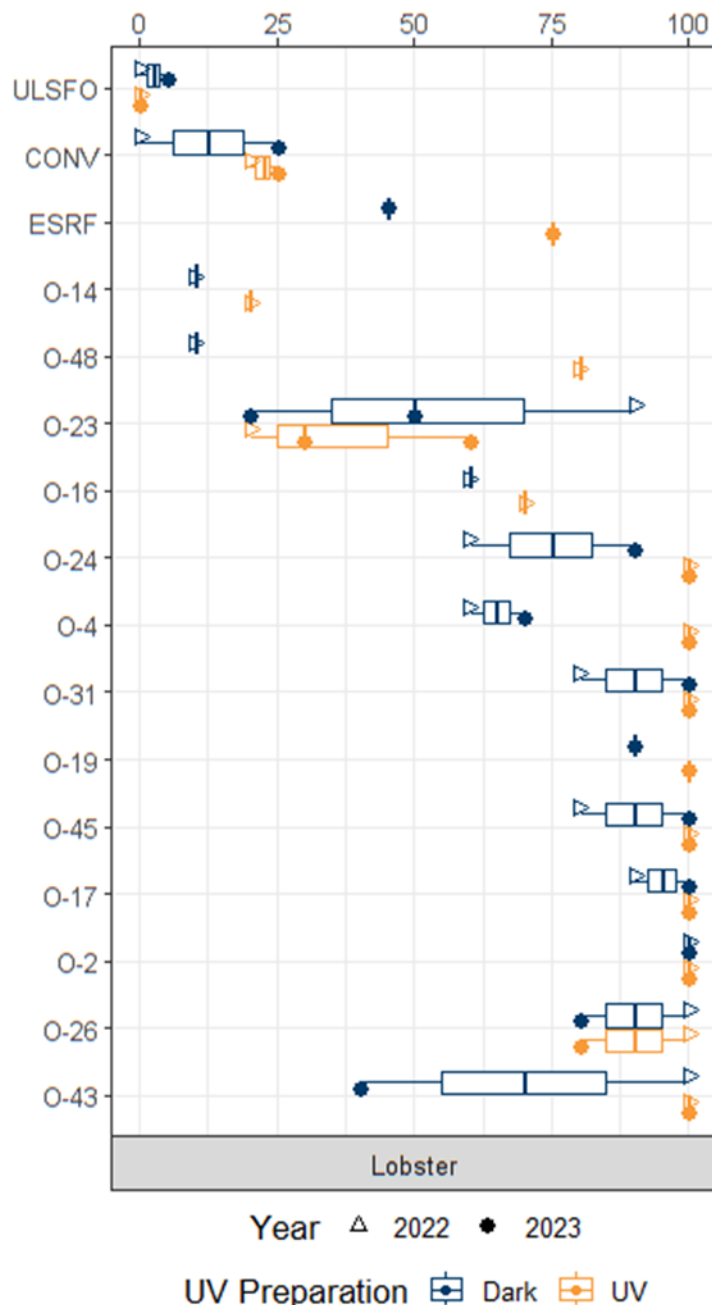
 816 *Figure 28: Predicted and observed toxicity. Dashed line is 1:1 with the dotted lines bounding 20%.*

 817 Using only waterborne PAC concentration, the toxic unit model consistently
 818 underestimates the toxicity of many of the VLSFOs products, both with and without UV.
 819 Other aspects that are not measured by traditional GC-MS (e.g., oxidized products) are
 820 likely contributing to the toxicity.

 821 The results of two seasons of lobster testing are presented in **Error! Reference source**
 822 **not found.** Stage I lobster larvae were sensitive to both UV-treated and non-irradiated
 823 WAF, and in many cases showed increased toxicity following photomodification. The
 824 results between the years were consistent for most products, with the notable exception
 825 of O-23 and O-45. With O-23, this product was selected for a repeat exposure based on
 826 the observed result of reduced toxicity following photo-modification. In the 2023 exposure,
 827 we were not able to repeat that result and on the basis of the exposure metrics (e.g.,
 828 TOC, fluorometry, and BE-SPME) believe the 2022 result to be anomalous. O-43 was
 829 selected for a repeat exposure in 2023 based on the 100% immobilization in both the UV-
 830 treated and non-irradiated WAF, and because the AMSA report had suggested that this
 831 product had been mislabelled (suspected to be RMD80 specification oil, and not
 832 RMD380). This may have also had an impact on the stability of the sample, which would
 833 explain the decrease in toxicity in 2023 compared to 2022 for the non-irradiated WAF,

834 however the UV-treated WAF in each year elicited a 100% immobilization response in the
835 larval lobsters.

836



837

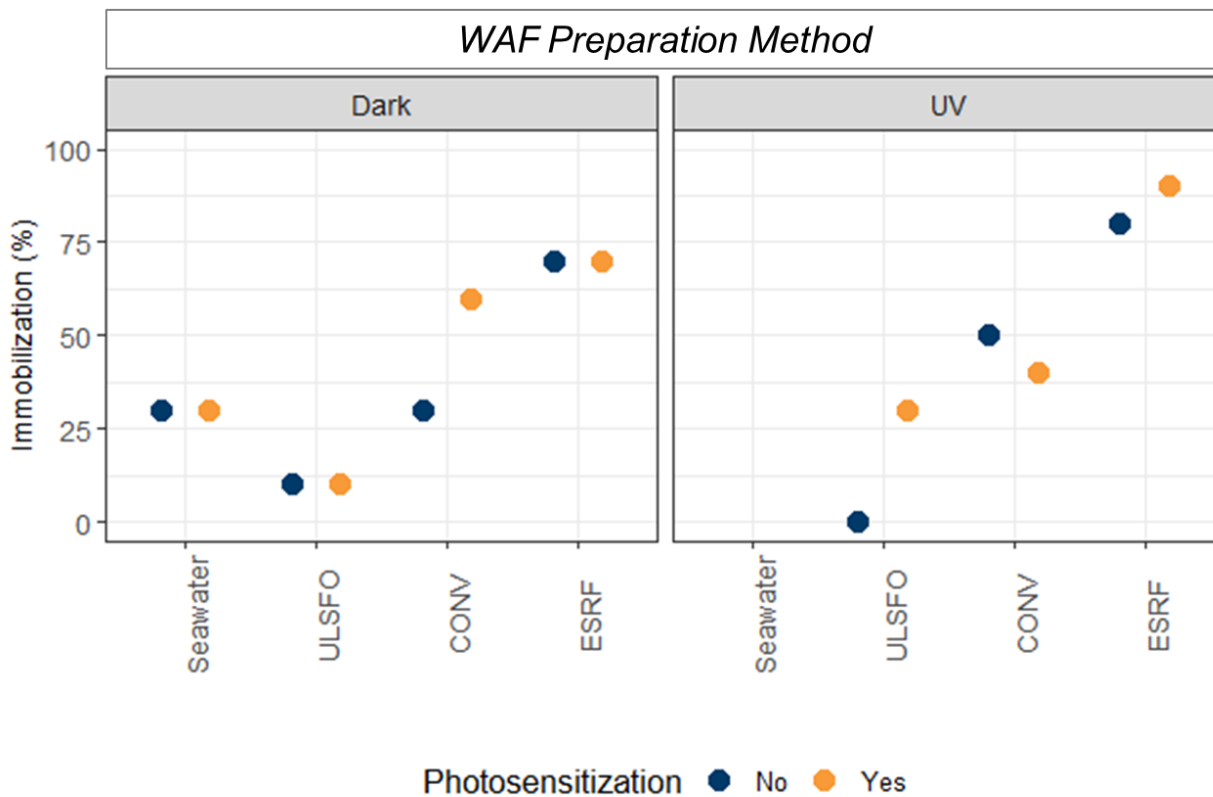
838 *Figure 29: Summary of the lobster immobilization in response to 24-hr exposure to irradiated (orange) and*
 839 *non-irradiated (blue) WAFs in the 2022 (open triangles) and 2023 (filled circles) testing season. Where the*
 840 *product was tested in both years the boxplot illustrates the range and mean response.*

841

3.3.1.1. Photo-modification and Photo-sensitization in lobster

842 American lobster larvae were exposed to dark-WAF or UV-WAF at 100% strength for 24-
 843 hrs. Afterwards the larvae were transferred into clean seawater, and a subset of replicates

844 from each treatment (dark or UV-WAF) were directed towards a photo-sensitization
 845 exposure involving a 3-hour exposure to a single UV dose, while the other units remained
 846 in the dark. Each unit was then followed for an additional 24-hours (under dark conditions)
 847 of monitoring to assess mortality. The results of which are shown in Figure 30.



848

849 *Figure 30: Summary of the photo-modification and photo-sensitization combined trial. The panel on the left*
 850 *represent WAF media that was prepared in the dark (no photo-modification), while the panel on the right is*
 851 *WAF media prepared under UV light (photo-modification). The colours of the points within each panel*
 852 *indicate whether following 24-hrs of exposure to media the replicate (individual point) was placed under UV*
 853 *light for 3-hours (photo-sensitization; orange circles), or left in the dark (blue circles).*

854 Photosensitization (orange points) had minimal effect on larval lobsters exposed to these
 855 WAFs under either photomodification regime. While there was an increase in the toxicity
 856 observed in the photo-modified ULSFO WAF, the relatively high control responses
 857 prevents us from saying with confidence that this is a true effect.

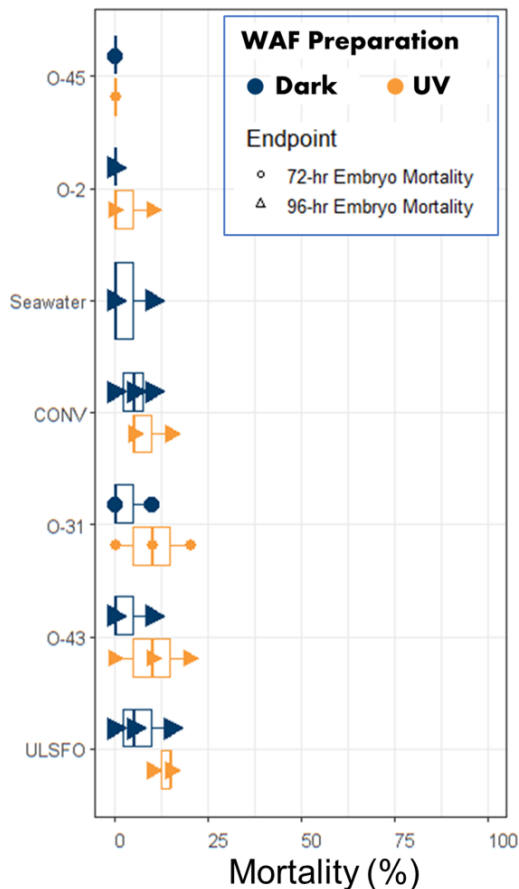
858 3.3.2. Atlantic cod results

859 3.3.2.1. *Embryo*

860 Six products (5 VLSFOs, and 1 conventional crude) were screened for toxicity with cod
 861 embryo exposures. WAFs were prepared at a single loading (1 g/L) under UV light and in
 862 the dark and were tested using only 100% strength solution of the WAF, with a 24-hr

863 exposure, followed by transfer to clean seawater for monitoring for 96 hours. The
 864 objective of this screening was to determine the relative toxicity of the different products,
 865 and to identify any products which showed a significant effect of photomodification (e.g.,
 866 a change in toxicity relative to the dark preparation).

867 The embryo trials showed either no toxicity response (Figure 31) or failed our validity
 868 criteria due to poor embryo performance (data not shown).



869

870 *Figure 31: Summary of embryo responses following either 72 (circles) or 96 (triangles) exposure to UV-*
 871 *treated (orange) or dark (blue) WAF.*

872 Due to the embryo quality issues, some of the trials were only valid for 72-hours (as shown
 873 by triangles in Figure 31) as compared to the others which ran for 96-hours. In each case
 874 there was little mortality response nor indication of significant differences between WAF
 875 preparation methods. Given the lack of sensitivity (potentially owing to reduced
 876 permeability of the embryo) and the embryo quality issues, the focus of the testing shifted
 877 to the larval life stage.

878 3.3.2.2. *Larval*

879 Larval cod were more sensitive to exposure than embryos, so product testing was
880 expanded to include 14 products (12 VLSFOs, and 2 conventional crudes), with the
881 results summarized in Table 4 and Figure 32.

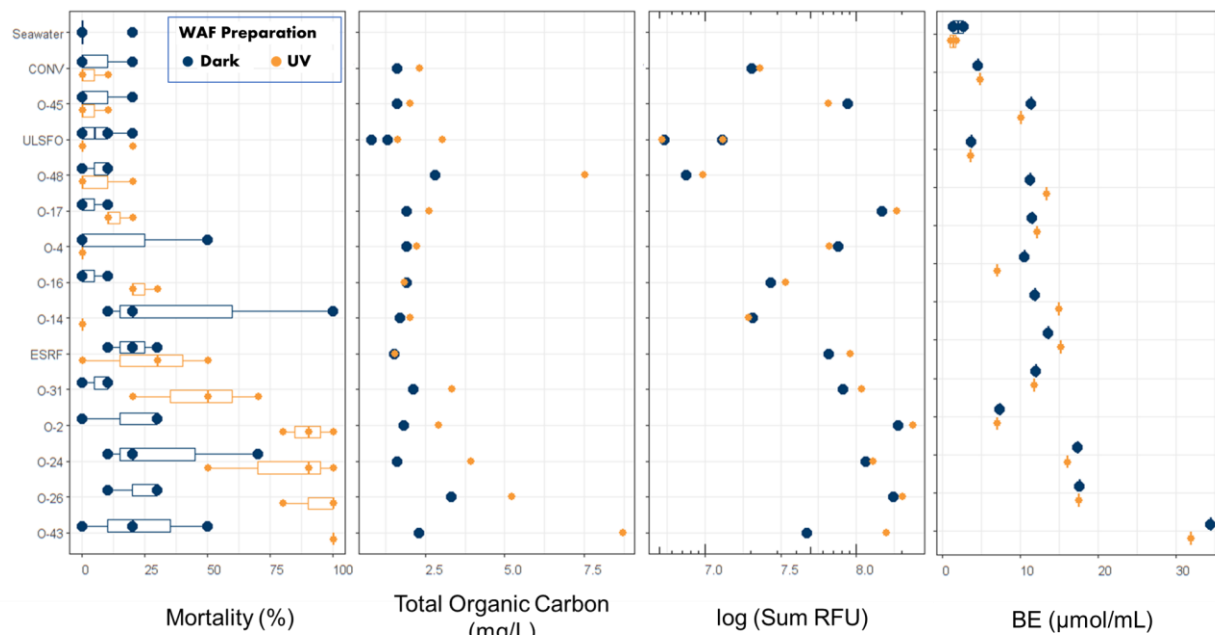
882

Table 4: Results of larval cod toxicity screening prepared in the dark and under 18 hours of irradiation.

Oil	UV	Average Mortality (%)	TOC	Sum RFU	BE-SPME	Fold Increase (UV to Dark)			
						Mortality	TOC	Sum RFU	BE-SPME
CONV	Dark	6.7	1.6	20243420	4.50	0.49	1.44	1.13	1.06
	UV	3.3	2.3	22789404	4.77				
ESRF	Dark	20	1.5	65196965	11.25	1.34	1.00	1.37	1.18
	UV	26.7	1.5	89577332	13.29				
ULSFO	Dark	6.7	0.8	13004722	1.30	1.00	3.75	0.99	0.75
	UV	6.7	3.0	12861002	0.98				
O-17	Dark	3.3	1.9	148216323	17.57	4.03	1.37	1.23	0.99
	UV	13.3	2.6	183013329	17.47				
O-26	Dark	23.3	3.3	176393893	17.34	4.00	1.58	1.13	0.92
	UV	93.3	5.2	198524518	15.91				
O-31	Dark	6.7	2.1	81886893	11.90	6.97	1.57	1.30	0.98
	UV	46.7	3.3	106750433	11.72				
O-45	Dark	6.7	1.6	87111250	7.36	0.49	1.25	0.74	0.93
	UV	3.3	2	64872312	6.88				
O-2	Dark	20	1.8	187227317	34.45	4.50	1.61	1.25	0.92
	UV	90	2.9	233979691	31.85				
O-43	Dark	23.3	2.3	47085476	11.83	4.29	3.78	3.33	1.26
	UV	100	8.7	156743506	14.87				
O-24	Dark	33.3	1.6	114884479	13.56	2.40	2.44	1.11	1.12
	UV	80	3.9	127287034	15.13				
O-4	Dark	16.7	1.9	75681677	10.44	0.00	1.16	0.87	0.66
	UV	0	2.2	65543284	6.93				
O-14	Dark	43.3	1.7	20628964	11.37	0.00	1.18	0.92	0.88
	UV	0	2.0	18994446	10.04				
O-16	Dark	3.3	1.9	27143889	11.41	7.06	0.95	1.23	1.05
	UV	23.3	1.8	33425179	12.01				
O-48	Dark	6.7	2.8	7476462	3.64	1.00	2.68	1.27	0.98
	UV	6.7	7.5	9518965	3.55				

883

884

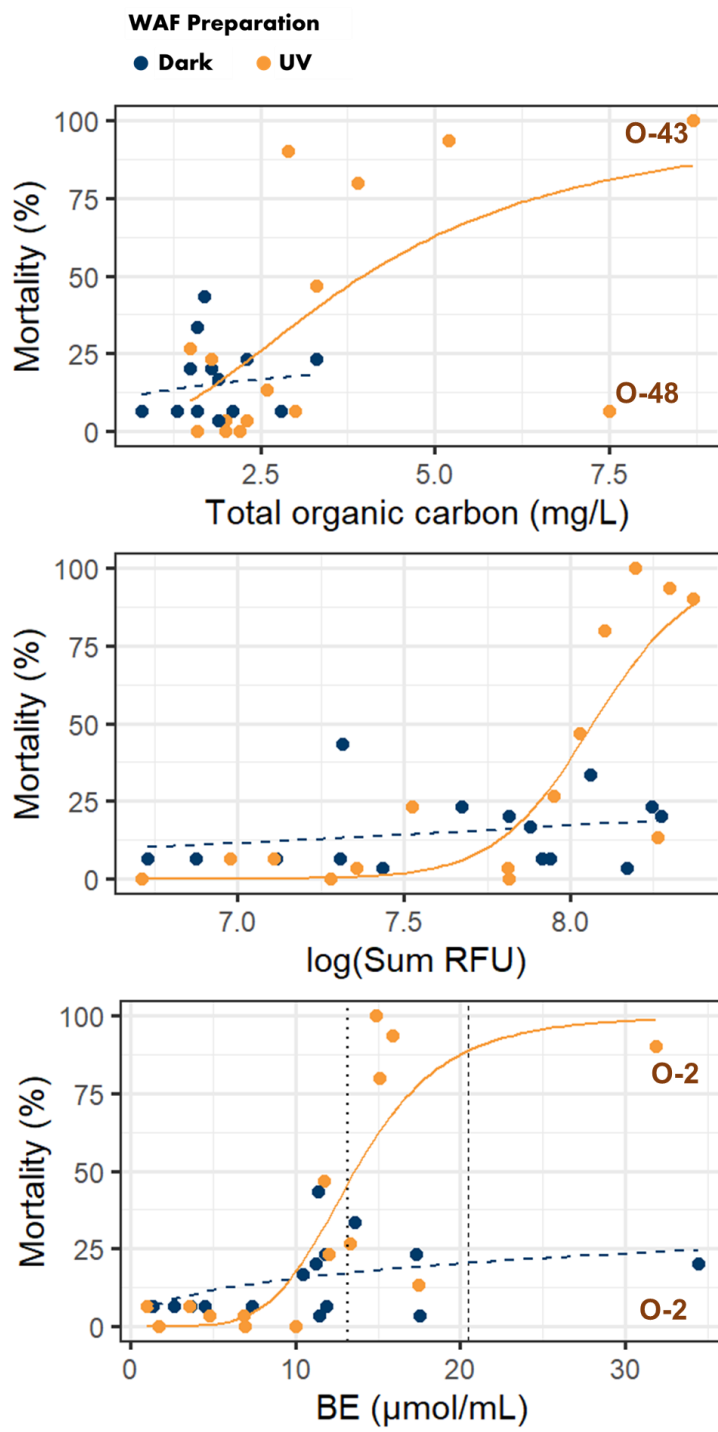


885

886 *Figure 32: Summary of the larval mortality (left; each point represents a replicate, with the box bounding*
 887 *the interquartile range), total organic carbon measurements (middle-left), the relative fluorometry signal*
 888 *(middle-right), and the BE-SPME (right) for the UV-treated (orange) and dark (blue) WAFs. The products*
 889 *are listed on the y-axis in decreasing order of toxicity based on the UV-treated WAFs (e.g., products on the*
 890 *bottom are more toxic)*

891 In nearly all cases the observed toxicity in the UV treated WAF (orange circles in Figure
 892 32) was equal or greater than the WAF prepared in the dark (blue circles). For all products
 893 tested, there was an increase in TOC with UV treatment. While the fluorometer can only
 894 measure compounds that fluoresce, in all but one case (O-45) there was an increase in
 895 the relative fluorometric signal in the UV treated WAFs compared to their non-irradiated
 896 counterpart. It should be noted, however, other compounds may have been formed that
 897 are not detectable with this method. There was less difference in the BE values between
 898 the irradiated and dark counterparts, however the increase in BE concentration generally
 899 followed with increases in toxicity. The increased TOC and RFUs after irradiation suggest
 900 that there were additional photoproducts being formed and that the amount formed varied
 901 between oil samples. The VLSFO WAFs showed a full range of mortality response from
 902 0 to 100% when irradiated, however there was seldom more than 50% mortality for any
 903 VLSFO WAF prepared in the dark.

904 The mortality data was modelled using the TOC, RFU, and BE-SPME as exposure
 905 metrics (Figure 33).



906

907 *Figure 33: Fitting the larval cod mortality data to the exposure metrics of total organic carbon (top), relative
 908 fluorometry signal (middle), and BE (bottom) for the UV-treated (orange) and dark (blue) WAFs.*

909 As TOC increased greater than 2.5 mg/L there was more pronounced mortality, with the
 910 notable exception of O-48, which had the second highest TOC concentration (7.5 mg/L),

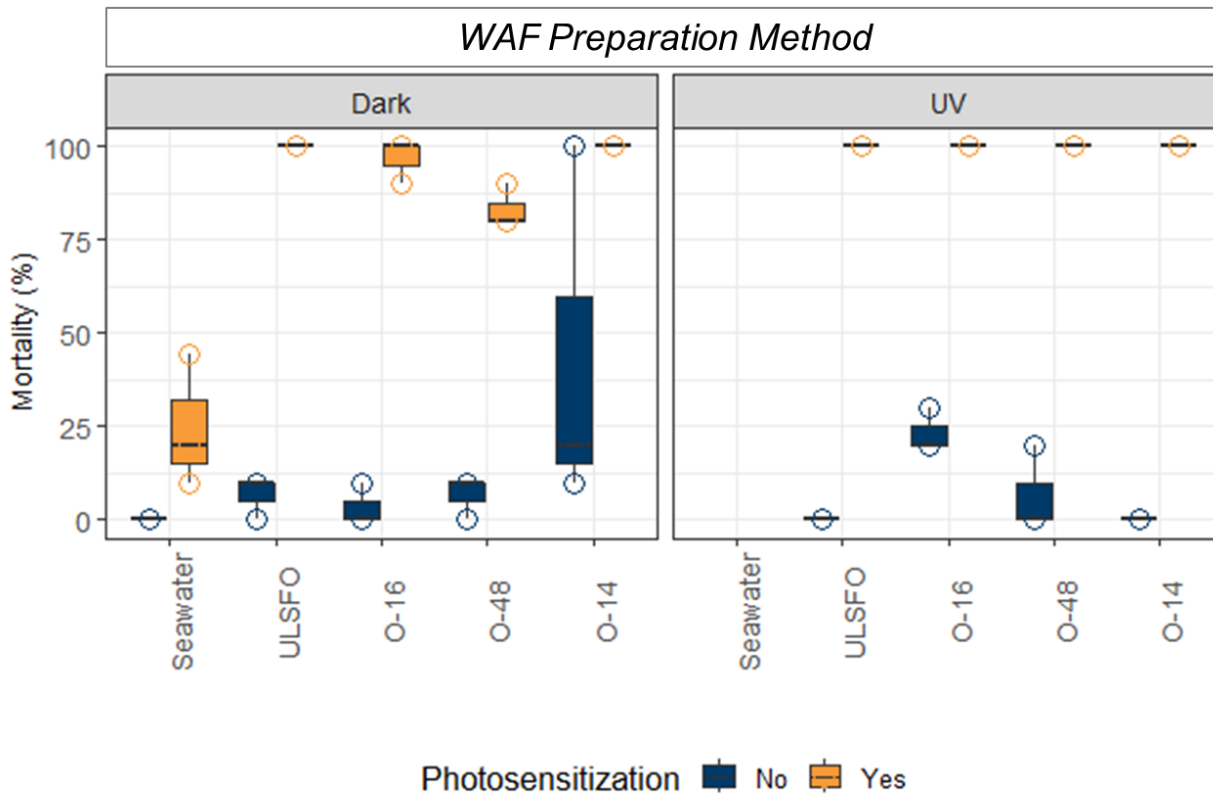
911 but very little mortality (mean 6.7% mortality). The greatest TOC measurements were
912 from WAFs that had been irradiated, highlighting the formation of photoproducts. There
913 was a stronger relationship with the fluorometry signal strength (RFU) and the observed
914 mortality when looking at the WAFs prepared under UV light. However, the dark WAFs
915 did not have as strong of a relationship, partially owing to the limited mortality seen in the
916 dark preparations. If the formed photoproducts are not detectable by fluorescence, this
917 may explain why at similar RFUs there is increased mortality observed in the UV WAFs
918 than those in the dark.

919 The BE exposure metric ($\mu\text{mol/L}$) generally increased with increasing mortality. There
920 were three results from the same trial where the BE-values were high (e.g., 17.3 – 17.5
921 $\mu\text{mol/L}$) but showed less mortality than expected. These values came from O-17 (UV and
922 dark) and O-26 (dark) and are consistent with the magnitude observed in the lobster
923 studies for those products (18.9 – 24.5 $\mu\text{mol/L}$). For lobster, these two products were
924 among the most toxic, however in cod they presented a much lower response. This could
925 be due to an overall reduced sensitivity of cod as compared to lobster or may reflect that
926 the exposure and monitoring time in the colder temperature cod, was not sufficient to
927 observe the toxicological effects (e.g., may have required >24-hrs to observe the effects).
928 The other result of interest for the BE relationship is O-2, which exhibited the greatest BE
929 concentrations (31.9 and 34.5 $\mu\text{mol/L}$ for UV and dark preparation respectively; again in
930 line with the measured values from the lobster studies), and also showed extreme
931 differences in mortality, 20% for the dark preparation and 90% for the UV preparation.
932 The lower than expected mortality in the dark preparation of O-2 may be due to the colder
933 temperatures and requiring more time to observe mortality, or could be due to the higher
934 degree of variability observed within Atlantic cod and their responses to petroleum
935 products (Scovil et al. 2022); however as the fish were from the same batch, the latter
936 explanation is less likely in this case. A concentration response model was applied to the
937 BE and mortality results, both with all the data and excluding the 4 data points where the
938 mortality was lower than expected, yielding a BE-critical value of 20.5 $\mu\text{mol/L}$ (5.9
939 standard error) and 13.2 $\mu\text{mol/L}$ (0.5 standard error) respectively (indicated as the dashed
940 and dotted vertical lines in the bottom panel of Figure 33). The BE-critical value is greater
941 than the value for lobster (6.3 $\mu\text{mol/L}$), confirming the greater acute sensitivity of lobster
942 as compared to cod larvae.

943 3.3.2.3. *Photo-modification and Photo-sensitization in cod*

944 Larval cod were exposed to dark-WAF or UV-WAF at 100% strength for 24-hrs.
945 Afterwards the cod were transferred into clean seawater, and a subset of replicates from
946 each treatment (dark and UV-WAF) were directed towards a photo-sensitization exposure
947 involving a 3-hour exposure to a single UV dose, while the other units remained in the

948 dark. Each unit was then followed for an additional 24-hours (under dark conditions) of
 949 monitoring to assess mortality. The results of which are shown in Figure 34.



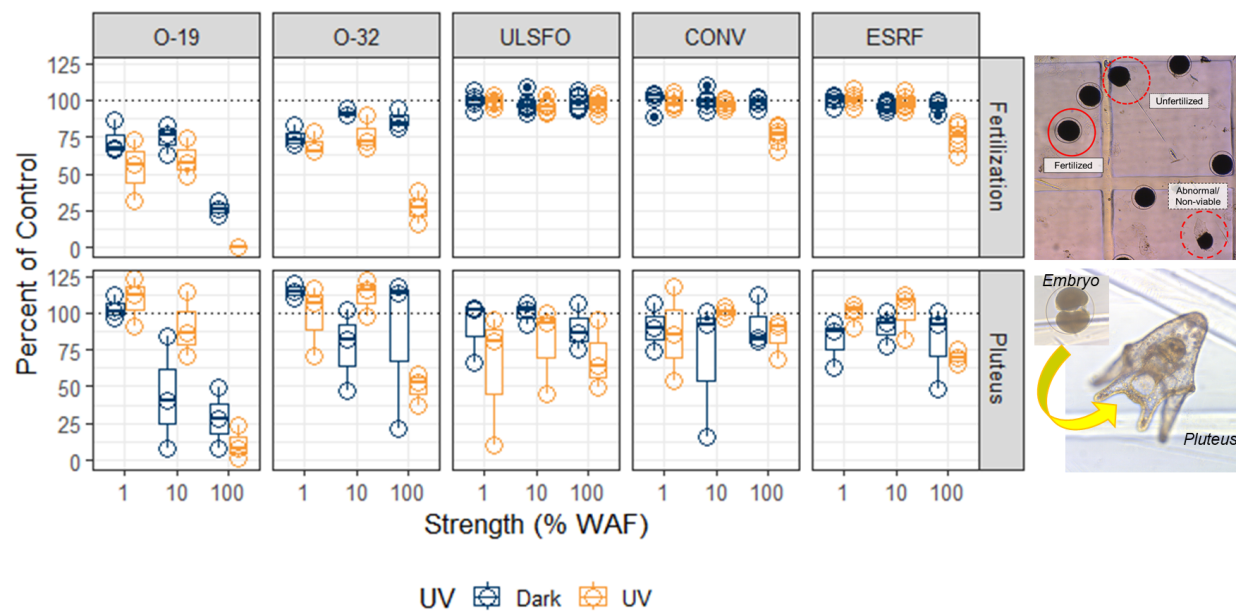
950

951 *Figure 34: Summary of the photo-modification and photo-sensitization combined trial. The panel on the left*
 952 *represent WAF media that was prepared in the dark (no photo-modification), while the panel on the right is*
 953 *WAF media prepared under UV light (photo-modification). The colours of the boxes within each panel*
 954 *indicate whether following 24-hrs of exposure to media the replicate (individual point) was placed under UV*
 955 *light for 3-hours (photo-sensitization; orange boxes), or left in the dark (blue boxes).*

956 Photo-sensitization (orange boxes) had a slightly greater effect on organisms pre-
 957 exposed to a photo-modified WAF (right panel) than the dark-WAF (left panel). This result
 958 could indicate that photo-products generated during irradiation were bioavailable to the
 959 organism, were at least mildly persistent within the organism, and were photo-reactive.
 960 However, because the responses in the photo-sensitization exposure units were so high
 961 (nearly showing 100% mortality) it is difficult to tease out the magnitude of the difference
 962 between the photo-sensitization potential of photo-modified products compared to their
 963 non-modified counterparts. It is also worth noting that in the seawater alone control
 964 treatment, a 3-hour UV exposure did result in mortality that was not observed in the no
 965 photo-sensitization group. This highlights that photo-sensitization exposures are
 966 fundamentally a co-exposure of two stressors (photo-reactive compounds and UV
 967 irradiation) and their potential synergistic effect (Alloy et al. 2023). The impact of photo-

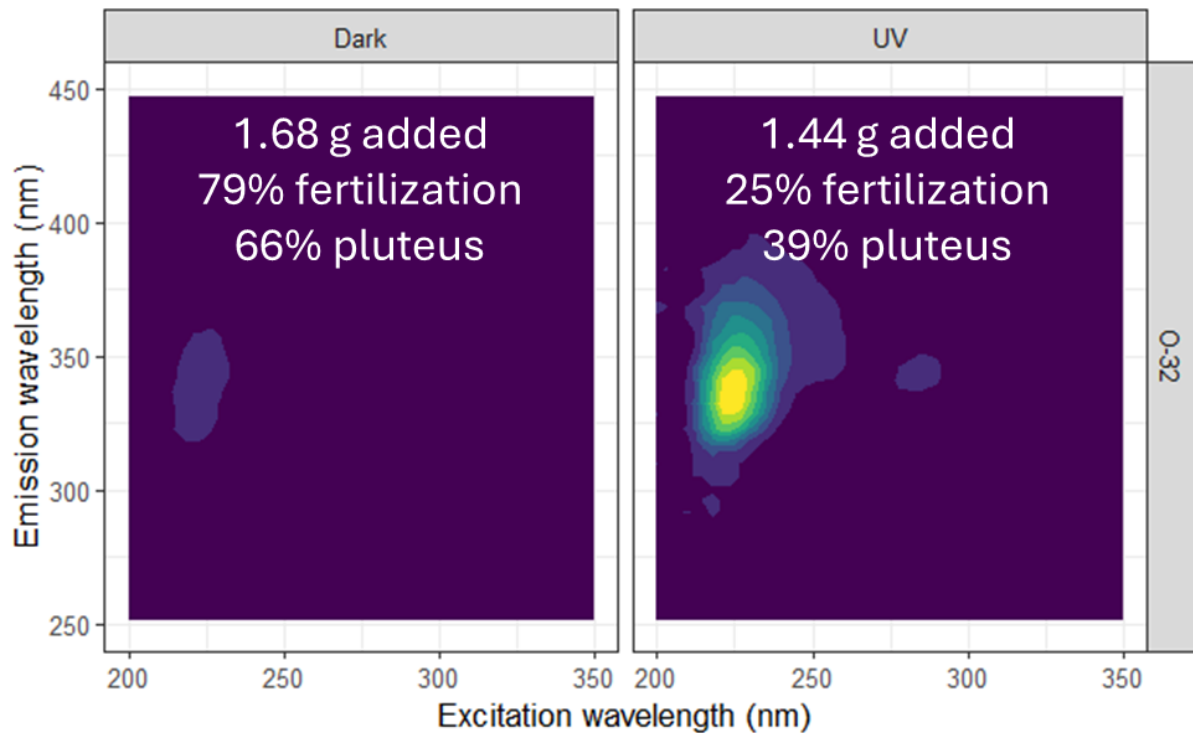
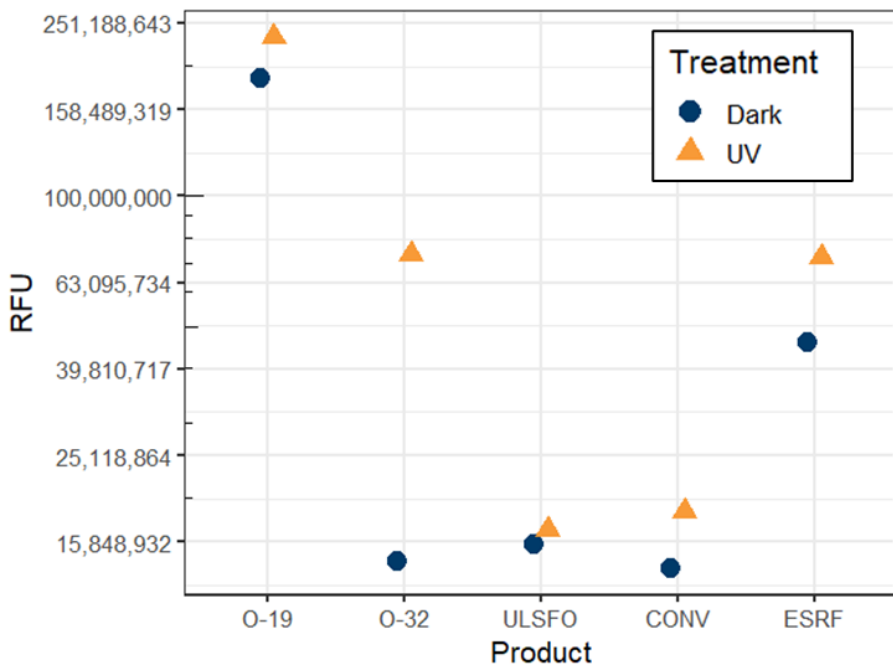
968 sensitization was greater in cod larvae than what was observed in lobster. This difference
 969 may be attributable to the different biology of the organisms, where the larval lobster has
 970 a semi-transparent carapace made of chitin which may limit the transmission of UV light
 971 into the body, whereas the larval cod are more transparent and thus allow more UV light
 972 into the body where it may react with the accumulated PACs, which otherwise may have
 973 been at levels where toxicity would not be expected to occur.

974 **3.3.3. Green sea urchin results**
 975 Five products (3 VLSFOs, and 2 conventional crudes) were screened for toxicity with
 976 green sea-urchin bioassays. WAFs were prepared at a single loading (1 g/L) under UV
 977 light and in the dark and were diluted to generate exposure solutions of 100, 10, and 1%
 978 strength. The urchin results are presented in Figure 35 for fertilization and development.



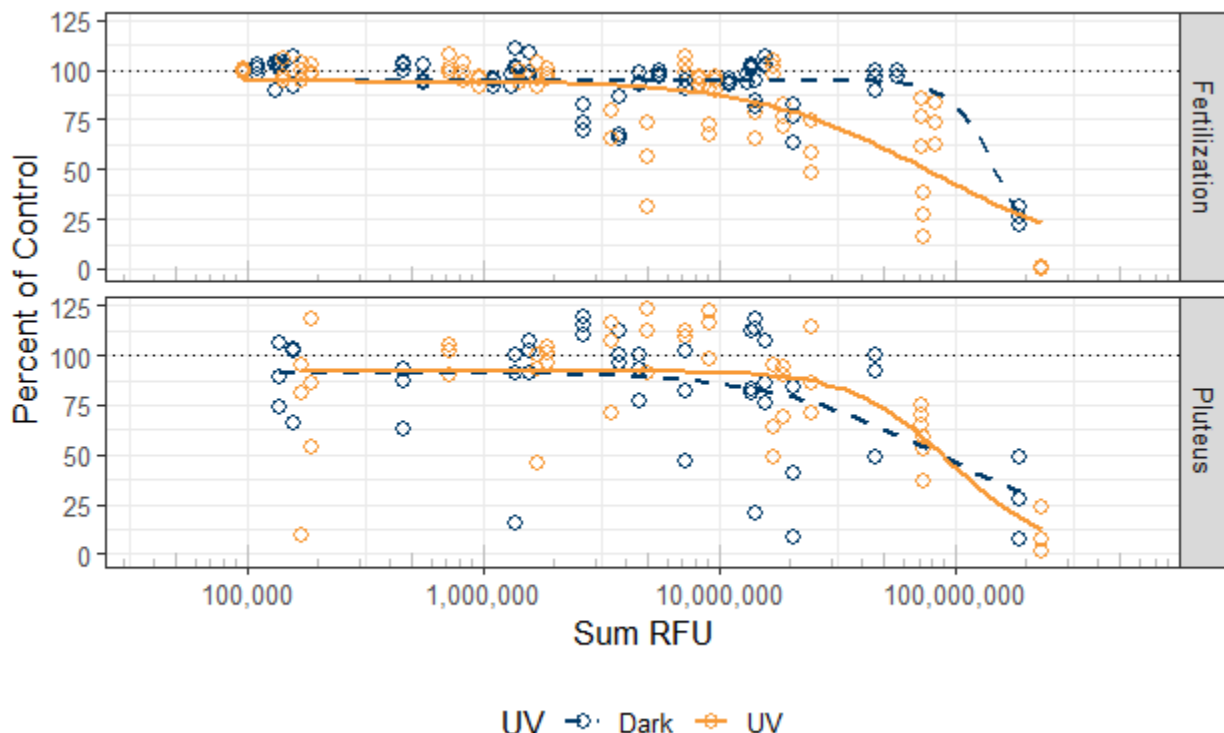
979
 980 *Figure 35: Urchin fertilization (top) and development (bottom) results for the UV-treated (orange) and dark*
 981 *(blue) WAFs.*

982 Fertilization and development are sensitive toxicological endpoints, and at the highest
 983 tested concentrations, both VLSFO products, O-19 and O-32, exhibited a significant
 984 decrease relative to the control performance, while there was minimal impact on these
 985 endpoints for the ULSFO, Conventional Heavy Crude (CONV) or the offshore
 986 Newfoundland crude (ESRF). For the VLSFOs, O-19 and O-32, the UV treated WAFs did
 987 exhibit greater toxicity for both endpoints than did the WAFs prepared in the dark, and
 988 demonstrated an increase in fluorometric signal following irradiation (Figure 36).



989
 990 *Figure 36: (top) The sum of the fluorometric signals from the urchin exposures for the WAFs prepared in*
 991 *the dark (blue circles) and under UV (orange triangles). (bottom) Summary of the fluorometry excitation*
 992 *and emission spectra (colour represents signal intensity with yellow being the most intense and purple the*
 993 *least) and toxicological responses for O-32.*

995 At the time of reporting, only the fluorometry data was available for the urchin exposures,
 996 and it was used to fit the fertilization and development responses (Figure 37).



997

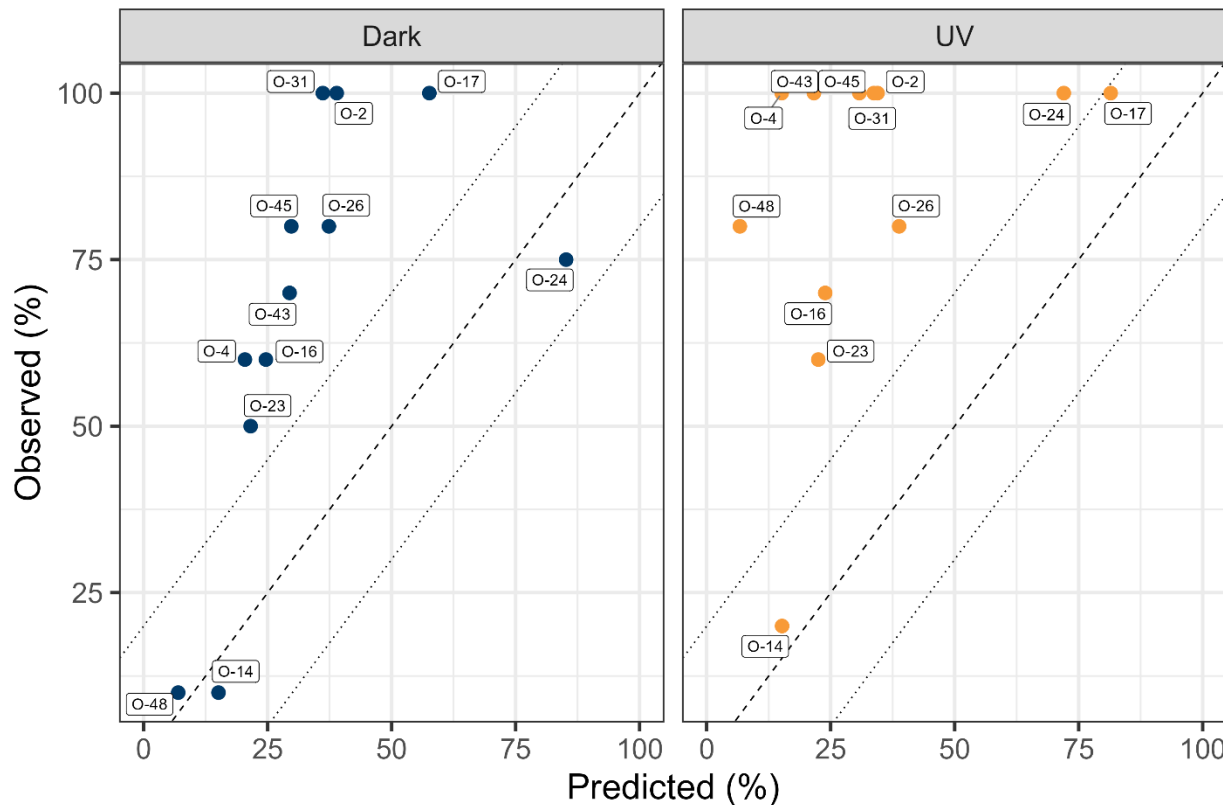
998 *Figure 37: Concentration response relationship for the UV-treated (orange) and dark (blue) WAFs.*

999 The response for both endpoints generally followed that with increasing fluorometric
 1000 signal there was reduction in the percent fertilized and reduced development to the
 1001 pluteus stage. When modelling the response data with both preparations combined, the
 1002 EC50 for fertilization was 99,981,951 (sum RFUs) and the EC50 for development to
 1003 pluteus was 82,994,263 (sum RFUs). This highlights that the development endpoint is
 1004 slightly more sensitive than the fertilization. However, as the fertilization bioassay can be
 1005 run in a single day (as compared to the 4-5 days for the development endpoint), it offers
 1006 a better opportunity to rapidly screen for toxicity.

1007 **3.4. Modelling**

1008 Using the measured PAC and alkane concentrations in the products (3.1.1), collected
 1009 after making WAF in both the dark and under UV, the expected concentrations in the
 1010 WAF were estimated, and those were used to calculate toxic units to the lobster and
 1011 predict the immobilization response. To estimate the concentrations, the mass of the
 1012 analyte in the sample was multiplied by partitioning transfer rate (estimated based on log
 1013 KOW), and the equilibrium partitioning between water and oil. The estimated values were

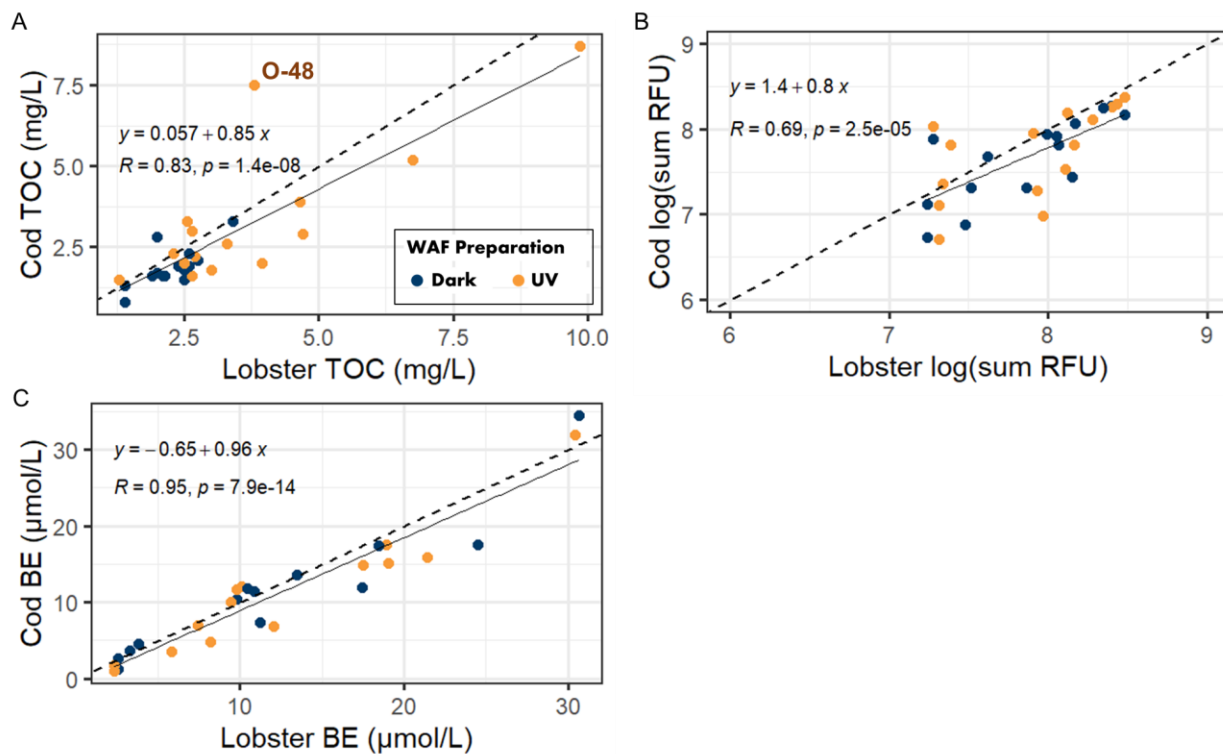
1014 compared to the subcooled solubility to ensure the modelled estimates did not exceed
 1015 solubility. From the estimated water concentrations, the toxic unit approach was applied
 1016 to predict the toxicity. The predicted and observed toxicity to American lobster larvae for
 1017 the products tested in presented in Figure 38.



1018

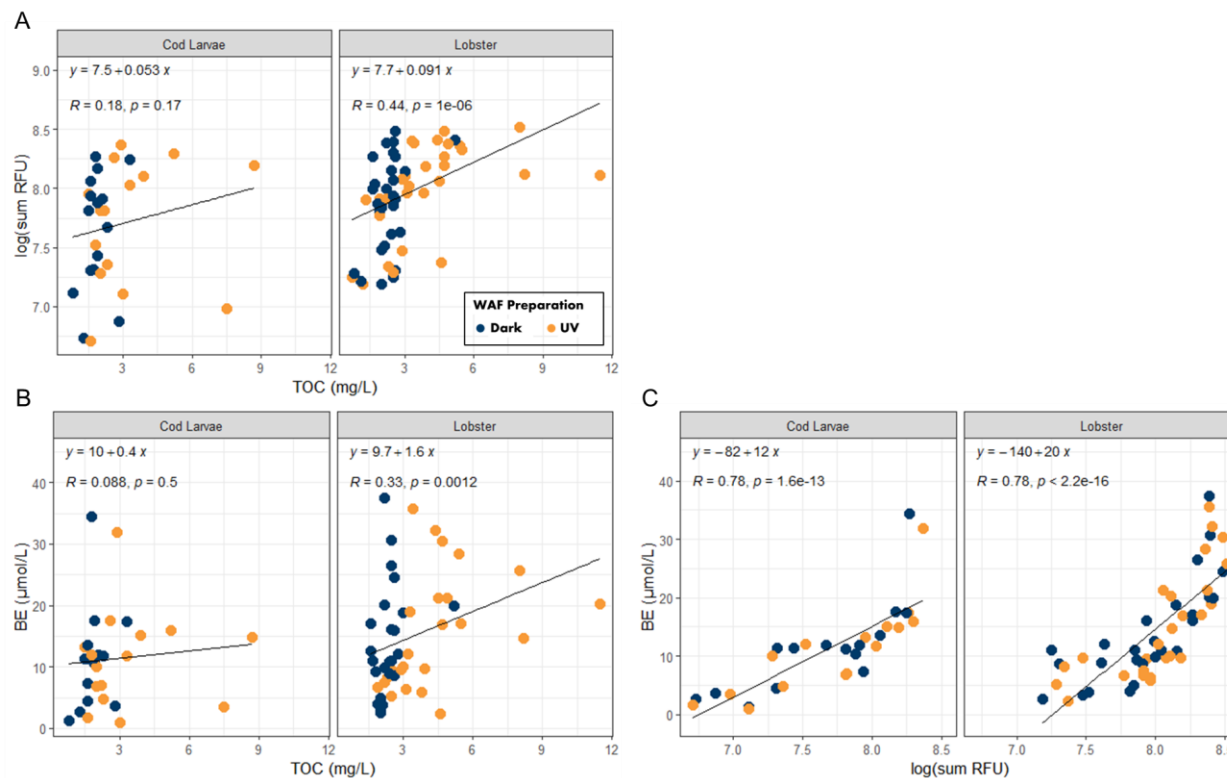
1019 *Figure 38: Predicted toxicity (as immobilization) to American lobster larvae based on the measured*
 1020 *concentrations in the source oil following the preparation of a WAF in the dark (left) or under UV light*
 1021 *(right). The dashed line is showing 1:1 and the dotted lines bound a +/- 20%.*

1022 In the case of the dark and irradiated VLSFO, the predicted toxicity was consistently less
 1023 than the observed toxicity, with only 3 products (O-14, O-24, O-48) in the dark preparation
 1024 and 2 products (O-14 and O-71) in the UV preparation having predictions within 20% of
 1025 the observed response. The dark preparations have a slightly better predictive ability
 1026 (e.g., more points closer to equality), than the UV preparations, again suggesting the
 1027 formation of compounds that are not accounted for in traditional chemical analysis but are
 1028 contributing to toxicity. These results highlight that to have more accurate predictions of
 1029 toxicity more comprehensive and additional characterization of test media (e.g.,
 1030 fractionation and liquid chromatography high resolution mass spectrometry (LC-HRMS),
 1031 gas chromatography-quadrupole time-of-flight mass spectrometry (GC-QTOF)) is
 1032 required.

1033 3.4.1. Relationships in water chemistry
 1034 When comparing the WAF preparations for lobster and cod, there was generally
 1035 consistent relationship between the measurements of the exposure metrics (Figure 39).

 1036
 1037 *Figure 39: Comparison between the measured exposure metrics TOC (A), RFU (B), and BE-SPME (C)*
 1038 *between lobster (x-axis) and cod (y-axis) for the same products (n = 15) prepared in the dark (blue*
 1039 *circles) and under UV light (orange circles). The dashed diagonal line is 1:1 and the solid line is the linear*
 1040 *regression relationship with the equation in the insert.*

 1041 In nearly all cases, the measured values in the cod preparations are slightly lower than
 1042 the same product prepared in the lobster testing (e.g., points tend to fall below the dashed
 1043 diagonal line at 1:1 in Figure 39). This difference may be attributable to two things. The
 1044 first being temperature, with the WAFs used in lobster testing having been prepared at
 1045 15°C, while the WAFs for cod testing were prepared at 6°C, the warmer temperature may
 1046 have impacted the dissolution rates, resulting in greater concentration in the lobster
 1047 preparation. The second option could reflect weathering state/stability of the products, as
 1048 the lobster testing was performed first, followed by the cod testing approximately 4
 1049 months later. However, the closeness of the data, and the significant relationship between
 1050 the preparations for each species highlights that a consistent WAF preparation and
 1051 analytical characterization was performed for all trials.

1052 In comparing between exposure metrics, there is a significant relationship the fluorometric
 1053 signal and the BE values (Figure 40), while the other relationships are less strong or
 1054 consistent.



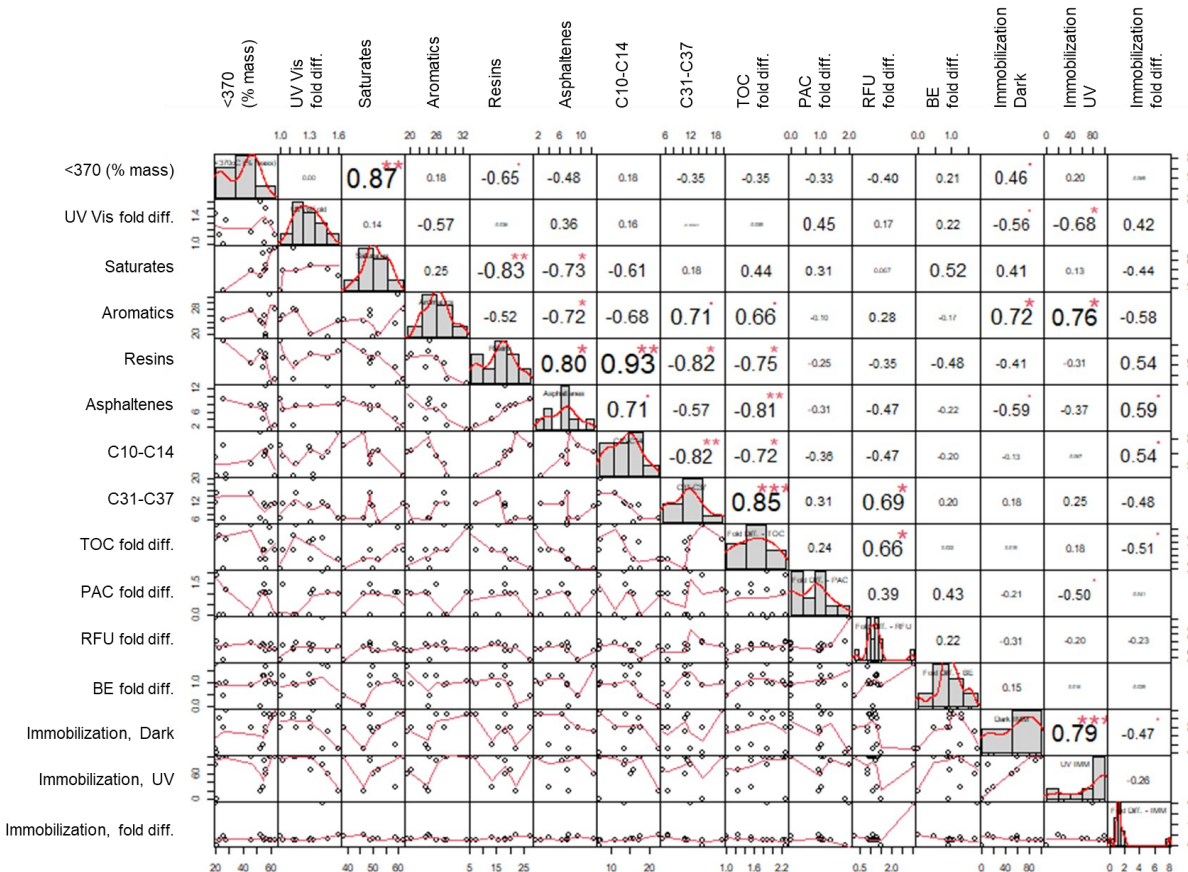
1055

1056 *Figure 40: Relationship between the exposure metrics TOC and RFU (A), TOC and BE (B), and RFU and*
 1057 *BE (C) prepared in the dark (blue circles) and under UV light (orange circles).*

1058 The relationship between the different exposure metrics highlights the importance of fully
 1059 characterizing exposure solutions, as each measurement method can only detect certain
 1060 compounds (e.g., fluorometry can only detect compounds which fluoresce) and each of
 1061 those compounds may be contributing towards toxicity in a different manner. The BE
 1062 metric, which measures the non-descript bioavailable fraction, has a good relationship
 1063 with observed toxicity in both lobster and cod, and can account for compounds which may
 1064 not be typically analyzed by other methods. This metric should be further explored as a
 1065 rapid analytical tool that can provide information regarding the potential impact of a water
 1066 sample.

1067 **3.4.2. Relationships between properties of the VLSFOs and bioassay results**
 1068 The physical and chemical properties of the tested products (only considering the
 1069 VLSFOs and ULSFOs; excluding O-43 and the conventional products) were examined
 1070 against the measured changes in exposure metrics (e.g., TOC, PAC, RFU, and BE) and

1071 the toxicological response (lobster immobilization in dark, with UV, and fold difference),
 1072 to identify significant relationships (Figure 41).



1073

1074 **Figure 41: Correlation matrix with scatterplots (lower half), histograms (diagonal), and significance levels**
 1075 **(upper half) for a suite of measures.**

1076 The diagonal shows histograms representing the distribution of each measure. The lower
 1077 triangle displays scatterplots illustrating pairwise relationships between the measures,
 1078 while the upper triangle contains the Spearman correlation coefficients (r) for each pair.
 1079 Asterisks (*, **, ***) in the upper triangle indicate the significance of the correlations: * (p
 1080 ≤ 0.05), ** (p ≤ 0.01), *** (p ≤ 0.001). Cells without asterisks represent correlations that
 1081 are not statistically significant (p > 0.05).

1082 The physical-chemical properties of the VLSFOs are related to each other, as can be
 1083 seen by the significant correlations between the SARA components. When looking at the
 1084 changes in exposure metric concentration from UV to dark, there were few of these
 1085 physical-chemical properties that had significant relationships. With fold increase in TOC
 1086 concentrations, there was a positive and significant relationship with aromatics and the

1087 C31-C37 fractions. This suggests that for a product with more aromatics and more in the
1088 C31-C37 fraction, there is likely to be more of an increase in TOC, as photoproducts,
1089 following UV irradiation. Similarly, there was a negative and significant relationship with
1090 resins, asphaltenes, and the C10-C14 fraction, suggesting that as those measures
1091 increase there is less of an increase in TOC following irradiation. There was also a
1092 positive and significant relationship between fold increase in RFUs and the C31-C37
1093 fraction of the VLSFOs. There were no significant relationships for fold increase in PAC
1094 or BE with any of the physical-chemical measures.

1095 The toxicological responses for lobster, immobilization in the dark WAF exposure,
1096 immobilization in the UV WAF exposure, and fold difference in immobilization following
1097 UV exposure, did have significant correlations with some of the physical-chemical
1098 measures. Notably the immobilization in the dark and UV were both positively and
1099 significantly correlated to the percent aromatic (e.g., greater the percent aromatic, the
1100 greater the immobilization); however the percent aromatic was not statistically correlated
1101 to the fold difference in immobilization response. The fold difference in immobilization was
1102 weakly correlated with the percent asphaltenes and the C10-C14 fraction (increasing
1103 amounts of each being correlated with a greater fold difference in immobilization), and
1104 the fold difference in TOC (increasing difference in TOC correlated to reduced difference
1105 in immobilization); however, the Spearman correlation coefficient for these relationships
1106 were all less than 0.6 and should be interpreted with caution.

1107 The SARA components, specifically the aromatics and asphaltenes, proved to have
1108 significant relationships with whether photomodification is likely to occur, and whether
1109 there is likely to be toxicity. The percent aromatics were significantly correlated with an
1110 increase in TOC (suggesting more formation of photoproducts), as well as the observed
1111 toxicity in the dark and UV WAFs. The percent asphaltenes was significantly correlated
1112 with increases in TOC following UV irradiation, and whether there would be an increase
1113 in immobilization following UV irradiation (albeit a weaker relationship). These
1114 relationships may provide a first pass screening value to determine the likelihood of
1115 photomodification and the significance of the photoproducts towards increasing the
1116 toxicity of the product.

1117 **4. Conclusions**

1118 There was an incredible diversity in the physical appearance, behaviour, and toxicity of
1119 the WAFs made with the VLSFOs, both alone and in the presence of UV light.

1120 The results highlight a wide range of responses across fuel types, with significant
1121 differences in sensitivity across species. Some of the VLSFOs and the ULSFO showed
1122 very little acute toxicity in these bioassays, while others resulted in significant changes

1123 (e.g., immobilization, mortality, delayed development). Lobster immobilization was the
1124 most sensitive endpoint, however the Atlantic cod saw significant increases in toxicity
1125 following a photo-sensitization exposure. The differences between these sensitivity to
1126 photo-modification and photo-sensitization highlight the importance of testing multiple
1127 species with different life histories and biology to ensure that the potential impacts of a
1128 contaminant are fully understood.

1129 The impact of UV light on the observed toxicity underscores the importance of addressing
1130 and incorporating modifying factors when determining the toxicity of complex mixtures in
1131 the laboratory. The likelihood of a product undergoing photomodification seems to be
1132 reasonably predicted by the SARA fraction, however this relationship should be further
1133 explored with more detailed characterization of the photoproducts. Photomodification can
1134 significantly increase the toxicity of some VLSFOs and it should be considered when
1135 assessing the potential damage these products can cause in a fuel spill scenario.

1136 The toxicity of many of the tested VLSFOs did not follow that of traditional crude oils,
1137 where PACs alone may adequately describe toxicity. The SARA components, particularly
1138 the percent aromatic, provided a general estimate for observing toxicity in larval lobster.
1139 The percent asphaltenes had a weakly significant relationship with the increase in toxicity
1140 observed following irradiation, and may provide an indicator for the potential toxicity of
1141 the formed photoproducts. Additional work needs to be done to understand what
1142 components within these VLSFOs are contributing towards toxicity, and the data
1143 generated in this study will help to develop and validate models to predict and assess the
1144 toxicity of these new generation fuel oils.

1145 5. Dissemination

1146 During this project the results of this study were presented at numerous scientific
1147 conferences:

1148 **SETAC-Europe Dublin, IRE: April 30th – May 4th 2023**

1149 **AMOP Technical Seminar, Edmonton, AB, CAN: June 6 – 8th 2023**

1150 **Canadian Ecotoxicology Workshop Ottawa, ON, CAN: October 2 – 5th 2023**

1151 **SETAC-North America Louisville, KY, USA: Nov 12 – 16th 2023**

1152 **SETAC-North Atlantic Chapter, Woods Hole, MA, USA: April 11 – 12th, 2024**

1153 **ACCESS/BoFEP Joint Conference, St. Andrews, NB: June 4 – 7th, 2024**

1154 **Canadian Ecotoxicology Workshop Kitchener, ON, CAN: October 6 – 9th 2024**

1155 Additionally, aspects of the research were presented to 19 high school and University
1156 groups from New Brunswick, Quebec, and Ontario, Canada. The findings presented in
1157 this study are being prepared for publication in the peer reviewed literature.

1158

6. References

1159

Aeppli C, Nelson RK, Radović JR, Carmichael CA, Valentine DL, Reddy CM (2014) Recalcitrance and degradation of petroleum biomarkers upon abiotic and biotic natural weathering of Deepwater Horizon oil. *Environmental Science & Technology* 48:6726–6734.

1160

1161

1162

1163

1164

1165

1166

Alloy M, Finch B, Ward C, Redman A, Bejarano AC, Barron M. (2023). Recommendations for Advancing Test Protocols Examining the Photo-induced Toxicity of Petroleum and Polycyclic Aromatic Compounds. *Aquatic Toxicology*, 256. <https://doi.org/10.1016/j.aquatox.2022.106390>

1167

1168

1169

1170

de Jourdan, B., Boloori, T., and Burridge, L. (2022). Newly hatched stage I American Lobster (*Homarus americanus*) survival following exposure to physically and chemically dispersed crude oil. *Archives of Environmental Contamination and Toxicology* 82. DOI 10.21203/rs.3.rs-781438/v1

1171

1172

1173

1174

1175

Dettman, H., Wade, T.L., French-McCay, D.P., Bejarano, A.C., Hollebone, B.P., Faksness, L., Mirnaghi, F.S., Yang, Z., Loughery, J.R., Pretorius, T., de Jourdan, B. (2023). Recommendations for the advancement of oil-in-water media and source oil characterization in aquatic toxicity studies. *Aquatic Toxicology* 261. <https://doi.org/10.1016/j.aquatox.2023.106582>

1176

1177

1178

Environment Canada. 2011. Biological test method: Fertilization assay using echinoids (sea urchins and sand dollars). EPS 1/RM/27 Second Edition. Science and Technology Branch, Environment Canada.

1179

1180

1181

1182

Heshka, N.E., Peru, K.M., Xin, Q., Dettman, H.D., Headley, J.V., 2022. High resolution Orbitrap mass spectrometry analysis of oxidized hydrocarbons found in freshwater following a simulated spill of crude oil. *Chemosphere* 292 (133415), 1–8. <https://doi.org/10.1016/j.chemosphere.2021.133415>.

1183

1184

1185

1186

Katz, S.D., Chen, H., Fields, D.M., Beirne, E.C., Keyes, P., Drozd, G.T., and Aeppli, C. (2022). Changes in Chemical Composition and Copepod Toxicity during Petroleum Photo-oxidation. *Environmental Science & Technology* 56 (9). DOI: 10.1021/acs.est.2c00251

1187

1188

1189

1190

Lara-Jacobo, L.R., Gauthier, C., Xin, Q., Dupont, F., Couture, P., Triffault-Bouchet, G., Dettman, H.D., Langlois, V.S., 2021. Fate and fathead minnow embryotoxicity of weathering crude oil in a pilot-scale spill tank. *Environ. Toxicol. Chem.* 40, 127–138. <https://doi.org/10.1002/etc.4891>

1191

1192

1193

McGrath, J.A., Fanelli, C.J., Di Toro, D.M., Parkerton, T.F., Redman, A.D., Leon Paumen, M., Comber, M., Eadsforth, C.V., den Haan, K., 2018. Re-evaluation of target lipid model-derived HC5 predictions for hydrocarbons. *Environ. Chem. Toxicol.* 37 (6), 1579–1593.

1194

1195

1196

McGrath, J., Getzinger, G., Redman, A.D., Edwards, M., Martin Aparicio, A., Vaiopoulou, E., 2021. Application of the target lipid model to assess toxicity of heterocyclic aromatic compounds to aquatic organisms. *Environ. Toxicol. Chem.* 40 (11), 3000–3009.

1197 Philibert, D., Parkerton, T., Marteinson, S., and de Jourdan B. (2021). Assessing the
1198 toxicity of individual aromatic compounds and mixtures to American lobster (*Homarus*
1199 *americanus*) larvae using a passive dosing system. *Environmental Toxicology and*
1200 *Chemistry* 40(5). DOI 10.1002/etc.4988

1201 Parkerton, T.F., French-McCay, D., De Jourdan, B., Lee, K., Coelho, G., 2023. Adopting
1202 a toxic unit model paradigm in design, analysis and interpretation of oil toxicity testing.
1203 *Aquatic Toxicology* 255, 106392. <https://doi.org/10.1016/j.aquatox.2022.106392>

1204 Scovil, A.M., de Jourdan, B., Speers-Roesch, B., 2022. Intraspecific Variation in the
1205 Sublethal Effects of Physically and Chemically Dispersed Crude Oil on Early Life Stages
1206 of Atlantic Cod (*Gadus morhua*). *Environmental Toxicology and Chemistry* 41(8). DOI
1207 10.1002/etc.5394

1208 Singer, M.M., Aurand, D., Bragin, G.E., Clark, J.R., Coelho, G.M., Sowby, M.L.,
1209 Tjeerdema, R.S., 2000. Standardization of the Preparation and Quantitation of Water-
1210 accommodated Fractions of Petroleum for Toxicity Testing. *Marine Pollution Bulletin* 40,
1211 1007–1016. [https://doi.org/10.1016/S0025-326X\(00\)00045-X](https://doi.org/10.1016/S0025-326X(00)00045-X)

1212

1213

1214 **7. Appendix**

1215

1216 **7.1. Alkanes and PAC Data from VLSFOs**

1217

1218

1219

1220

1221

Instrument	071124co_15.D	071124co_16.D	071124co_17.D	071124co_18.D	071124co_19.D	071124co_20.D	071124co_21.D	071124co_22.D	071124co_23.D	071124co_24.D	071124co_25.D	071124co_26.D	071124co_27.D	071124co_28.D	071124co_29.D	071124co_30.D	071124co_31.D	071124co_32.D
Sample->	Source O-2	Source O-4	Source O-14	Source O-16	Source O-17	Source O-23	Source O-24	Source O-26	Source O-31	Source O-43	Source O-45	Source O-48	Extract O-2	Extract O-4	Extract O-16	Extract O-31		
	7/12/2024 4:05 PM	7/12/2024 5:07 PM	7/12/2024 6:09 PM	7/12/2024 7:11 PM	7/12/2024 8:13 PM	7/12/2024 9:14 PM	7/12/2024 10:16 PM	7/12/2024 11:18 PM	7/13/2024 12:20 AM	7/13/2024 1:22 AM	7/13/2024 4:28 AM	7/13/2024 5:30 AM	7/13/2024 6:31 AM	7/13/2024 7:33 AM	7/13/2024 8:35 AM	7/13/2024 9:37 AM		
biphenyl	6.005	1.456	2.693	1.01	8.617	2.37	1.574	10.131	1.351	1.58	1.126	0.506	7.024	1.5	0.968	1.254		
ACE	1.069	0.327	1.783	0.582	2.582	0.449	0.585	2.909	0.524	0.212	0.85	0.131	1.344	0.317	0.536	0.534		
ACY	3.668	1.887	1.541	2.509	8.632	1.595	2.066	4.762	1.884	1.093	3.362	0.454	4.488	2.004	2.515	1.796		
naph	40.307	11.824	24.832	9.199	63.142	24.247	7.689	68.104	12.897	8.746	14.429	5.421	43.79	10.851	7.995	10.407		
naph-2me	91.404	20.462	24.369	27.123	186.215	35.975	32.652	46.57	35.525	17.16	35.932	7.644	107.247	22.217	28.237	34.332		
naph-1me	52.338	13.539	15.971	17.746	111.833	20.994	19.277	32.64	20.991	14.484	23.106	4.874	65.98	14.737	18.212	20.15		
naph-C2	322.15	88.323	81.01	130.085	772.316	123.764	153.435	101.189	137.906	76.319	166.202	27.656	419.594	97.801	137.26	137.323		
naph-C3	4096.68	1261.1541	1087.134	1815.572	8478.686	1509.028	2217.449	1044.202	1823.054	993.871	2361.32	395.61	5166.814	1349.282	1846.659	1789.674		
naph-C4	2531.944	1055.301	806.764	1419.602	6404.362	997.239	1583.269	702.678	1296.107	918.719	1733.6	353.451	3170.652	1126.643	1427.471	1264.136		
fluo	4.938	2.014	2.158	2.255	11.001	2.53	2.449	5.795	1.964	1.68	2.664	0.69	5.947	2.1	2.179	1.86		
fluo-C1	14.081	5.208	4.709	8.272	33.482	6.955	9.59	7.345	7.455	3.256	9.641	2.204	16.932	5.477	8.296	7.089		
fluo-C2	21.626	11.055	9.423	19.226	62.802	13.938	22.861	12.289	16.965	6.904	21.401	6.337	25.187	11.339	19.03	15.867		
fluo-C3	14.71	9.79	8.61	18.865	46.613	13.137	25.667	15.408	16.835	6.357	21.332	7.485	16.977	9.846	18.642	15.302		
fluo-C4	14.668	14.233	12.061	24.597	35.827	16.087	37.588	25.739	22.137	10.595	25.354	14.841	17.138	13.93	24.824	21.942		
anthr	1.681	0.966	1.322	1.363	3.306	1.041	2.175	13.383	1.01	0.25	1.883	0.422	2.078	0.932	0.918	1.764		
phen	12.644	6.658	5.751	11.13	34.444	8.647	12.648	12.259	9.029	3.182	13.975	2.661	15.616	6.987	11.355	9.145		
phen-C1	50.611	25.35	28.147	51.895	143.977	45.349	81.081	46.002	54.842	9.948	69.786	15.334	60.801	25.321	52.193	55.238		
phen-C2	33.261	24.375	27.444	52.104	103.944	45.046	122.144	77.058	65.176	9.767	71.085	16.817	40.775	24.643	52.824	66.556		
phen-C3	39.813	44.05	47.55	85.681	103.623	70.663	289.961	174.216	122.641	17.806	113.378	30.711	47.981	43.822	85.165	123.569		
phen-C4	8.956	14.157	13.056	21.824	20.73	17.496	75.192	49.382	30.193	6.644	26.326	10.733	10.582	13.738	21.03	29.654		
DBT	1.436	1.903	0.559	1.569	7.38	1.195	0.781	0.883	0.81	1.241	2.02	0.388	1.689	1.968	1.623	0.812		
DBT-C1	2.11	3.148	1.301	3.139	12.654	2.885	1.899	2.475	1.705	1.591	4.263	0.989	2.509	3.209	3.198	1.71		
DBT-C2	313.395	471.454	240.15	448.496	1564.362	503.367	390.007	847.099	306.375	246.92	602.937	176.111	368.231	464.506	445.595	305.408		
DBT-C3	279.692	447.421	254.441	356.805	960.602	470.415	556.053	1381.483	366.691	221.239	527.149	204.871	333.238	440.652	371.418	363.037		
DBT-C4	156.769	242.765	139.9	182.951	354.262	226.325	338.718	844.377	202.185	133.739	250.036	136.999	183.202	236.103	182.951	202.579		
flanth	0.312	0.98	0.424	0.498	1.165	0.627	1.634	1.853	0.743	0.092	0.787	0.113	0.361	0.85	0.671			
pyr	2.274	3.375	2.94	4.694	5.007	4.076	18.563	9.809	7.91	0.382	7.137	1.433	2.777	3.565	4.83	8.166		
pyr-C1	623.936	1149.858	1097.635	1463.576	1369.915	1643.803	7502.554	3840.208	2952.412	256.67	2203.027	509.555	752.507	1202.365	1471.429	2980.605		
pyr-C2	1238.127	2997.446	2660.076	3209.555	2037.275	3355.535	24673.888	8667.55	7711.637	381.835	4746.452	1136.708	1516.844	3180.795	3215.043	7801.135		
pyr-C3	1107.758	2731.693	2498.013	3448.245	1753.169	2983.917	20516.083	8204.636	6580.322	466.509	4768.833	1310.122	1366.036	2893.377	3399.622	6556.197		
pyr-C4	910.974	2548.439	2068.874	3399.622	1469.631	2990.918	15919.678	6329.518	517.1408	7116.37	4488.269	1340.114	1205.393	2748.25	3456.481	5476.604		
chr/tri/BAA	1.908	4.563	4.033	7.357	1.946	5.394	12.992	10.491	8.17	0.756	9.336	1.899	2.255	4.713	7.23	8.003		
chrys-C1	4.207	11.265	9.09	15.85	4.164	11.078	50.35	27.01	19.879	1.352	20.447	3.817	5.073	11.603	15.777	20.285		
chrys-C2	10.335	30.62	21.068	37.363	11.017	25.55	135.68	71.359	52.001	3.918	50.268	10.884	12.713	32.875	36.528	51.073		
chrys-C3	8.211	26.985	17.688	31.012	9.691	19.777	120.12	57.939	42.47	3.637	40.31	9.609	10.123	28.615	29.852	41.174		
chrys-C4	6.638	21.547	11.766	20.288	7.035	12.027	66.54	35.443	26.248	3.836	24.886	7.954	8.103	22.953	19.147	26.189		
BBF	0.433	1.528	0.759	1.396	0.33	1.073	5.222	2.47	1.937	0.117	2.228	0.233	0.529	1.708	1.403	1.907		
BEP	0.493	1.985	0.89	1.58	0.397	1.109	5.4	3.019	2.485	0.207	2.272	0.592	0.614	2.146	1.57	2.536		
BAP	0.317	2.262	0.643	0.961	0.77	0.9	5.821	1.957	1.714	0.294	1.332	0.298	0.402	2.398	0.836	1.674		
PER	0.126	0.899	0.255	0.382	0.306	0.358	2.313	0.778	0.681	0.117	0.529	0.118	0.16	0.953	0.332	0.665		
IND	0.373	4.104	1.062	0.709	0.196	0.763	3.81	1.625	1.148	0.11	0.921	0.303	0.49	4.119	0.632	1.083		
GHI	0.339	3.736	0.966	0.646	0.178	0.695	3.468	1.479	1.045	0.1	0.839	0.276	0.446	3.749	0.575	0.986		
ANTANT	0.132	0.652	0.261	0.4	0.107	0.35	1.568	0.615	0.494	0.018	0.48	0.078	0.167	0.702	0.352	0.402		
nC10	2.935	7.063	27.68	17.71	7.298	20.774	3.826	9.396	14.491	74.997	17.326	4.786	3.578	7.962	16.661	11.967		
nC11	8.964	16.121	31.19	23.125	11.863	26.686	6.789	13.231	20.699	102.678	20.76	6.653	9.554	16.616	22.601	19.02		
nC12	8.875	20.94	30.023	26.366	22.604	28.186	10.682	15.242	20.059	89.535	22.705	7.384	10.385	21.753	26.113	19.295		
nC13	8.895	23.587	30.222	32.494	31.378	30.314	12.814	17.175	19.403	86.537	24.942	8.743	10.425	24.63	32.811	19.272		
nC14	10.695	26.884	32.381	40.196	40.331	33.954	15.773	19.231	22.088	81.808	28.959	11.284	12.657	28.131	40.313	22.074		
nC15	11.075	26.837	31.269	42.153	43.752	33.403	16.72	20.38	21.961	78.322	31.758	12.733	12.926	30.098	43.021	22.481		
nC16	13.667	31.143	32.151	44.666	54.592	37.997	19.052	21.758	23.67	70.679	32.858	16.1	15.815	31.14	45.393	24.588		
nC17	17.796	46.39	45.367	71.47	114.792	60.479	24.054	27.987	21.365	30.29	35.926	29.081	20.831	19.105	45.367	64.058		
pris	8.469	16.901	24.583	46.691	57.057	24.69	10.152	14.314	18.929	56.563	18.22	10.436	8.884	17.363	43.493	16.678		
nC18	20.007	46.315	45.026	67.981	133.64	62.012	27.598	32.277	27.819	81.172	45.984	25.718	21.776	45.91	60.575	24.724		
phyt	5.965	18.436	24.943	41.209	20.062	18.436	10.845	15.182	75.912	11.929	12.471	6.507</						

Instrument	071124co_33.D	071124co_34.D	071124co_35.D	071124co_36.D	071124co_39.D	071124co_40.D	071124co_41.D	071124co_42.D	071124co_43.D	071124co_44.D	071124co_45.D	071124co_46.D	071124co_47.D	071124co_48.D	071124co_51.D	071124co_52.D
Sample->	Extract O-2 UV	Extract O-4 UV	Extract O-6 UV	Extract O-31 UV	Extract O-14	Extract O-17	Extract O-24	Extract O-26	Extract O-14 UV	Extract O-17 UV	Extract O-24 UV	Extract O-26 UV	Extract O-23	Extract O-43	Extract O-48	Extract O-43 UV
	7/13/2024 10:39 AM	7/13/2024 11:40 AM	7/13/2024 12:42 PM	7/13/2024 1:44 PM	7/13/2024 4:49 PM	7/13/2024 5:51 PM	7/13/2024 6:53 PM	7/13/2024 7:55 PM	7/13/2024 8:57 PM	7/13/2024 9:59 PM	7/13/2024 11:00 PM	7/14/2024 12:02 AM	7/14/2024 1:04 AM	7/14/2024 2:06 AM	7/14/2024 5:11 AM	7/14/2024 6:13 AM
biphenyl	6.106	1.128	0.902	1.122	2.356	6.109	1.454	9.543	2.524	8.542	1.191	10.023	2.054	0.978	0.466	2.114
ACE	1.194	0.227	0.519	0.477	1.656	2.141	0.582	2.84	1.68	2.936	0.483	2.973	0.433	0.704	0.127	0.446
ACY	3.93	1.498	2.436	1.639	1.415	6.782	1.982	4.484	1.452	9.514	1.636	4.711	1.455	3.034	0.428	1.503
naph	37.19	8.309	7.084	8.406	21.69	43.836	6.429	65.822	19.245	66.215	5.304	67.735	20.168	11.719	4.639	21.227
naph-2me	98.69	17.234	26.638	31.127	24.479	159.112	34.605	49.994	21.837	220.705	30.233	50.907	37.221	32.948	7.226	38.697
naph-1me	59.841	11.263	17.433	18.548	15.765	96.344	20.436	34.237	15.253	134.678	17.585	36.097	21.036	21.981	4.536	21.434
naph-C2	381.713	74.382	132.928	128.319	78.258	671.091	160.131	99.231	81.111	940.198	135.548	104.822	125.02	161.86	26.224	126.904
naph-C3	4622.916	1008.31	1784.014	1653.12	1005.025	7077.084	2193.153	971.425	930.895	9699.144	1811.679	991.773	1390.53	1996.659	371.977	1405.522
naph-C4	2741.717	814.798	1363.998	1148.316	713.501	4995.141	1499.586	642.38	779.79	7223.716	1200.773	659.829	900.055	1601.298	332.109	910.022
fluo	5.436	1.631	2.152	1.722	2.02	9.207	2.423	5.62	2.129	13.383	2.022	5.89	2.337	2.489	0.647	2.393
fluo-C1	14.942	4.143	8.098	6.543	4.315	27.364	9.515	6.989	4.181	29.801	7.868	7.269	6.483	8.082	2.181	6.525
fluo-C2	21.763	8.107	18.336	14.427	8.4	49.308	22.029	11.526	9.186	72.622	17.868	11.766	12.798	19.768	5.954	12.725
fluo-C3	14.539	6.962	17.761	14.138	7.706	34.93	25.038	14.305	8.458	51.495	20.207	14.87	12.375	19.61	6.837	12.4
fluo-C4	15.023	10.014	23.643	20.459	10.512	26.689	37.81	25.351	11.377	39.43	30.602	26.251	14.585	23.654	13.581	14.45
anthr	1.698	0.93	1.357	1.153	1.225	2.593	1.752	1.712	0.968	3.768	1.253	1.847	1.019	1.852	0.429	1.01
phen	14.239	5.401	11.463	8.661	5.56	30.155	13.249	12.466	5.474	42.977	11.013	13.147	8.768	13.329	2.661	8.664
phen-C1	54.421	19.154	51.94	51.94	26.388	123.457	85.897	44.975	21.94	153.714	68.725	46.374	43.609	56.255	14.905	43.243
phen-C2	35.778	18.18	51.51	61.395	25.172	85.232	131.412	77.562	26.963	127.185	104.604	81.755	43.926	69.754	16.181	43.722
phen-C3	41.258	31.774	82.066	112.373	42.264	77.809	313.013	175.454	46.39	116.934	247.222	185.764	65.994	109.54	29.086	65.491
phen-C4	9.115	9.926	20.058	26.916	11.096	14.711	77.456	47.804	12.023	22.147	61.151	50.451	15.43	23.983	10.024	15.233
DBT	1.456	1.453	1.583	0.756	0.523	5.902	0.716	0.793	0.518	8.836	0.584	0.821	1.113	1.827	0.389	1.109
DBT-C1	2.212	2.387	3.13	1.588	1.208	9.745	1.832	2.312	1.294	14.497	1.487	2.378	2.759	3.925	0.948	2.729
DBT-C2	326.827	345.451	434.527	284.241	222.994	1186.605	378.403	803.725	234.599	1760.351	319.878	823.854	475.287	559.742	169.305	470.415
DBT-C3	290.616	324.928	353.259	334.885	232.987	693.696	561.605	1337.213	255.337	1044.592	465.115	1390.079	440.437	490.723	190.079	438.216
DBT-C4	160.888	175.466	177.722	186.927	124.499	249.391	350.251	816.297	137.034	372.6	297.457	852.042	205.05	231.447	131.375	204.799
flanth	0.332	0.691	0.461	0.76	0.397	0.937	1.464	1.704	0.546	0.488	1.272	1.853	0.58	0.665	0.138	0.574
pyr	2.357	2.691	4.73	7.817	2.855	4.06	20.243	10.557	2.778	5.819	17.232	11.013	4.188	6.273	1.458	4.133
pyr-C1	664.144	898.959	1438.884	2829.801	1022.422	1071.523	7041.154	3892.337	904.163	1582.498	5838.221	3934.059	1587.701	1604.068	508.136	1577.578
pyr-C2	1337.181	2347.588	3140.776	7279.47	2471.712	1577.105	27464.806	8986.187	2795.932	2378.997	23710.312	9633.302	3304.73	4841.911	1151.939	3309.555
pyr-C3	1203.311	2121.665	3300.284	6034.532	257.427	1346.452	2234.721	8378.24	253.888	2068.212	19240.303	9013.623	8254.588	4752.318	1322.99	2880.322
pyr-C4	1073.415	2008.325	3355.724	5115.796	1906.042	1177.2	17536.613	6707.001	2161.022	1798.859	1445.936	7107.096	2255.535	4535.099	1450.142	2249.669
chr/tri/BAA	2	3.558	7.128	7.532	3.867	1.525	11.572	8.946	2.079	1.872	299.874	7.764	4.793	4.302	1.885	4.836
chrys-C1	4.534	8.72	15.203	18.713	8.571	3.215	49.039	25.445	7.735	4.408	1313.987	26.168	9.88	17.585	3.752	9.924
chrys-C2	11.244	24.334	35.369	47.322	19.636	8.412	126.663	64.42	18.757	12.279	3280.528	64.675	22.891	40.073	10.751	23.141
chrys-C3	8.815	21.04	28.922	37.339	15.572	7.71	113.384	52.614	16.939	11.422	2807.852	53.776	17.438	38.409	9.583	17.642
chrys-C4	7.069	16.478	18.161	23.522	9.95	5.5	64.559	31.16	10.965	8.04	1584.049	31.021	10.737	24.82	7.604	10.847
BBF	0.463	1.256	1.226	1.745	0.637	0.276	6.573	1.783	0.953	0.397	116.33	1.662	0.948	1.441	0.326	0.939
BEP	0.548	1.644	1.534	2.372	0.848	0.323	0.581	2.868	0.784	0.465	141.534	2.89	1.052	1.896	0.596	1.056
BAP	0.356	1.768	0.881	1.521	0.617	0.715	13.345	1.405	1.605	0.509	109.218	1.244	0.727	0.984	0.271	0.725
PER	0.141	0.702	0.35	0.604	0.245	0.284	5.303	0.636	0.198	0.202	41.426	0.604	0.276	0.342	0.109	0.287
IND	0.375	3.043	0.613	0.963	0.94	0.135	0.537	1.321	0.071	0.178	11.709	1.288	0.547	0.131	0.265	0.543
GHI	0.341	2.77	0.558	0.877	0.855	0.123	0.488	1.202	0.668	0.162	57.203	1.172	0.498	0.511	0.241	0.495
ANTANT	0.133	0.465	0.323	0.351	0.213	0.072	0.241	0.411	0.184	0.097	27.404	0.411	0.245	0.071	0.061	0.237
nC10	2.812	5.399	14.35	11.467	24.587	4.644	2.381	7.842	17.306	6.459	2.357	7.205	16.621	12.593	4.017	16.809
nC11	9.306	12.718	21.764	19.43	30.589	8.645	5.945	12.46	25.247	12.514	5.119	11.996	25.323	17.31	6.157	24.8
nC12	9.572	16.816	25.607	19.528	29.931	17.645	10.162	15.053	26.342	25.46	8.718	15.094	28.938	20.232	7.068	28.452
nC13	9.844	19.26	32.993	19.509	30.417	26.949	13.321	17.806	27.577	39.419	12.065	18.57	32.974	24.27	9.024	33.615
nC14	11.776	21.931	41.41	22.089	33.562	33.901	16.417	20.193	28.905	49.048	14.563	20.895	37.408	27.393	12.293	38.932
nC15	12.162	22.901	41.236	22.436	32.526	35.973	16.28	21.298	29.842	57.856	14.964	21.32	38.337	28.084	15.753	40.502
nC16	14.809	25.695	45.997	23.878	34.465	47.247	22.036	28.98	69.105	17.742	23.666	42.749	33.548	19.183	45.148	
nC17	14.728	30.607	57.476	22.141	31.981	49.125	23.067	45.591	114.824	15.655	23.61	45.048	39.297	14.281	43.546	
pris	7.229	13.149	36.972	15.792	18.439	36.664	8.427	10.287	23.264	58.157	7.169	10.543	18.952	15.554	8.786	18.3
nC18</td																

Instrument	071124co_53.D	071124co_54.D	071124co_63.D	071124co_64.D
Sample->	Extract O-45 UV	Extract O-48 UV	Extract O-23 UV	Extract O-45
	7/14/2024 7:15 AM	7/14/2024 8:17 AM	7/15/2024 1:25 PM	7/15/2024 2:27 PM
biphenyl	0.952	0.45	2.066	0.879
ACE	0.776	0.132	0.468	0.661
ACY	2.962	0.402	1.549	2.834
naph	9.969	4.325	23.711	12.203
naph-2me	33.825	6.96	41.783	34.919
naph-1me	21.316	4.35	22	21.304
naph-C2	160.126	25.112	130.55	150.848
naph-C3	2069.023	346.853	1523.247	2043.705
naph-C4	1540.447	301.242	975.207	1431.971
fluo	2.577	0.667	2.394	2.493
fluo-C1	8.805	2.135	6.737	8.794
fluo-C2	19.106	5.874	13.1	19.162
fluo-C3	18.865	6.777	12.701	19.188
fluo-C4	23.293	13.476	14.995	22.441
anthr	1.682	0.372	1.027	1.843
phen	13.835	2.634	8.853	13.377
phen-C1	64.469	14.145	46.14	66.929
phen-C2	68.526	15.635	44.094	65.531
phen-C3	105.098	27.937	66.14	100.733
phen-C4	23.367	9.579	15.582	22.49
DBT	1.775	0.365	1.134	1.793
DBT-C1	3.863	0.913	2.752	3.762
DBT-C2	548.854	165.688	479.513	537.894
DBT-C3	488.789	189.685	437.643	461.497
DBT-C4	226.397	130.91	208.56	216.798
flanth	0.672	0.132	0.596	0.695
pyr	6.618	1.371	4.3	6.531
pyr-C1	2071.334	503.784	1634.059	2068.212
pyr-C2	4655.345	1129.328	3272.564	4373.888
pyr-C3	4643.898	1313.245	2782.308	4291.012
pyr-C4	4519.678	1437.465	2094.229	4087.512
chr/tri/BAA	5.734	1.81	5.391	8.873
chrys-C1	18.091	3.565	10.915	19.311
chrys-C2	42.293	10.216	24.213	46.001
chrys-C3	37.72	8.968	17.918	36.199
chrys-C4	21.838	7.107	10.692	22.058
BBF	1.381	0.311	0.981	1.919
BEP	1.96	0.588	1.122	2.204
BAP	0.753	0.225	0.88	1.214
PER	0.381	0.095	0.35	0.483
IND	0.739	0.249	0.544	0.692
GHI	0.672	0.227	0.495	0.63
ANTANT	0.227	0.054	0.223	0.31
nC10	11.854	3.826	19.185	15.574
nC11	17.072	6.034	29.418	20.841
nC12	21.049	7.147	33.386	24.019
nC13	26.36	9.107	39.008	28.931
nC14	31.484	12.381	45.307	33.557
nC15	34.498	14.04	47.381	39.012
nC16	37.842	18.991	54.953	43.204
nC17	36.677	14.345	42.748	32.077
pris	15.326	8.12	19.936	13.69
nC18	36.514	17.797	41.82	30.803
phyt	9.76	7.591	11.387	7.049
nC19	41.965	34.975	68.683	49.761
nC20	37.094	36.794	61.948	46.293
nC21	41.571	41.786	69.484	51.865
nC22	43.688	44.559	70.573	54.739
nC23	46.676	50.865	75.13	58.765
nC24	43.98	47.254	63.709	53.923
nC25	44.799	44.306	64.636	57.017
nC26	46.502	42.673	61.902	59.576
nC27	52.516	43.654	69.025	66.178
nC28	50.236	42.736	64.869	63.396
nC29	47.392	42.05	62.06	60.369
nC30	42.359	36.591	55.186	53.299
nC31	36.076	34.156	49.801	45.821
nC32	25.785	24.804	35.633	32.701
nC33	25.338	21.836	28.898	27.471
nC34	15.555	17.533	21.975	19.701
nC35	13.897	15.73	17.618	15.435
nC36	11.278	13.563	14.391	11.867
nC37	9.314	11.177	12.271	9.504
nC17pris	55	36.13	84.321	63.606
nC18phyt	52.421	42.264	81.873	60.614
oTP	0	0.011	0.01	0.01
C30hop	34.098	12.188	19.914	29.499